



**Centro de Investigación y de Estudios
Avanzados del Instituto Politécnico Nacional**

DEPARTAMENTO DE FÍSICA

“Diseño de dispositivos en aleaciones de $\text{Ge}_{(1-x)}\text{Sn}_x$ que operan a temperatura ambiente y su caracterización termoeléctrica”

Tesis que presenta

Jhonny Tiscareño Ramirez

Para obtener el grado de

Maestro en Ciencias

en la Especialidad de

Física

Director de tesis: **Dr. Salvador Gallardo Hernández**

Ciudad de México

Julio, 2023



**Centro de Investigación y de Estudios
Avanzados del Instituto Politécnico Nacional**

PHYSICS DEPARTMENT

**“Devices design on $\text{Ge}_{(1-x)}\text{Sn}_x$ alloys operating at room
temperature and their thermoelectric characterization”**

Thesis submitted by

Jhonny Tiscareño Ramirez

In order to obtain the

Master of Science

degree, specialty of

Physics

Supervisor: **Dr. Salvador Gallardo Hernandez**

Mexico City

July, 2023

To Irari,

My everlasting source of support, trust, and love.

My eternal light that illuminates the path even in my darkest hours.

My everything, forever.

¿Sabes tú para qué son los camiones?

¿Sabes tú por qué hay estrellas y constelaciones?

Eso no lo sé, solo sé

Que es muy interesante

— 31 Minutos (La señora interesante)

This work is a collaboration between **Centro de Investigación y de Estudios Avanzados del Instituto Politécnico Nacional** (CINVESTAV - IPN) in Mexico and **Forschungszentrum Jülich** (FZJ) in Germany. The experimental development and part of the data analysis was carried out at FZJ in the **Peter Grünberg Institute 9** (PGI-9) as the result of a short research stay from January to April 2023 in the **Silicon-based epitaxy and photonics** group led by **Dr. Dan Buca**. The training process, operation of characterization equipment and fabrication of devices was supervised by **Dr. Omar Concepción Díaz**. The data analysis and interpretation of the results was completed in CINVESTAV in the Department of Physics supervised by **Dr. Salvador Gallardo Hernandez**.

Content

CONTENT	13
AGRADECIMIENTOS.....	17
ACKNOWLEDGEMENTS.....	19
RESUMEN.....	21
ABSTRACT	23
CHAPTER 1. CONCEPTS ON THERMOELECTRICS	25
Figure of merit	26
The Seebeck coefficient	29
Electrical conductivity	29
Thermal conductivity	30
CHAPTER 2. SI-GE-SN ALLOYS GROWTH AND CHARACTERIZATION	32
Epitaxial Growth	33
RBS	35
RBS simulations using RUMP.....	38
XRD	40
The 3ω Method	42
Experimental part.....	43
Theoretical part.....	44
Thermal conductivity	46
Seebeck coefficient	50
Temperature Coefficient of Resistance (TCR)	50
Electrical conductivity	51
CHAPTER 3. EXPERIMENTAL PROCESS	53

Growth and characterization.....	53
<i>GeSn</i> thicknesses set.....	54
<i>Sn</i> concentration set.....	54
RBS.....	55
XRD.....	56
Set-up build up and calibration	58
Python script.....	61
The K device.....	64
Results for the TCR	67
Validation of the 3ω method.....	69
SiO ₂ thickness study.....	72
Lattice thermal conductivity measurements	77
<i>GeSn</i> thicknesses	77
<i>Sn</i> concentration.....	78
Improved devices.....	81
The K-S device.....	81
The σ device	90
CHAPTER 4. DISCUSSION AND CONCLUSIONS	91
REFERENCES	95
LIST OF TABLES.....	97
LIST OF FIGURES.....	99
COMPLEMENTS.....	101
Python scripts	101
utils.py	101
TE_measurement.py.....	102
Mask for K design.....	124
Complete	124
Detail.....	125
Mask for K-S design.....	126
All layers	126

First layer	127
Second layer	128
Third layer	129
Fourth layer	130
Fifth layer	131
Mask for the K-S-σ design	132
All layers	132
First layer (only σ device)	133
Second layer (only σ device)	134
Third layer (only σ device)	135
Run sheet for K-S and K-S-σ design	136

Agradecimientos

A Irari Jiménez López por ser la mejor compañera que pude haber encontrado en esta vida. Gracias por apoyar todas mis ideas y proyectos. Si no fuera por tu sabio consejo nunca habría conseguido superarme en lo académico y en lo personal. Es por ti que he tomado las decisiones correctas a lo largo de mi vida. Me siento completo a tu lado. Este trabajo es el resultado de tantos días que compartimos estudiando lado a lado como lo ha sido desde que nos conocimos. Nos queda todo un futuro por delante. Dedico a ti todo el esfuerzo y trabajo que implicó esta tesis. Gracias por todo.

A mi padre Geovani Tiscareño Hernández, a mi madre Norma Ramírez Betancourt y a mi hermana Nelly Tiscareño Ramírez, porque a pesar de las carencias y dificultades siempre han sabido sacar adelante a la familia y el más grande ejemplo es este trabajo. Les agradezco por haber depositado toda su confianza en mí y haberme encaminado hasta este punto de mi vida. Aprovecharé muy bien todo el esfuerzo que han hecho para que yo me encuentre aquí.

A Manuel Jiménez Villanueva, Laura López Jiménez y Mextli Daniela Jiménez López por haberme acompañado durante este proceso y arroparme como parte de su familia desde el momento en que los conocí. Les agradezco el apoyo y cariño que me han brindado. Ustedes han sido parte fundamental de mi vida los últimos años y espero seguir compartiendo muy buenos momentos a su lado.

A Carolina Sánchez López, Pedro Montes Tolentino, Alonso Reyes López y Elizabeth Machuca de la Paz por ser mi gran inspiración y motivación para seguir adelante. Ustedes son y serán siempre mi ejemplo a seguir. Antes de conocerlos mis metas en la vida eran mucho menos ambiciosas. Les agradezco mucho por todo su apoyo y cariño.

A Misael Sánchez Pérez y Fernanda Escobedo Montaña por abrirme las puertas a su equipo de trabajo y brindarme un medio para poder pagar la estancia que resultó en esta tesis. Gracias, no solo por ser un excelente equipo, sino por ser un gran apoyo emocional y motivarme a seguir adelante.

A Daniel Arturo López Aguilar, Humberto Parrilla de la O, Miguel Alfonso Zapata de la Cruz, Ramon Eduardo López Villamil y Darly Yaritza Castro Cárdenas por haberme apoyado y acompañado a lo largo de la maestría. Siempre llevaré en mi memoria los buenos momentos, los desvelos constantes por las tareas y exámenes, tantas risas, dificultades y alegrías que pasamos juntos. Sin su apoyo nunca habría llegado tan lejos.

A mis amigos de “Pura Vida” que durante el primer semestre me ayudaron con tareas, explicaciones, consejos y con quienes pasé momentos muy agradables. Ramon, Zapata, Roberto, Julio, Bladimir, José, Picón y Alexander. Gracias a ustedes pude terminar exitosamente el primer semestre, estoy infinitamente agradecido con cada uno. Y quiero que sepan que merecían mucho más que yo continuar en la maestría. Es inaceptable y decepcionante que por culpa de los procesos de evaluación subjetivos y de algunos evaluadores en este departamento no se pueda dimensionar lo brillantes que son todos ustedes.

Al Dr. Salvador Gallardo Hernández, le agradezco sus sabios consejos desde la licenciatura y durante toda la maestría. Aún conservo el libro que me obsequió cuando ingresé al proceso de admisión del departamento de física. “Por valiente”, incluso recuerdo sus palabras. Le agradezco infinitamente la sugerencia de contactar al Dr. Omar y el apoyo que me brindó para hacer posible la estancia de investigación que resultó en este gran trabajo.

Acknowledgements

To Professor Detlev Grützmacher for accepting the research stay during which I developed this work. I am indebted to you for this great opportunity. Thank you for everything.

To Dan Buca for allowing me to be part of his research group and for giving me the opportunity to learn about *GeSn* alloys which was a completely new topic for me some months ago. Thanks to you I was able to have a deep understanding of what it really is to do research.

To Omar Concepción Díaz for his wonderful support since we met, for his kind explanations about the growth process of *GeSn* alloys on the CVD and for teaching me everything about RBS and XRD characterization techniques. Thank you for all your attention and for guiding me through the development of this work. I have learned lots of things from you. Thank you for all your patience, your advice, your friendship and for caring so much about me.

To Oliver Krause for taking the time to explain to me on detail everything related to the 3ω method and the thermoelectrics of *GeSn* alloys. I really appreciate all the time you spent with me until I was able to continue the work by myself. I can not imagine what I would have done without your valuable help.

To Thorsten Brazda for his kind help during the low temperature measurements. I know I was unable to learn the whole process of measuring a sample using the cryostat, but you were patient enough to walk me through it more than three times.

To Prateek Kaul for being a great partner during my stay in FZJ. When I arrived, I was very nervous about the English language and my poor communication skills. I am very grateful because you, maybe without being aware of it, had always something to tell to keep the conversation alive and that made me feel more and more confident to improve my speaking skills.

To Jin Hee Bae for her valuable help with the TEM and SEM images. I will always remember that day I forgot my card to have lunch and you paid for it. I really appreciate that.

To Patric Bernardy, Karl-Heinz Deussen and Andreas Tiedemann for their kind support in the CVD lab. Your work is essential for the progress of this research because without being able to grow semiconductor nothing else makes sense. Thank you so much.

To Qing-Tai Zhao, Teren Liu, Yi Han, Jingxuan Sun, Dong Yang, Yannik Junk, Jiayuan Zhang and, in general, all people working on PGI-9 for all their advises, suggestions, for their help, for all those cake days, for every conversation we had. I loved spending time at PGI-9 because all of you made me feel a part of that place. I immediately felt the collaboration and support from all of you. Thank you so much for everything.

Resumen

Las propiedades termoeléctricas de aleaciones binarias de $GeSn$ fueron estudiadas por las cantidades que involucra la figura de mérito ZT que determina qué tan bueno es un material para la conversión entre calor y electricidad. El $GeSn$ se creció en una capa de Ge recocido post-deposición (PDA por sus siglas en inglés) sobre un sustrato de Si . Las técnicas de Difracción de Rayos X (XRD por sus siglas en inglés) y Espectrometría de Retrodispersión de Rutherford (RBS por sus siglas en inglés) fueron utilizadas para obtener la composición de las muestras y asegurar que presentan una estructura cristalina.

Dispositivos microelectrónicos dedicados que permiten la extracción de la conductividad eléctrica, conductividad térmica de red y el coeficiente Seebeck de aleaciones de $GeSn$ fueron fabricados. Este trabajo está principalmente enfocado en la conductividad térmica de red para la cual un estudio de las aleaciones de $GeSn$ a diferentes concentraciones de Sn y a diferentes espesores fue realizado. El método 3ω se explica a detalle y las fórmulas utilizadas para calcular la conductividad térmica y el coeficiente Seebeck son derivadas. Más específicamente, el método diferencial 3ω es aplicado, el cual elimina los efectos parásitos debido a los contactos y otras capas de heteroestructura involucradas en la medición. El primer dispositivo (Dispositivo K) es el diseño común de 4 contactos y un calentador de línea para medir solo la conductividad térmica del material. El segundo dispositivo (Dispositivo K-S) ofrece la posibilidad de medir de forma simultánea la conductividad térmica y el coeficiente Seebeck mediante un contacto metálico en contacto directo con el material a medir y un calentador en serpentín en lugar de uno de línea. El último dispositivo (Dispositivo σ) permite que la corriente fluya directamente a través del material para medir la caída de voltaje y calcular la conductividad eléctrica. Los dispositivos K-S y σ fueron diseñados en este trabajo y el K-S fue también fabricado para probar el concepto y su funcionalidad. Todos los datos medidos que se muestran aquí fueron obtenidos del dispositivo K.

Las mediciones fueron realizadas utilizando un amplificador Lock-in controlado por un script en Python a través de la librería Zhinst. El escaneo de frecuencia, el escaneo de voltaje y la

medición de resistencia son las tres opciones disponibles para analizar utilizando el script. Los datos experimentales, la configuración y las gráficas son almacenados de forma separada en archivos para el posterior procesamiento de datos y extracción de parámetros.

Para el estudio de la dependencia de la conductividad térmica con el espesor de *GeSn* un comportamiento asintótico fue encontrado a medida que el grosor incrementa, atribuido a la gran dispersión de fonones producida en la interfaz de las capas a medida que el material se vuelve más delgado. Para reforzar la observación, una muestra muy gruesa (700 nm) crecida en un substrato virtual de Ge (*GeVS* por sus siglas en inglés) de alta calidad confirmó que existe un grosor crítico para el cual la conductividad térmica alcanza el valor correcto.

Para el estudio de la dependencia de la conductividad térmica con la concentración de *Sn*, existe una clara tendencia decreciente para concentraciones de *Sn* arriba del 5% mostrando un valor muy pequeño de $\sim 4 \frac{W}{mK}$ para concentraciones del 12%. Este es un indicador de que el *Sn* está, definitivamente, incrementando la dispersión de fonones en la red. Sin embargo, la razón por la cual el decremento cambia a concentraciones más altas tiene sus raíces en las peculiaridades del material como se discute posteriormente. Para continuar la investigación, un set de nuevas muestras debe crearse y medirse en buffers de *GeVS* de alta calidad y se debe apuntar hacia mayores grosores de *GeSn* y mayores concentraciones de *Sn*.

Finalmente, los dispositivos K-S y σ deben ser probados y, de ser necesario, mejorados para una determinación confiable del coeficiente Seebeck y la conductividad eléctrica. La figura de mérito ZT puede, entonces, ser calculada para probar que el *GeSn* es útil para aplicaciones termoeléctricas.

Abstract

The thermoelectric properties of $GeSn$ binary alloys were studied by the quantities involved in the figure of merit ZT which determines how good is a material to convert heat into electricity. The $GeSn$ was grown on a Ge post-deposition annealed (PDA) buffer over a Si substrate. X-ray diffraction (XRD) and Rutherford backscattering spectrometry (RBS) techniques were used to obtain the composition and ensure the crystalline structure of the samples.

Dedicated microelectronic devices were fabricated that allows the extraction of the electrical conductivity, lattice thermal conductivity and the Seebeck of $GeSn$ alloys. This work is mainly focused on the lattice thermal conductivity for which the study of $GeSn$ alloys of different Sn concentration and thickness was carried out. The 3ω method is explained on detail and the formulas used to calculate the thermal conductivity and Seebeck coefficient are derived. More specific, the 3ω differential method is applied which eliminates the parasitic effects due to the contact pads and other heterostructure layers involved in the measurement. The first device (K device) is the common 4-pads heater stripe design to measure only the thermal conductivity of the material. The second device (K-S device) provides the possibility to measure simultaneously the thermal conductivity and the Seebeck coefficient by a metal pad in direct contact with the material to measure and a serpentine heater instead of a stripe. The last device (σ device) allows a current to flow directly through the material to measure the voltage drop and calculate the electrical conductivity. The K-S and the σ devices were designed in this work and the K-S was also fabricated for testing the concept and its functionality. All measured data showed here were obtained from the K device.

The measurements were carried out using a Lock-in Amplifier controlled by a Python script through the Zhinst library. A frequency scan, a voltage scan and a resistance measurement are the three available options to analyze by using the script. The experimental data, the configuration and the plots are stored in separated files to further processing of data and parameters extraction.

For the study of the thermal conductivity dependence on the $GeSn$ thickness, an asymptotic behavior was found as the thickness increases which is attributed to the large phonon scattering produced in the interface of the layers as the material becomes thinner. To reinforce the observation, a very thick sample (700 nm) grown on a high-quality Ge virtual substrate ($GeVS$) confirmed that there is a critical thickness for which the thermal conductivity reaches a right value.

For the study of the thermal conductivity dependence on the Sn concentration, there is first a clear decreasing tendency for Sn concentrations above 5 at %. showing a very low value of $\sim 4 \frac{W}{mK}$ at Sn content of 12 at %. This is an indicator that Sn is definitely increasing phonon scattering in the lattice. However, the reason why the decrease change at higher Sn has roots in the material “peculiarities” as discussed later. To continue the investigation, new set of samples must be grown and measured on high quality $GeVS$ buffers and higher $GeSn$ thicknesses and Sn concentrations must be targeted.

Finally, the K-S and the σ devices must be tested and, if necessary, improved for reliable Seebeck coefficient and electrical conductivity determination. The ZT figure of merit can be then calculated and prove that this $GeSn$ material is useful for thermoelectric applications.

Chapter 1. Concepts on thermoelectrics

Thermoelectric materials are a class of materials that can generate a voltage drop in response to a temperature gradient and vice versa. This is known as the Seebeck effect, and it happens because some materials tend to accumulate charges in a significant degree at one end of the material when are exposed to heat. These materials can also produce a temperature gradient when are subjected to an external voltage, which is known as the Peltier effect. And finally, the Thomson effect refers to the reversible heating or cooling of a material when both, an electric current and a temperature gradient are applied. For energy harvesting applications the Seebeck effect is the most important one. This is the basis for the development and fabrication of thermoelectric devices, which can have a wide range of applications, including refrigeration, temperature sensing and, for our concerns, energy harvesting. However, they are not yet as efficient as other methods of energy harvesting, most of them nor compatible with CMOS technology nor efficient enough at room temperature. Providing a solution to the previous challenges is the main objective of this work.

Research in the thermoelectric field is lately strongly accelerated, with the aim of developing materials with higher energy recovery efficiency. Different techniques such as the increasing of the Seebeck coefficient (which indicates the ratio of the generated voltage to the temperature gradient) by using doping or alloying, the decrease of the thermal conductivity by increasing the phonon scattering, and the exploration of different nanostructures have been investigated to improve the thermoelectric properties of these materials.

The thermoelectric capability of a material depends on many different properties. For this reason, the figure of merit (ZT) group these characteristics and provides a quantitative value to determine the usefulness of a thermoelectric material.

Figure of merit

The figure of merit (ZT) is a key parameter used to quantify the efficiency of a thermoelectric material as it was first defined by A.F. Ioffe [1] as:

$$ZT = \frac{S^2 \sigma}{k} T \quad (1)$$

where S is the Seebeck coefficient, σ is the electrical conductivity, k is the thermal conductivity, and T is the temperature.

A higher value of ZT indicates a more efficient thermoelectric material which means that it can generate a larger voltage in response to a temperature gradient minimizing the heat loss through thermal conduction. By selecting materials with high Seebeck coefficients, high electrical conductivity, and low thermal conductivity, it is possible to maximize the efficiency of thermoelectric devices as it is explained on detail by H. Julian Goldsmid. [2]

By the end of the 1960's it was thought that the upper limit for the ZT value might be near 1 which is not considered to be useful for practical thermoelectric applications. The interest renewed in the 1990's when the engineered structures seemed to be a promising solution to improve the ZT value. Many nanostructured materials have been developed since then. Fig. 1 shows that many thermoelectric materials as for 2010 does not reach a ZT value of 1 and, except for Bi_2Te_3 (bulk and nanostructured), none of them is useful at room temperature ($\sim 300K$). In that time it was believed that the new thermoelectric materials would have a $ZT \sim 2$ with a conversion efficiency increase over 20% compared to the $ZT \sim (1.3 - 1.7)$ and conversion efficiency $\sim (5\% - 6\%)$ of that moment [3].

In Fig. 2, Sb_2Te_3 is reported as a thermoelectric p-type material in the room temperature range. The research of thermoelectric materials continued the following years but rarely focused on room temperatures.

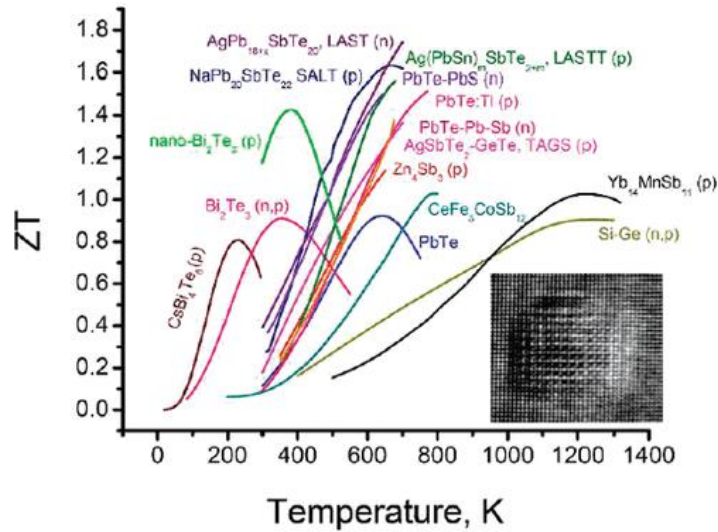


Fig. 1 State of the art thermoelectric materials as for 2010 [3]

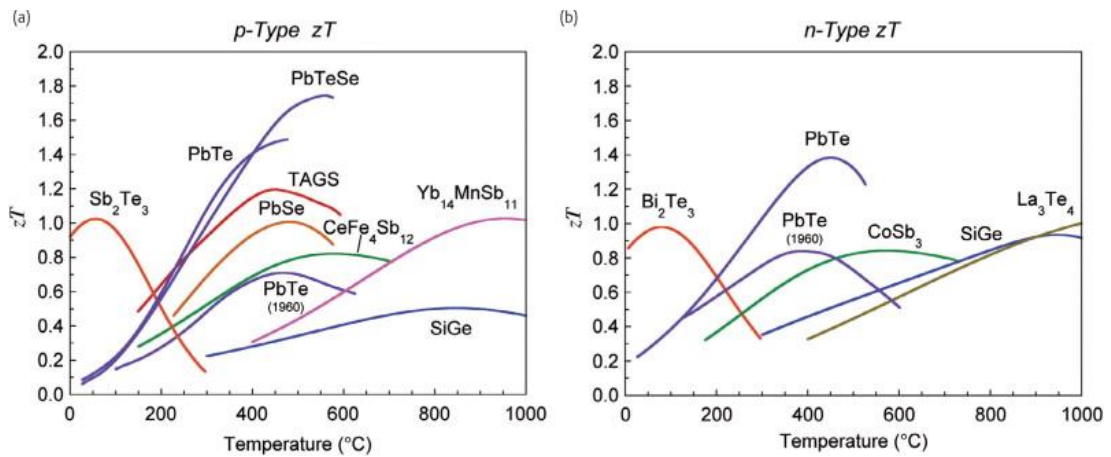


Fig. 2 State of art common thermoelectric materials as for 2011 [4]

Nowadays, a ZT value of 1 is generally considered to be the minimum threshold for practical thermoelectric applications and the upper limit for ZT is still to be studied for many materials. One example of this is the recently obtained upper limit value for n- and p-type $PbTe$ reported as $ZT = 2$ and $ZT = 3$, respectively [5]. However, Pb is a toxic heavy metal which can produce several damages to multiple body systems.

As for 2013, the Half-Heusler materials gain research interest because they are environmentally friendly, mechanically, and thermally robusts. These materials consist of a XYZ chemical composition with X being a transition metal, noble metal or rare-earth element, Y a transition metal or noble metal, an Z the main group element. In Fig. 3 the

detailed composition for the Half-Heusler materials are Half-Heusler (n): $Hf_{0.25}Zr_{0.75}NiSn_{0.99}Sb_{0.01}$ and Half-Heusler (p): $Hf_{0.44}Zr_{0.44}Ti_{0.12}CoSn_{0.8}Sb_{0.2}$. The only material in this figure reported to be useful at room temperature is the *Bi-Te* which have a detailed composition of *Bi-Te* (n): $Cu_{0.01}Bi_2Te_{2.7}Se_{0.3}$ [6] and *Bi-Te* (p): $Bi_xSb_{2-x}Te_3$ [7]. For the n-type material the Cu-doping along with the nanostructured engineering of the material resulted on the increase of *ZT* compared to previous results, while for the p-type the nanocrystalline bulk alloy was responsible of this increase.

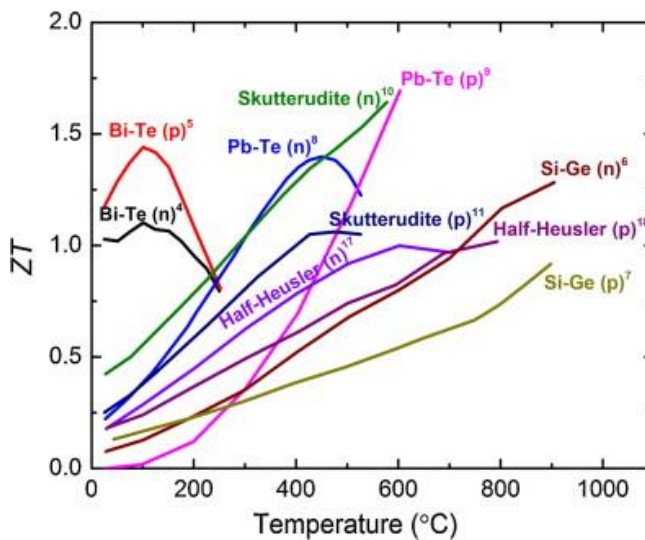


Fig. 3 Half-Heusler thermoelectric materials compared to nanostructured compounds [8]

In the last years, some alternatives have been studied to achieve room temperature thermoelectric materials such as the n-type Mg_3Sb_2 -based materials which exhibits a $ZT \sim 1$ [9]. Even though the *SiGe* alloys have been widely used as thermoelectric materials for high temperatures, a fully CMOS technology compatible material working at room temperatures had not yet been reported until 2021 with a not-yet studied material in the thermoelectric field, the *GeSn* binary alloy. This material shows, in early stages of research, a $ZT \sim 0.4$ at room temperature [10] which is a low value compared to the common *Bi-Te* and *Sb-Te* -based materials but offers the possibility of monolithic integration on Si-based devices. It is worth to mention that the *ZT* of this material is not yet the highest value that could be achieved since there is no doping and more atoms could be added to the alloy such as *Si* to get a *SiGeSn* alloy.

Body energy harvesting using Bi_2Te_3 have been studied in the last years reaching an output of $4.15 V$ and generates up to $8.6 \frac{\mu W}{cm^2}$ with an efficiency of 30% being able to power a low-consumption device [10]. Considering the $ZT \sim 1.2$ of Bi_2Te_3 , the real goal for a Si-based portable energy harvesting device is to find a material with similar ZT than that of the Bi_2Te_3 . To achieve an improvement of the thermoelectric capabilities of a material it is important to detail the quantities involved in the figure of merit.

The Seebeck coefficient

The Seebeck effect is a physical effect found by Thomas Johann Seebeck in 1821, it is defined as the ratio of the generated voltage to the temperature difference between the two ends of a material as:

$$S = \frac{\Delta V}{\Delta T} \quad (2)$$

It is an important property of the thermoelectric materials, causing the ZT value to increase as it also increases. Moreover, the Seebeck Coefficient is dependent on the properties of the material, such as its electrical conductivity, thermal conductivity, and the density of states of the electrons near the Fermi level, for that reason tuning the Seebeck Coefficient is not a very common strategy to increase the ZT of a thermoelectric material. Despite intrinsic semiconductors exhibit a $S = 0$, the doping level rapidly increases the coefficient until reaching a peak after which it decreases again [11].

Electrical conductivity

The electrical conductivity (σ) measures the ability of a material to conduct an electrical current. It is a fundamental property of materials with charge carriers. In semiconductors, the electrical conductivity is typically much lower than in metals due to the smaller number of free electrons. However, this value can be increased by doping the material with impurities. The electrical conductivity for semiconductors is defined as:

$$\sigma = ne\mu_e + pe\mu_h \quad (3)$$

Where e is the electron charge, μ_e and μ_h are the electron and hole mobilities, respectively, and n and p are the charge carrier concentrations for electrons and holes, respectively.

The conductivity can be increased by doping the material with impurities, although too high concentrations can lead to impurity scattering and reduced mobility of the charge carriers. Yet, it is important to notice that the temperature dependence for the electrical conductivity in extrinsic semiconductors is very important. Therefore, the operation temperature range for a thermoelectric material should satisfy the following inequality [12]:

$$T \leq \frac{E_g}{10 k_B} \quad (4)$$

where E_g is the band gap of the material and k_B the Boltzmann constant.

Thus, this work is mainly focused on the thermal conductivity for which a study on its dependance with both $GeSn$ thickness and the Sn concentration was carried out, looking for a future enhancement of the figure of merit ZT .

Thermal conductivity

Thermal conductivity (k) is a measure of the material ability to conduct heat. It is defined as:

$$k = \frac{Qd}{A\Delta T} \quad (5)$$

Where, Q is the amount of heat transferred, d the distance between two isothermal planes, A is the area of the surface and ΔT the temperature gradient.

Materials with high thermal conductivity are good conductors of heat such as metals. For semiconductors, as Group IV materials, the thermal conductivity depends on the crystal structure, the strength, and type of atomic bonds and the presence of defects or impurities in the crystal lattice. It is common to separate the thermal conductivity as:

$$k = k_e + k_{ph} \quad (6)$$

Where k_e is the contribution due to the free charge carriers, called the electronic thermal conductivity, and k_{ph} is the contribution due to phonons, called the lattice thermal

conductivity. Phonons are quantized units of lattice vibration, which dissipates the heat by transferring energy from one atom to another through the lattice so for complex crystal structures, such as *GeSn* or *SiGeSn* the thermal conductivity is expected to be low due to the alloy scattering. Phonon scattering reduces the phonons mean free path, leading to a reduction in thermal conductivity.

Intrinsic semiconductors, such as silicon and germanium, have a simple crystal structure and strong covalent bonds between neighboring atoms. For that reason, these materials have relatively high thermal conductivities: $k_{Ge} \sim 58 \frac{W}{K m}$ and $k_{Si} \sim 142 \frac{W}{K m}$ [13], due to the efficient transport of lattice vibrations through the crystal lattice.

Extrinsic semiconductors, doped with impurities to modify their electrical properties, can have significantly different thermal conductivities depending on the type and concentration of impurities by increasing the phonon scattering.

This work is mainly based on the study of the thermal conductivity of *GeSn* alloys at different *GeSn* thicknesses and different *Sn* concentrations. For the electrical conductivity and the Seebeck coefficient extraction, some devices were designed and fabricated and will be discussed in the next chapters.

Chapter 2. Si-Ge-Sn alloys growth and characterization

GeSn and *SiGeSn* alloys are materials belonging to the Group IV of elements, also called Silicon-group, which have recently gained the interest in the semiconductors research field because of their potential monolithical integration of electronic, photonic and, more recently, thermoelectric functions. These materials are binary and ternary alloys, respectively, with large lattice mismatch and large atomic size variations. The lattice parameters of each element are: $a_{Si} = 5.431 \text{ \AA}$, $a_{Ge} = 5.646 \text{ \AA}$ and $a_{\alpha Sn} = 6.489 \text{ \AA}$ [14]. These values represent the equilibrium interatomic distance between adjacent atoms in the elemental lattice.

By adding *Sn* to the *Ge* crystal lattice, the bandgap of the material can be reduced, making it more suitable for infrared optoelectronic applications. Additionally, the incorporation of *Sn* into the crystalline lattice of *Ge* can modify the properties of the material, such as increasing the electron mobility and reducing the thermal conductivity. In the other hand, by introducing *Sn* into the *SiGe* crystal lattice, the bandgap of the material can be tuned achieving the direct bandgap for optoelectronic applications [15].

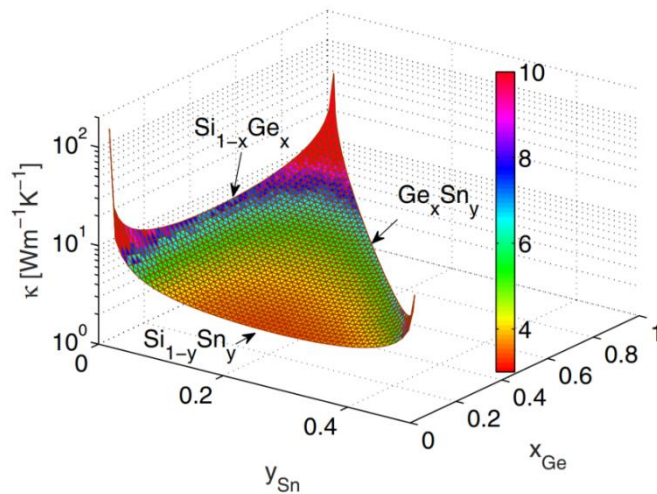


Fig. 4 Thermal conductivity of *SiGe*, *GeSn*, and *SiSn* alloys at different concentrations [16].

Both materials have a reduced thermal conductivity and a high electrical conductivity, by adding doping impurities, which make them suitable for thermoelectric applications. According to the theory, the thermal conductivity of *GeSn* and *SiGe* and *SiSn* alloys should rapidly decrease by increasing the *Sn* concentration up to a minimum after which it increases again as shown in Fig. 4.

Epitaxial Growth

Chemical Vapor Deposition (CVD) is a widely used method for the growth of thin films and coatings on various substrates. In CVD, a gaseous precursor is introduced into a reactor chamber to form a solid film on the substrate surface of a wafer. The process is typically carried out under vacuum or low-pressure conditions to minimize gas-phase reactions. Once the precursor gases are introduced in the reactor chamber, the substrate wafer adsorbs the gas molecules leading to surface reactions and the formation of a solid film. The growth rate, composition and other properties can be controlled by the temperature, pressure, gas flow rate and kind of substrate material.

CVD is widely used in the fabrication of semiconductor devices because it allows for precise control of film thickness, composition, and crystal structure, which is important for our concerns to achieve a good thermoelectric material. CVD is the best method for growing *GeSn* and *SiGeSn* thin layers due to its ability to produce high-quality and economic crystalline films which cannot be achieved by other techniques such as MBE.

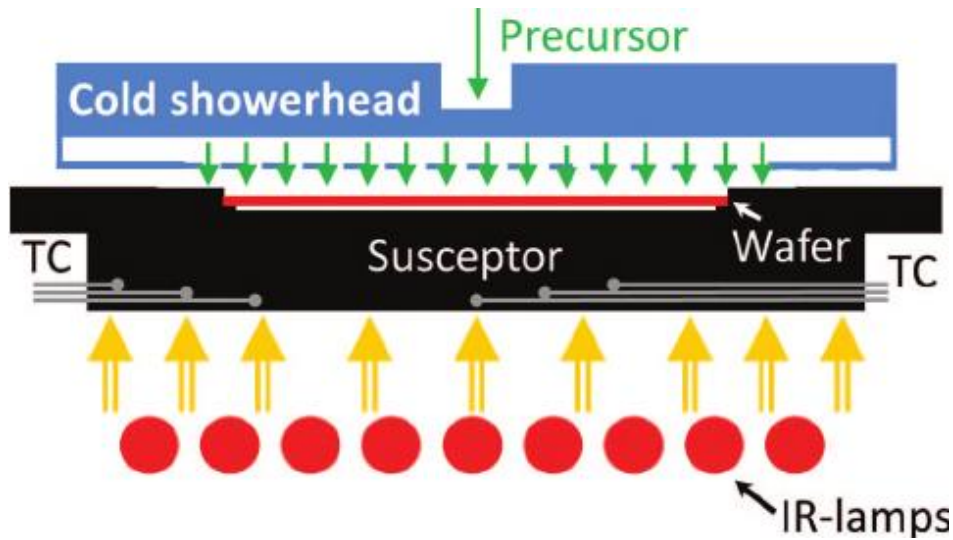


Fig. 5 Schematic of the reaction chamber of the CVD machine as shown in [17]

One of the challenges in growing $GeSn$ and $SiGeSn$ thin films is the large lattice mismatch between Ge , Sn and Si atoms, which can result in defects and dislocations in the film which has been improved over the years by a Ge buffer layer and a post-deposition annealing (PDA) process. For the deposition of $GeSn$ and $SiGeSn$ alloys low temperatures (250 - 300 °C) are required for a growing rate governed by surface reactions. This is called the kinetic growth regime. In this regime, the growth rate and thickness uniformity depend on the temperature.



Fig. 6 $GeSn$ thin film grown over a Ge buffer on a Si substrate

For this work, an industry-standard AIXTRON Tricent Reduced Pressure Chemical Vapor Deposition (RP-CVD) reactor was used. A showerhead system delivers the precursor gases to the rotating wafer. To prevent the premature reaction of the precursor gases separated tubes are used. The wafer is heated by nine infrared lights as the susceptor carrier, mounted on a quartz support, continuously rotates to provide a homogeneous temperature distribution, and reduce heating variances. Six thermocouples measure the temperature during the growing process. The uniformity of temperature is of big importance to ensure the uniformity of the grown layer thickness.

RBS

The Rutherford Backscattering Spectrometry (RBS) is a characterization technique used to study the composition and structure of materials. In RBS, a beam of high-energy ions is directed at the sample, and the ions are scattered by the nuclei of atoms that compose the sample. The scattered ions are then detected and analyzed to determine the composition and depth distribution of the elements in the sample. It is especially useful to determine the composition of thin layers.

As the ions beam, 1.4MeV He^+ for our case, goes through the sample, elastic scattering occurs. The incident ions interact with the nuclei in the sample and are deflected in various directions the energy and direction of the scattered ions establishes a very accurate measurement of the thickness, composition, and crystalline structure of the sample.

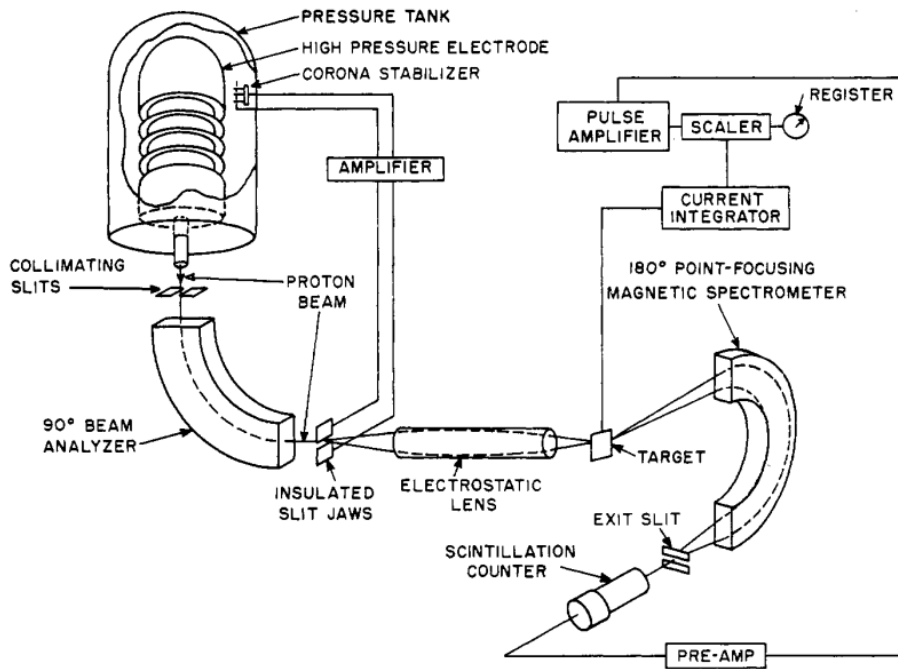


Fig. 7 Schematic drawing of RBS apparatus taken from [18]

The RBS technique was first described for chemical analysis in 1957 [18]. The schematic drawing of the process is shown in Fig. 7 for the detection of *O, Al, Si, S, Ca, Fe, Cu, Ag, Ba* and *Pb*. Nowadays the technique is used to determine the composition, thickness, and structure of many different elements. The nuclear properties of the elements are used to distinguish between them due to the interaction energies on the beam collision with the sample.

The theory is based on the elastic scattering method which considers the velocity V_s of a particle of mass M_1 and initial velocity V_0 which is elastically scattered at angle θ by a particle of mass M_0 initially at rest.

$$V_s = \frac{V_0}{M_0 + M_1} \left[M_1 \cos \theta + (M_0^2 - M_1^2 \sin^2 \theta)^{\frac{1}{2}} \right] \quad (7)$$

Or, in terms of the energy:

$$E_s = kE_0 \quad (8)$$

$$k = \frac{E_s}{E_0} = \left[\frac{M_1 \cos \theta + (M_0^2 - M_1^2 \sin^2 \theta)^{\frac{1}{2}}}{M_0 + M_1} \right]^2 \quad (9)$$

where k is the ratio of the particle energy after scattering to the energy before scattering.

The elements in the sample are identified by the change in the energy of the scattered particles. Narrow peaks are produced by very thin films and increase their width as the thickness also increases due to a loss of energy by ionization in the sample depending on the penetration depth as shown in Fig. 8

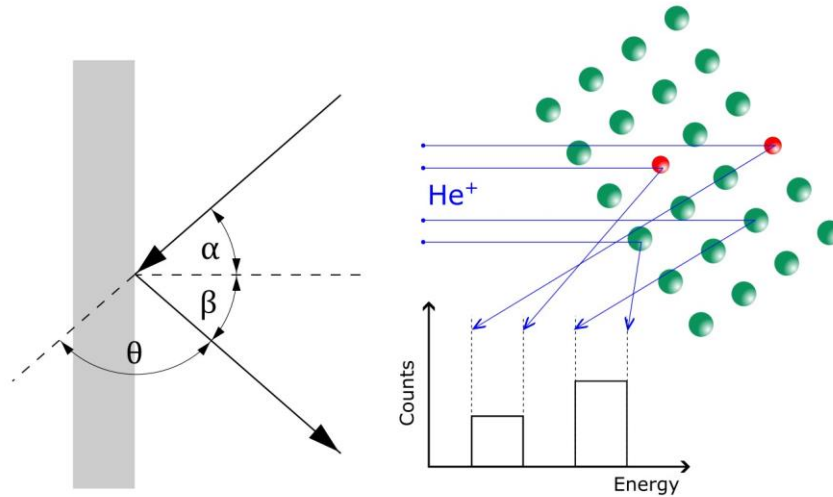


Fig. 8 Schematic of RBS technique

For elements of $Z > 30$ the Rutherford formula for scattering cross section is accurate enough and the sensitivity increases by increasing Z_1 and Z_0 or by decreasing E .

$$\frac{d\sigma}{d\Omega} \equiv \sigma(\theta) = \left(\frac{Z_1 Z_0 e^2}{4 E \sin^2 \left(\frac{\theta}{2} \right)} \right)^2 \quad (10)$$

For a target material with various elements a_i , the following formula gives the number of particles Y_i scattered from an element a_i counted in the momentum interval determined by the resolution factor R_s

$$Y_i = 1.2 \times 10^{13} \left(\frac{d\sigma}{d\Omega} \right)_i \frac{q\Omega E_1 n_i}{R_s} \left[\sum_i n_i \left(\epsilon_{i1} + \frac{\epsilon_{i2} \cos \theta_1}{k_i \cos \theta_2} \right) \right]^{-1} \quad (11)$$

where R_s is the spectrometer resolution factor, E_1 is the incident particle energy, q is the incident charge in μC , Ω is the spectrometer solid angle, ϵ is the atomic stopping cross section of each atomic species, subscript 1 before scattering and subscript 2 after scattering, θ the angles between the normal of the target and the incident and scattered beams, subscripts 1 and 2 respectively. The composition of the elements can be determined by application of these formulas [18] or by comparison with measurements on a reference sample of known concentrations.

RBS simulations using RUMP

RUMP is a Rutherford Backscattering Spectroscopy analysis package built on Genplot which provides comprehensive tools for simulating RBS spectra. Even though last update of the package was on august 2013 it provides accurate results on RBS analysis through customizable parameters and plotting capabilities.

To calibrate our simulations a sample reference with known composition, as described below, is measured along the samples of interest each time.

Reference sample:

1. 7 nm Sr 1.1% Ti 1% O 2.5%
2. 7 nm Gd 1.05% Sc 1% O 2.5%
3. 2000 nm Si 100%

Later, by adjusting the *conversion (conv)* factor, the *channel off (choff)* factor and the *correction (corr)* factor, the simulation curve is fitted to the experimental curve as shown in Fig. 9.

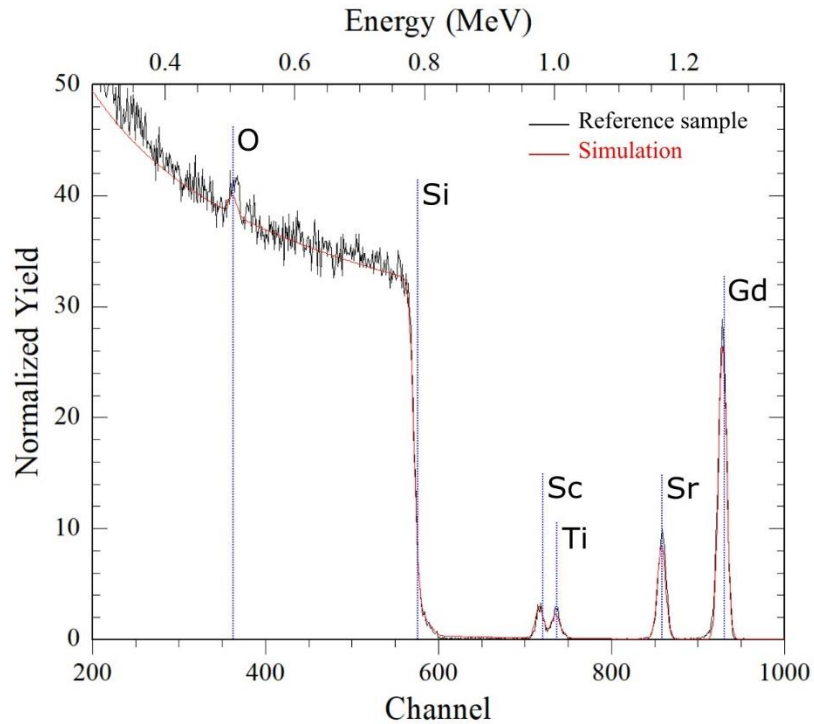


Fig. 9 RBS experimental over simulation curve for the reference sample

The following script leads to the simulation and plot of Fig. 9 results.

```

conv
1.334
21.201820

reg 200 1000
reg y 0 50
sim
la 1 th 7 nm co Sr 1.1 Ti 1 0
2.5 /
la 2 th 7 nm co Gd 1.05 Sc 1 0
2.5 /
la 3 th 2000 nm co Si 100 /
compa

choff 14 / compa
corr 1.65 / compa

```

Code 1 Script for simulating the reference sample

By using the previously determined *conv* factor, the samples can be simulated to obtain the composition of all its layers. The following is the result for a *SiGeSn* sample grown on a *Ge* buffer and a *Si* substrate.

```
Sim Reset
Layer 1
  Thick 210 nm
  Composition Si 8 Ge 84.5 Sn
  7.5 /
  Fuzzy 20.000000 20
Next
  Thick 265 nm
  Composition Ge 100 /
  Fuzzy 10.000000 20
Next
  Thick 999 nm
  Composition Si 100 /
  Maxpth 200
  Foil disable
```

Code 2 Example of composition results for a SiGeSn sample

Since the Sn concentration is of great interest for our concerns, this technique is fundamental in the study of thermoelectrics of thin films. To further confirm the results, other techniques may be used in combination as secondary ion mass spectrometry (SIMS) and X-Ray Diffraction (XRD), to provide a complete notion of the composition and structure of the material. However, for this work, every sample was measured only using RBS and XRD.

XRD

X-ray diffraction (XRD) is a non-destructive analytical technique used to determine the crystallographic structure, chemical composition, and lattice parameters of materials. By analyzing the intensity and position of the diffraction peaks, it is possible to determine the crystal structure and composition of the material.

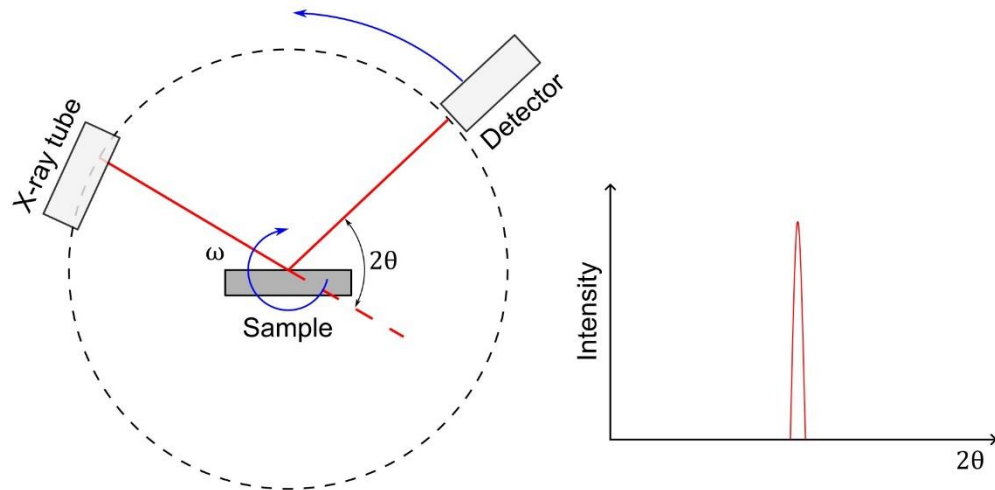


Fig. 10 Schematic drawing of the XRD technique

The detector moves in a circle around the sample which position is determined as the 2θ angle and records the number of X-rays observed at each position as counts or counts per second. Each diffraction pattern is a fingerprint of the measured material which also depends on the crystalline phase.

As well as the RBS analysis, the experimental XRD data can be compared to a reference pattern to determine the composition of the sample. An example of the expected curves for *GeSn/Ge/Si* samples are shown in Fig. 11.

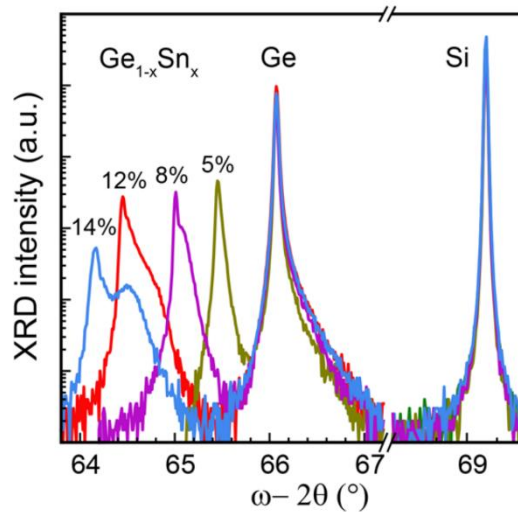


Fig. 11 XRD ω - 2θ rocking curves for *GeSn/Ge/Si* samples as shown in [19]

The 3ω Method

The method was developed to measure the thermal conductivity of thin films with high accuracy. It was described for the first time in 1987 by Cahill and Pohl [20] as a modification of the standard steady-state heat flow method. The original steady-state method involved measuring the temperature difference across a sample that is in contact with two heat reservoirs held at different temperatures. The thermal conductivity of the sample is then determined by applying Fourier's law of heat conduction, which relates the heat flow to the temperature gradient. It consists of applying a small AC current with frequency ω through a metallic heater stripe that is in thermal contact with the sample, then the AC current generates a temperature oscillation with frequency 2ω . The temperature oscillation propagates through the sample and is detected by a thermocouple or other temperature sensor in terms of a signal with frequency 3ω . It is also common to use the same metallic stripe as both, the heater, and the sensor. Fig. 12 shows the device Cahill and Pohl used to apply the method for bulk materials. In which it is assumed that the heat will be distributed equally below the heater stripe and below the contact pads.

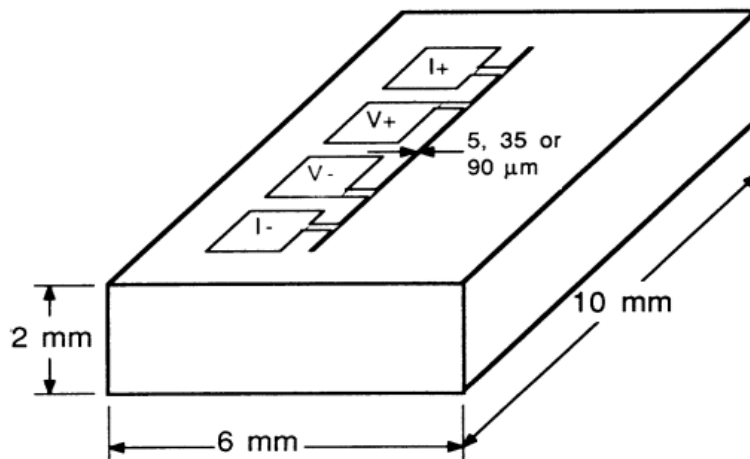


Fig. 12 Schematic drawing of the device for the 3ω method as presented by Cahill and Pohl in [20]

In this work, the thermal conductivity and the Seebeck coefficient are both extracted by applying the 3ω method.

Experimental part

In more detail, an AC current

$$I(t) = I_{1\omega} \cos(\omega t) \quad (12)$$

where ω is the angular frequency, is applied through the heater stripe which has a resistance R . The voltage drop on the resistance is expressed by:

$$V(t) = R I_{1\omega} \cos(\omega t) \quad (13)$$

Later, by Joule Effect, the power dissipation contains a 2ω component as:

$$P(t) = RI(t)^2 \quad (14)$$

$$P(t) = \frac{1}{2} R I_{1\omega}^2 [1 + \cos(2\omega t)] \quad (15)$$

recalling the squared of a cosine identity: $\cos^2(A) = \frac{1}{2}[1 + \cos(2A)]$.

The power input will generate a heating $\delta T(t)$ which also contains a 2ω oscillatory component. However, this heating oscillations will not, in general, reach the zero value as happens with the applied power specially when the oscillations are too fast compared to the thermal response time of the system. Due to the delay between the input power and the heating it is expected to find a dephase ϕ , so:

$$\delta T(t) = \delta T_0 + \delta T_{2\omega} \cos(2\omega t + \phi) \quad (16)$$

The variation in temperature will cause, back in the heater stripe, a change in resistance according to:

$$\frac{\delta R}{R} = \alpha \delta T \quad (17)$$

where α is the stripe's temperature coefficient of resistance (TCR) which will modify the voltage drop as:

$$V(t) = (R + \delta R(t)) I_{1\omega} \cos(\omega t) \quad (18)$$

$$V(t) = (1 + \alpha \delta T(t)) V_{1\omega} \cos(\omega t) \quad (19)$$

substituting Eq. 16 in Eq. 19 the voltage drop can be expressed as:

$$V(t) = (1 + \alpha(\delta T_0 + \delta T_{2\omega} \cos(2\omega + \phi))) V_{1\omega} \cos(\omega t) \quad (20)$$

$$V(t) = V_{1\omega} (\cos(\omega t) + \alpha \delta T_0 \cos(\omega t)) + V_{1\omega} \alpha \delta T_{2\omega} \cos(2\omega + \phi) \cos(\omega t) \quad (21)$$

By neglecting the average heating (due to the typically small value α), it follows that:

$$V(t) = V_{1\omega} \cos(\omega t) + \frac{1}{2} V_{1\omega} \alpha \delta T_{2\omega} [\cos(3\omega + \phi) + \cos(\omega t + \phi)] \quad (22)$$

recalling the sum of cosines identity: $\cos(A) + \cos(B) = 2 \cos\left(\frac{A+B}{2}\right) \cos\left(\frac{A-B}{2}\right)$.

$$V(t) = V_{1\omega} \cos(\omega t) + \frac{1}{2} V_{1\omega} \alpha \delta T_{2\omega} \cos(3\omega + \phi) + \frac{1}{2} V_{1\omega} \alpha \delta T_{2\omega} \cos(\omega t + \phi) \quad (23)$$

thus, the 3ω component (blue) is useful to experimentally determine the $\delta T_{2\omega}$ (note that an additional 1ω component was neglected again due to the small value α):

$$V_{3\omega} = \frac{1}{2} V_{1\omega} \alpha \delta T_{2\omega} \quad (24)$$

$$\delta T_{2\omega} = \frac{2 V_{3\omega}}{\alpha V_{1\omega}} \quad (25)$$

Theoretical part

By considering the stripe as a one-dimensional line heater on a semi-infinite sample, the propagation of heat can be modelled radially symmetric. Fourier's law describes the conduction of heat and states that the heat flux is proportional to the negative gradient of temperature:

$$\vec{J}_Q = -\kappa \nabla T$$

where \vec{J}_Q is the heat flux, ∇T is the temperature gradient and κ is the thermal conductivity. Later, considering that that no work is done on or by the sample, the conservation of energy finally leads to the heat diffusion equation:

$$\frac{\partial T}{\partial t} = D \nabla^2 T \quad (26)$$

where $D = \frac{\kappa}{\rho c}$ (ρ is the density of mass, c is the specific heat of the material and κ the thermal conductivity) is the thermal diffusivity. Recalling the geometry to analyze is a cylinder, the general heat diffusion equation in cylindrical coordinates is:

$$\frac{\partial T(r, t)}{\partial r^2} + \frac{1}{r} \frac{\partial T(r, t)}{\partial r} = \frac{1}{D} \frac{\partial T(r, t)}{\partial t} \quad (27)$$

The solution of this equation involves a zeroth order modified Bessel function of second kind as:

$$T(r, t) = \frac{P}{2\pi l \kappa} K_0(qr) e^{i2\omega t} \quad (28)$$

where P is the applied power, l the stripe length and q the wavenumber of the diffusive thermal wave defined as:

$$q = \sqrt{\frac{i2\omega}{D}} \quad (29)$$

Since we are not interested on the whole cylinder but only in the lower half, reducing the volume means a heat flux increase in the same proportion assuming there is no heat dispersion on the surface. Therefore, the final expression is:

$$T(r, t) = \frac{P}{\pi l \kappa} K_0(qr) e^{i2\omega t} \quad (30)$$

The approximation which leads to the final solution is only reasonable if the sample thickness is much greater than the thermal wavelength (λ).

$$\lambda = \frac{1}{|q|} = \sqrt{\frac{D}{2\omega}} \quad (31)$$

It is possible to consider the sample as semi-infinite if its thickness exceeds 5λ to ensure that the temperature oscillation is contained in the sample.

Finally, to achieve a better description of the experiment, the finite width heater stripe can be considered as an infinite number of 1D line heaters over its width ($2b$). By taking the convolution of the heating expression and a rectangular function which represents the heat going through the sample evenly over its width from $-b$ to b the approximate solution for the temperature increase, as suggested by Cahill (assuming the thermal penetration depth is large compared to the heater width) is:

$$T \approx \frac{P}{\pi l \kappa_s} \left[\ln 2 - i \frac{\pi}{4} - \frac{1}{2} \ln \left(\frac{2\omega b^2}{D_s} \right) \right] \quad (32)$$

A detailed description of the mathematical process to get to this expression can be found in [21].

A more accurate approximation was provided by Duquesne et al. [22] which is valid in the low frequency limit as $\omega \rightarrow 0$

$$T \approx \frac{P}{\pi l \kappa_s} \left[\frac{3}{2} - \gamma - i \frac{\pi}{4} - \frac{1}{2} \ln \left(\frac{2\omega b^2}{D_s} \right) \right] \quad (33)$$

where γ is the Euler-Mascheroni constant.

Thermal conductivity

The theoretical expression for the change in temperature and the experimental expression provides the possibility of extracting the thermal conductivity of the sample by using the *Slope method*. Before going on detail with the method, equating both temperature change equations allow to express the $V_{1\omega}$ in terms of the $V_{3\omega}$.

$$\delta T_{2\omega} = T \quad (34)$$

$$\frac{2 V_{3\omega}}{\alpha V_{1\omega}} = \frac{P_{2\omega}}{\pi l \kappa_s} \left[\frac{3}{2} - \gamma - i \frac{\pi}{4} - \frac{1}{2} \ln \left(\frac{2\omega b^2}{D_s} \right) \right] \quad (35)$$

and by expressing $P_{2\omega}$ in terms of $V_{1\omega}$ ($P_{2\omega} = \frac{V_{1\omega}^2}{R_0}$), the following expression arises:

$$V_{3\omega} = \frac{\alpha}{2\pi l \kappa_s R_0} V_{1\omega}^3 \left[\frac{3}{2} - \gamma - i \frac{\pi}{4} - \frac{1}{2} \ln \left(\frac{2b^2}{D_s} \right) - \frac{1}{2} \ln(\omega) \right] \quad (36)$$

The *Slope method* provides a way for extracting the thermal conductivity taking advantage of the linear dependency of the $V_{3\omega}$ with the logarithm of the frequency ω . To have a better understanding of the method the last expression can be rearranged as:

$$V_{3\omega} = -\frac{\alpha}{4\pi l \kappa_s R_0} V_{1\omega}^3 \ln(\omega) + \frac{\alpha}{2\pi l \kappa_s R_0} V_{1\omega}^3 \left[\frac{3}{2} - \gamma - \frac{1}{2} \ln \left(\frac{2b^2}{D_s} \right) \right] - i \frac{\alpha}{8l \kappa_s R_0} V_{1\omega}^3 \quad (37)$$

The linear behavior of the last expression for ω is now evident ($y = Ax + B$) plus an imaginary term which describes the dephase of the $V_{3\omega}$. Fitting the curve of the real part of the $V_{3\omega}$ against the $\ln(\omega)$ directly leads to extract the κ_s as all the other values are known. Even though the thermal conductivity could also be extracted from the out-of-phase term ($Im\{V_{3\omega}\}$), it is not usually performed that way because the signal is much smaller compared to the in-phase term ($Re\{V_{3\omega}\}$).

Finally, the thermal conductivity is calculated as:

$$\kappa_s = \frac{\alpha}{4\pi l R_0} \frac{V_{1\omega}^3}{A} \quad (38)$$

Where A is the value of the slope from the fitting. It is very important to note that this expression also provides a way of validating the method to ensure that the measured data makes sense.

Three points should be verified to ensure the validity of the 3ω method:

1. Linear dependency between $Re\{V_{3\omega}\}$ and $\ln(\omega)$ at constant voltage.
2. Constant dependency between $Im\{V_{3\omega}\}$ and $\ln(\omega)$ at constant voltage.
3. Cubic dependency between $V_{3\omega}$ and $V_{1\omega}$ at constant frequency.

For our purposes, however, the *Slope method* is not enough to analyze multilayered samples. Cahill et al. showed in the past [23] that the effect of thin films on a substrate can be simply considered as additional frequency independent terms. The previous applies in the case that the n-film thickness τ_n is much smaller than the width of the heater (2b) so that the edge effects during the heat flow can be neglected. The additional $\delta T_{2\omega}$ due to n-films can be expressed as:

$$\delta T_{2\omega_{films}} = \frac{P_{2\omega}}{l} \sum \frac{\tau_n}{2b\kappa_n} \quad (39)$$

The last expression leads to the so-called *Differential method* in which the thermal conductivity of a specific layer can be extracted by subtracting the $\delta T_{2\omega}$ from two samples, one without the layer of interest.

$$\delta T_{2\omega} = \delta T_{2\omega_{substrate}} + \sum \delta T_{2\omega_{n-film}} \quad (40)$$

$$\delta T_{2\omega_{film}} = \delta T_{2\omega_{substrate+film}} - \delta T_{2\omega_{substrate}} \quad (41)$$

The expression for $\delta T_{2\omega}$, considering the effect of thin films is:

$$\delta T_{2\omega} = \frac{P_{2\omega}}{l} \left\{ \frac{1}{\pi\kappa_s} \left[\frac{3}{2} - \gamma - i \frac{\pi}{4} - \frac{1}{2} \ln \left(\frac{2\omega b^2}{D} \right) \right] + \sum \frac{\tau_n}{2b\kappa_n} \right\} \quad (42)$$

The expression was rearranged to facilitate the understanding the *Differential method*. For our concerns, the measured samples have at least 3 layers: *Si substrate*, *Ge buffer*, and *GeSn* for example. By applying the 3ω method to a *Si/Ge* and a *Si/Ge/GeSn* samples is possible to isolate the thermal conductivity value of the *GeSn* layer from the equations, as:

$$\delta T_{2\omega_{Si/Ge/GeSn}} = \frac{P_{2\omega}}{l} \left\{ \frac{1}{\pi\kappa_{Si}} \left[\frac{3}{2} - \gamma - i \frac{\pi}{4} - \frac{1}{2} \ln \left(\frac{2\omega b^2}{D} \right) \right] + \frac{\tau_{Ge}}{2b\kappa_{Ge}} + \frac{\tau_{GeSn}}{2b\kappa_{GeSn}} \right\} \quad (43)$$

$$\delta T_{2\omega_{Si/Ge}} = \frac{P_{2\omega}}{l} \left\{ \frac{1}{\pi\kappa_{Si}} \left[\frac{3}{2} - \gamma - i \frac{\pi}{4} - \frac{1}{2} \ln \left(\frac{2\omega b^2}{D} \right) \right] + \frac{\tau_{Ge}}{2b\kappa_{Ge}} \right\} \quad (44)$$

$$\delta T_{2\omega_{Si/Ge/GeSn}} - \delta T_{2\omega_{Si/Ge}} = \frac{P_{2\omega}}{l} \frac{\tau_{GeSn}}{2b\kappa_{GeSn}} \quad (45)$$

Finally, the thermal conductivity of the $GeSn$ layer can be calculated as:

$$\kappa_{GeSn} = \frac{P_{2\omega}}{l} \frac{\tau_{GeSn}}{2b} \left[\left(\frac{2V_{3\omega}}{\alpha V_{1\omega}} \right)_{Si/Ge/GeSn} - \left(\frac{2V_{3\omega}}{\alpha V_{1\omega}} \right)_{Si/Ge} \right]^{-1} \quad (46)$$

A small variation of the method using a 2D micro-heater instead of the 1D stripe is described in [24], the *Differential method* is carried out by using two samples which increases the systemic errors due to small differences in the growth of both samples. Fig. 13 shows an alternative by fabricating two devices on the same sample. The etching of the thin film of interest everywhere on the sample except on a small mesa is required. The new expression for the thermal conductivity of the thin film of interest is:

$$\kappa_{film} = \frac{P_{2\omega}}{A} \tau_{film} \left[\left(\frac{2V_{3\omega}}{\alpha V_{1\omega}} \right)_{substrate+film} - \left(\frac{2V_{3\omega}}{\alpha V_{1\omega}} \right)_{substrate} \right]^{-1} \quad (47)$$

where A is the cross-sectional area of the thin film mesa.

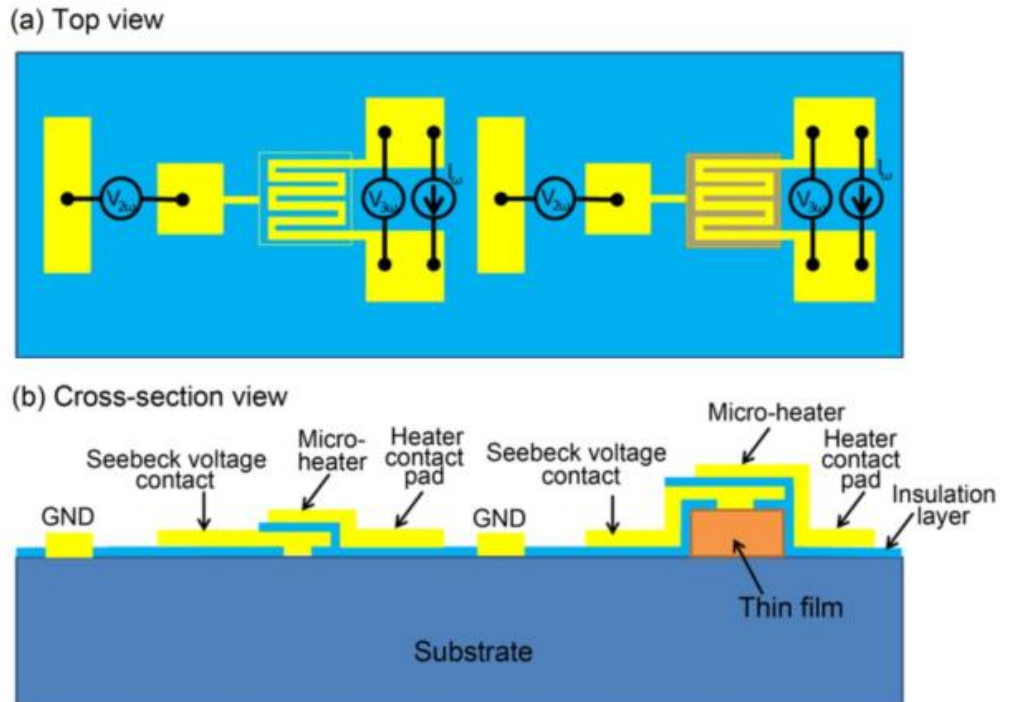


Fig. 13 Device for Seebeck coefficient and Thermal conductivity differential measurements, as shown in [24]

To measure this new device the $V_{1\omega}$ and the $V_{3\omega}$ are applied and measured, respectively, in the same contact pads, these contact pads are electrically isolated from the thin film mesa and the substrate, respectively for each device.

Seebeck coefficient

The Seebeck coefficient can be extracted from the improved device described in the previous section. By using the Seebeck voltage contact pad which is in direct contact with the material of interest it is possible to measure the generated voltage due to the heating of the material. Recalling the temperature change has a 2ω component, the generated voltage by Seebeck effect will also oscillate at frequency 2ω . Applying the *Differential method* to the Seebeck expression, follows that:

$$V_{2\omega_{film}} = V_{2\omega_{substrate+film}} - V_{2\omega_{substrate}} \quad (48)$$

Finally, the Seebeck coefficient is calculated as:

$$S_{film} = -\frac{V_{2\omega_{substrate+film}} - V_{2\omega_{substrate}}}{\delta T_{2\omega_{substrate+film}} - \delta T_{2\omega_{substrate}}} \quad (49)$$

$$S_{film} = -\frac{V_{2\omega_{substrate+film}} - V_{2\omega_{substrate}}}{\left(\frac{2}{\alpha} \frac{V_{3\omega}}{V_{1\omega}}\right)_{substrate+film} - \left(\frac{2}{\alpha} \frac{V_{3\omega}}{V_{1\omega}}\right)_{substrate}} \quad (50)$$

Temperature Coefficient of Resistance (TCR)

A fundamental parameter to apply the 3ω method is the TCR (α) which can be obtained by measuring the resistance of the material, Au/Cr in this case, at different temperatures. As a first order approximation, a linear fit of the curve is enough to determine the α value. A more accurate value can be obtained by repeating the process for different samples.

As the TCR is a property of the heater's material itself, it should be expected to get the same value regardless of the geometry or the amount of material being measured. In our case, the K-device provides a simple way for measuring this parameter by performing a resistance measurement of the heater stripe at different temperatures.

Recalling the variation of resistance as dependent on temperature:

$$\frac{\delta R}{R} = \alpha \delta T \quad (51)$$

The solution of this differential equation is:

$$R(T) = R_0 e^{\alpha \Delta T} \quad (52)$$

Which can be approximated by taking the first terms of its expansion. This approximation is valid if the temperature coefficient of resistance itself does not vary too much with the temperature and if $\alpha \Delta T \ll 1$. From the approximation it follows that

$$R(T) = R_0(1 + \alpha \Delta T) \quad (53)$$

Rearranging the terms, the parameters for the linear fit can be determined.

$$R(T) = R_0 \alpha T + R_0 - R_0 \alpha T_0 \quad (54)$$

$$R(T) = m T + n \quad (55)$$

where T_0 is the reference temperature. Finally, from these parameters the α value is calculated as

$$\alpha = \frac{m}{n + mT_0} \quad (56)$$

Electrical conductivity

The cross section electrical conductivity of the GeSn samples can be measured by the device proposed in Fig. 14. A mesa of the layer of interest is etched to establish the dimensions of the current path. A contact pad is deposited on top of the mesa and extends on both sides down the mesa. Separating the current and voltage pads the parasitic resistance from the current electrode can be excluded from the measurement.

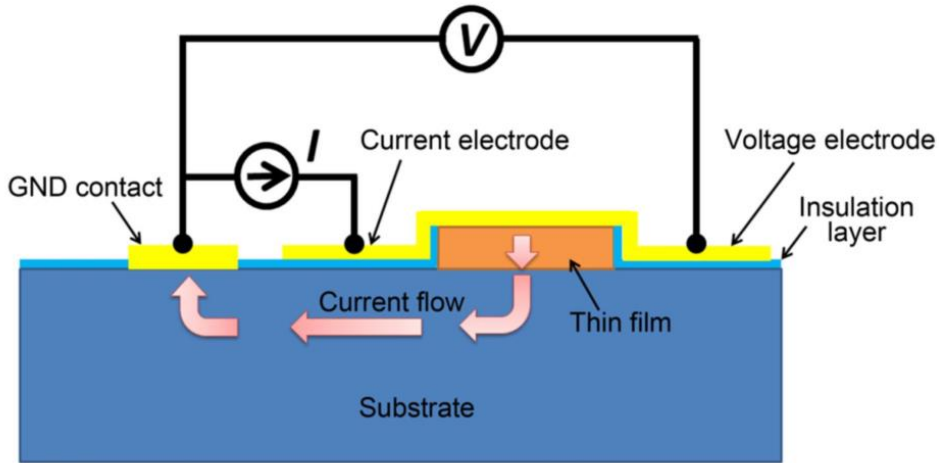


Fig. 14 Schematic of the cross-section view of a thin film electrical conductivity measuring device as shown in [24]

The measured resistance is in terms of the substrate resistance, the thin film resistance, and both contact pads [24].

$$R_{total} = \frac{r_{c, film}}{A} + \frac{l}{\sigma_{cross} A} + R_{sub} + \frac{r_{c, sub}}{A_{GND}} \quad (57)$$

where $r_{c, film}$ is the contact resistivity at the metal-film interface, A is the cross-sectional area of the mesa, σ_{cross} is the cross-plane electrical conductivity of the thin film, l is the thickness of the mesa, R_{sub} is the substrate resistance, $r_{c, sub}$ is the contact resistivity at the ground metal-substrate interface, and A_{GND} is the area of the ground contact. The last term of this equation becomes negligibly small as the ground contact area increases and the resistance of the substrate is typically much smaller than the mesa resistance due to its large thickness compared to that of the mesa. Both terms can be neglected by taking the previous considerations. To get a more accurate value a differential method can be performed. Two samples, one with an etched mesa and one only with the substrate can be measured and subtracted to get only the thin film resistance. If the deposition process for the contact pads is the same for both samples, the parasitic resistances should be the same.

$$\sigma_{cross} = \frac{l}{A} \frac{1}{(R_{total, film} - R_{total, sub})} \quad (58)$$

Chapter 3. Experimental process

Growth and characterization

The growth of $GeSn$ alloys was carried out in the CVD reactor using germane GeH_4 or digermane Ge_2H_6 and tin-tetrachloride $SnCl_4$ as precursor gases and N_2 as a carrier gas. The Sn concentration depends on the growth temperature (T), the reactor pressure (P), the total gas flow (Q_T) and the partial pressure ratio between the precursor gases. As described in [25], the reference conditions of growth are $p_{GeH_4}/p_{SnCl_4} = 1100$, $P = 60$ mbar, $Q_T = 9000$ sccm and $T = 300^\circ C$ which are represented by the black point in Fig. 15. Either by decreasing the temperature, decreasing the total gas flow, or increasing the reactor pressure leads to an increase in the Sn concentration.

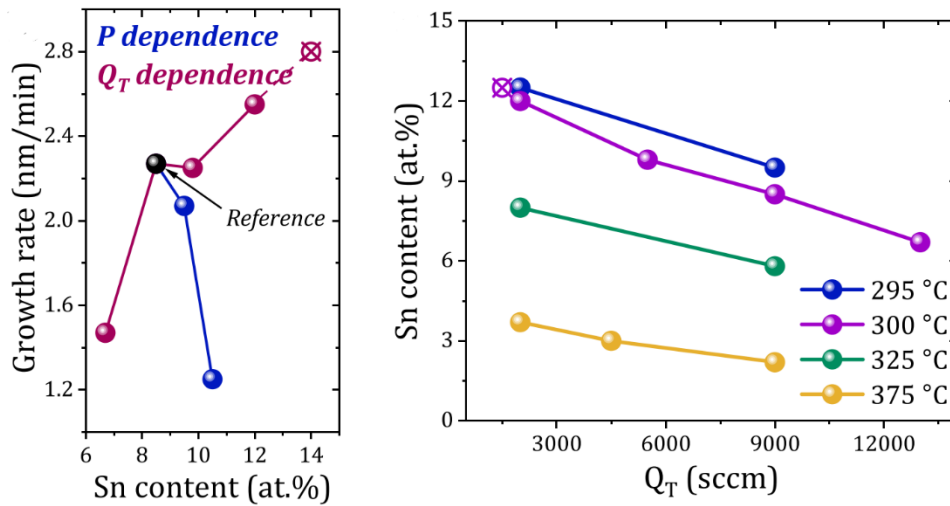


Fig. 15 (left) Grow rate as a function of Sn content for different reactor pressure (P) and total gas flow (Q_T) values. (right) Sn content as a function of the total gas flow (Q_T) at different temperatures as shown in [25].

In the case of monolayered structures, an isothermal growth by changing only the total gas flow is the best option due to its wide range of concentrations it offers considering the large variation in the grow rate in depending on the temperature. In the other hand, the growth of multilayered structures represents a new challenge since temperature can only decrease from layer to layer, but this is beyond the scope of this work.

GeSn thicknesses set

To compare the effect of the *GeSn* thickness on the thermal conductivity value, five samples with similar *Ge* buffer thickness of $\sim 310\text{nm}$ and *Sn* concentration of $\sim 12\%$ were chosen. An additional sample with a very thin *GeSn* layer (40nm) was added to the set to check the increase of the phonon scattering near the interface but the *Ge* buffer layer is much smaller than the other samples so a different *GePDA* sample (225nm) was used for the differential calculations. Finally, a sample with a very thick *GeSn* layer (705nm) grown on a high quality *Ge* substrate was added.

Sample	d_{GePDA} (nm)	d_{GeSn} (nm)	Sn %
GeSn_1	170	40	11.5
GeSn_2	265	109	12.5
GeSn_3	295	280	11.8
GeSn_4	315	310	12
GeSn_5	325	325	12
GeSn_6	310	385	12.3
GeSn_7	1500 (<i>GeVS</i>)	705	12.5
GePDA_2	265	--	--
GePDA_1	225	--	--
GeVS_1	1500 (<i>GeVS</i>)	--	--

Table 1 Set of samples to compare the thermal conductivity for different *GeSn* thicknesses

Sn concentration set

Theory states that the thermal conductivity rapidly decreases as the *Sn* concentration increases. A set of samples with concentrations from 0% to 11% were chosen with similar *GeSn* ($\sim 200\text{nm}$) and *Ge* ($\sim 400\text{nm}$) thicknesses to compare the theoretical results to the experimental ones.

Sample	d_{GePDA} (nm)	d_{GeSn} (nm)	Sn %
Sn_1	435	165	5
Sn_2	388	145	6
Sn_3	380	180	9
Sn_4	380	200	10
Sn_5	390	235	11
GePDA_3	410	--	0

Table 2 Set of samples to compare the effect of *Sn* concentration in the thermal conductivity

RBS

After fitting the curves using the RUMP software, the results for the RBS spectrum shows the Sn concentration for each sample. In Fig. 16 the RBS of all samples in the $GeSn$ -thickness set are compared to show the increase in the width of the Sn peak as the thickness of the layer increases. In counterpart, the height of the Sn peak remains the same for all samples which indicates that the Sn concentration for all samples is very similar.

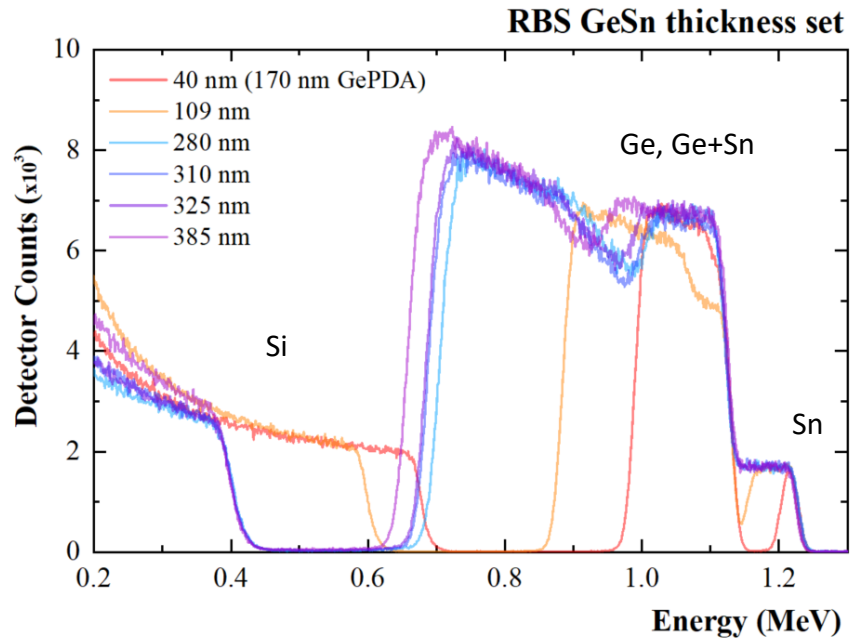


Fig. 16 RBS spectrum from $GeSn$ -thickness set samples

For the Sn concentration set of samples, all the Ge and Sn peaks should have similar widths while the height of the Sn peak should increase according to the Sn concentration.

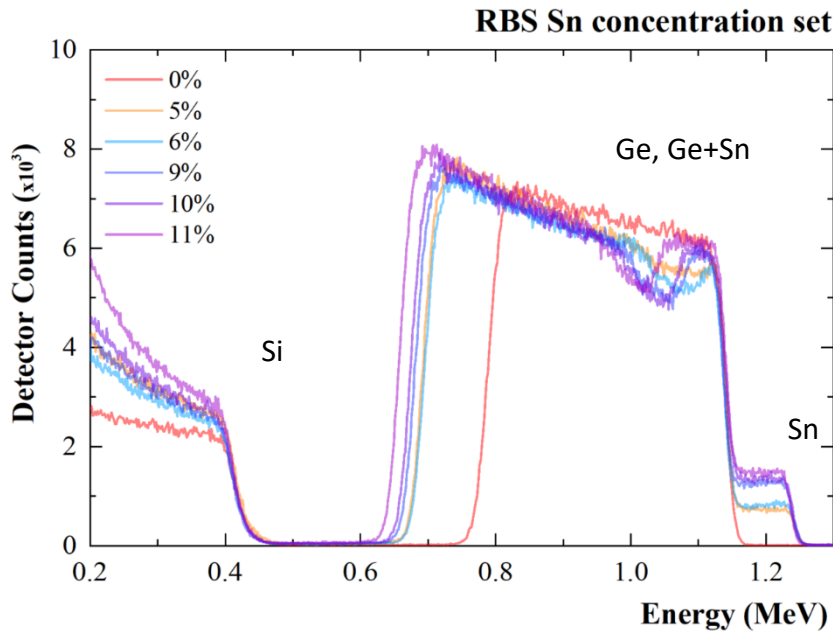


Fig. 17 RBS spectrum from Sn-concentration set samples

XRD

The XRD results for the *GeSn* thickness set, in Fig. 18, show the *Sn* concentration of all samples above 280 nm has a similar maximum value position for the *GeSn* peak, while for the *Ge* and *Si* peaks the difference is very small except for the 40 nm sample which has a small variation in the *Ge* signal because the *GePDA* layer is different from the rest. The difference of the 40nm and 109nm samples in the *GeSn* could be related to a different strain in the lattice. For the rest of the samples this is not the case, and it is visible in the two-peak shape of the signals which means the *GeSn* layer reached a critical thickness of relaxation after which the *Sn* changes and stay stable.

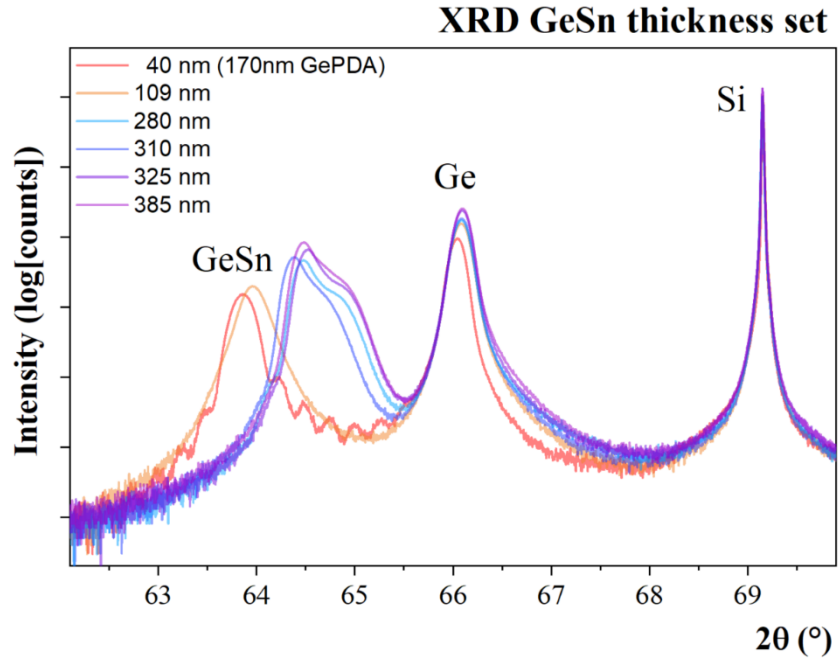


Fig. 18 XRD curves from GeSn-thickness set samples

The same behavior is shown in the 6% sample of the *Sn* concentration set of samples in Fig. 19, a single peak indicates the sample did not reach the critical thickness, in this set of samples the *Ge* buffers and the *Si* substrates of each sample show a very similar signal. For the *GeSn* peaks it is clear how the signal is left-shifted as the *Sn* concentration increases.

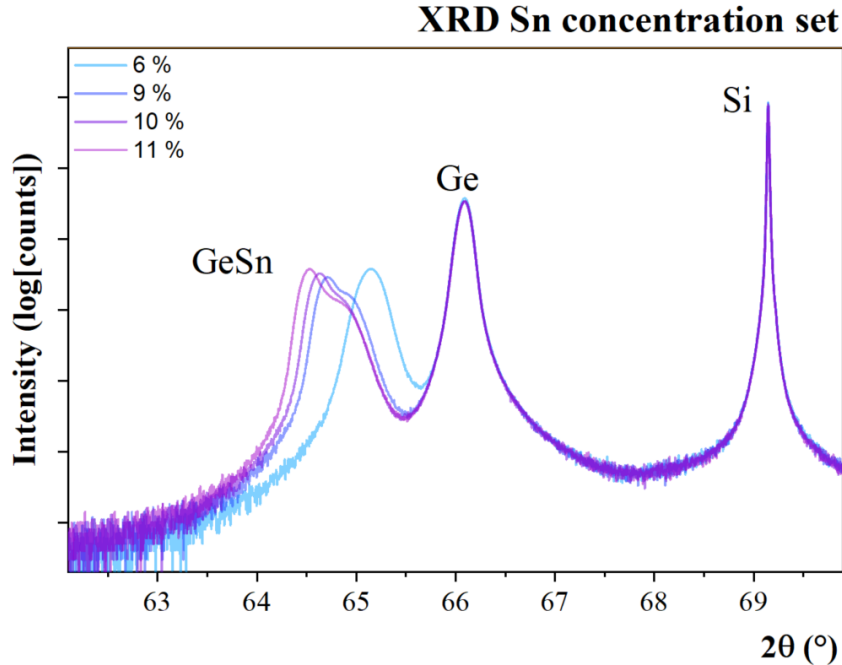


Fig. 19 XRD curves from Sn-concentration set samples

Set-up build up and calibration

A Printed Circuit Board (PCB) was previously designed and fabricated as described in [26] to make easier the connection between the sample and the Lock-in Amplifier. The 3ω method was applied with a Lock-in Amplifier (Zurich Instruments MFLI).

A chip carrier holds the sample with the fabricated devices and works as the connection interface between the PCB and the device. The chip has a square geometry with beveled borders, one of them smaller than the others. The convention used to glue a K device sample to the chip carrier is to make the smallest corner point down left. After that, the sample is glued with silver conductive glue with the short heater devices on the left side and the large ones on the right side. This glue was chosen because its working range of temperature is wide enough to carry out low and high temperature measurements. Each side of the chip has 7 contact pads making a total of 28.

The electrical bonding of the sample to the chip carrier was made on a F&S Bondtec Automatic Wire Bonder machine using *Al* wires. The connections map for the K device is shown in Fig. 20 and a picture of an actual chip carrier is shown in Fig. 21

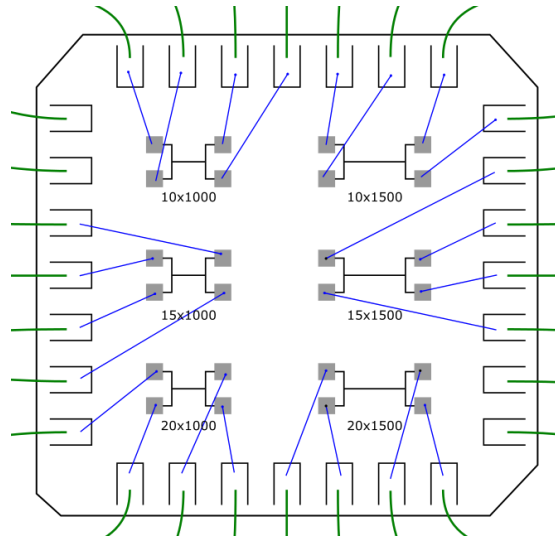


Fig. 20 Bonding map for the K device within the chip carrier

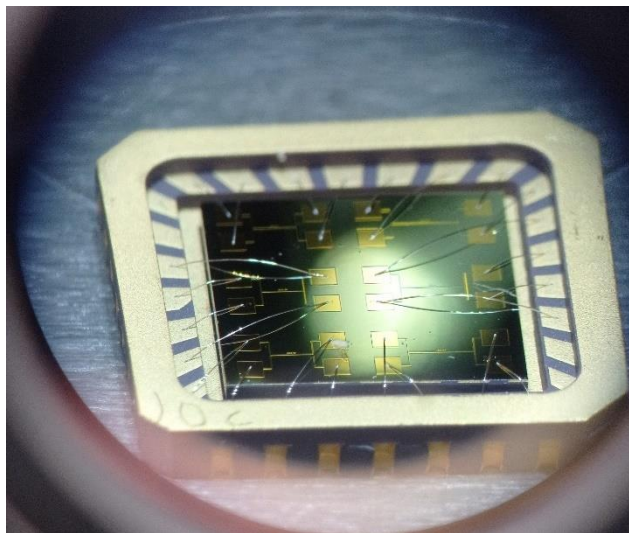


Fig. 21 K device sample glued and bonded to the chip carrier

Three types of measurements are useful for the 3ω method:

1. Voltage scan
2. Frequency scan
3. Resistance measurement

The first one is not required to extract the thermal conductivity of the samples but to validate the method. The voltage is applied through the differential output of the lock-in to a pair of contact pads to make the current flow through the heater. Through the differential

input the first and third harmonic are measured on the other pair of contact pads (For the K-S device the input and output connections share a single pair of contact pads). The applied voltage is increased throughout the experiment and the measured harmonics are plotted against it separating the in-phase component and the out-of-phase component of the signal.

For the frequency scan measurement, the connections are the same as for the voltage scan measurement. The difference is that now the frequency is increased as the applied voltage remains constant. The plot from this measurement should show a linear behavior for the in-phase component if the frequency axis has a logarithmic scale and a constant behavior for the out-of-phase component.

The resistance measurement requires only 2 cables to apply a voltage over the heater (for the K and K-S devices) and measure the current. By fitting the curve, the resistance value can be extracted. For the σ device, this is the only useful measurement, the goal is to extract the electric conductivity of the thin layer which is possible by performing a resistance measurement as

The connections diagram showed in Fig. 22 describes with a color code the position of each cable to perform either a frequency scan measurement or a resistance measurement on the K design. Even though, the measurement works as long as each pair of contact pads is plugged to the right input or output terminals, respectively, the convention showed in the picture is straightforward enough to speed up the measurement process. For the K-S device and the σ device a connections map has not yet been created because those devices are still under development and test. Despite the previous, the same PCB is useful for the three devices.

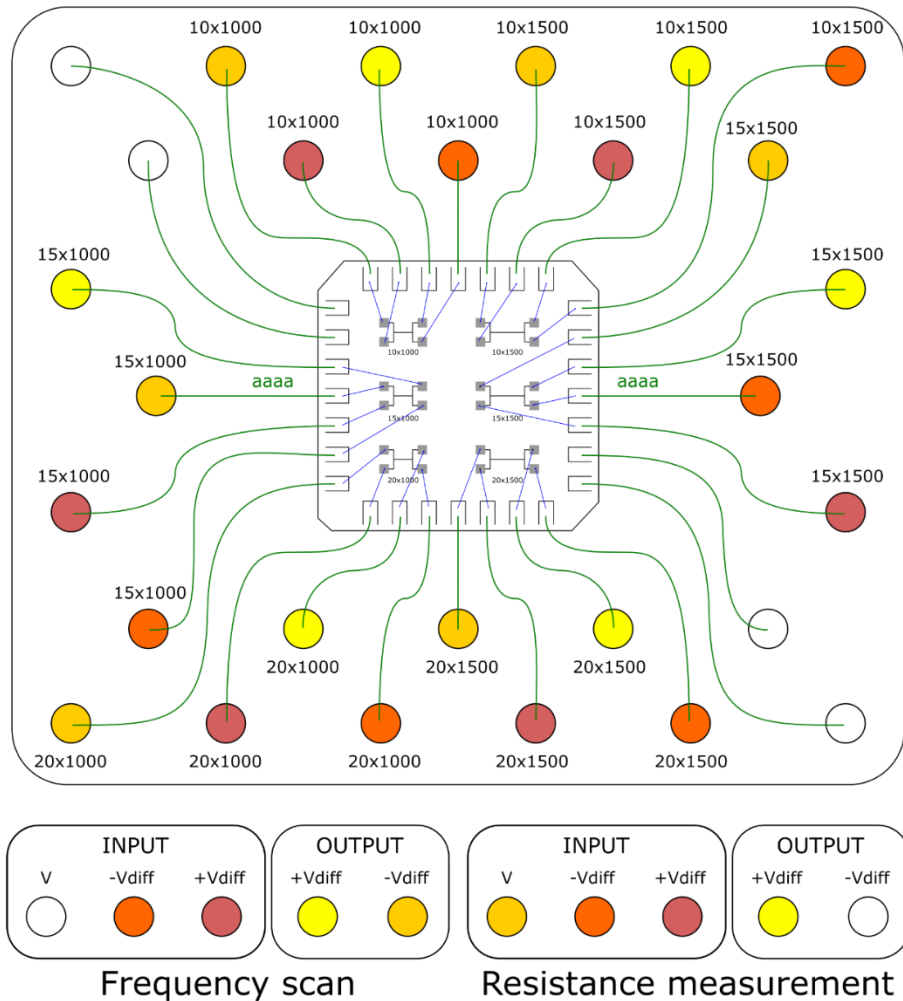


Fig. 22 Connections diagram between the chip carrier, the PCB and the Lock-in amplifier for the Frequency scan measurement and the Resistance measurement for the K device

Python script

A python script to automatically set the Lock-in Amplifier parameters was developed. The Zhinst library¹ is present in many different languages from which Python was chosen because it is a simple and open-source tool very well known around the scientific community.

The code has a partial Graphical User Interface (GUI) implementation to show the file prompts and to display the plots during the measurement. The Tkinter library² provides a

¹ Provided by Zurich Instruments https://docs.zhinst.com/labone_programming_manual/python.html

² Included into the Python standard library <https://docs.python.org/3/library/tkinter.html>

multi-platform GUI implementation for Python which includes windows, buttons, labels, prompts, among other useful tools. For plotting the data, the Matplotlib library³ is a well-known tool with many different customizable options. Finally, the Numpy library⁴ expands the Python mathematical processing capabilities. Those libraries along with the Zhinst library, to control the Lock-in Amplifier, are the basis for the script. An additional small script *Utils.py* provides useful tools to customize the appearance of the console messages for the user and will not be explained in detail because it is not a requirement for the script to work.

The first part of the *TE_measurement.py* script, which can be found in the Complements (Python scripts), a variable with name *options* contains the parameters for the connection to the Lock-in Amplifier as well as the parameters for the resistance, frequency scan and voltage scan measurements. All the measurements share three parameters, the number of points (*num_pts*), the number of measurements to average for each point (*num_pts_for_avg*), and the time to wait between a new value (frequency or voltage) is set and the measurement is performed. The other available parameters are, for the resistance measurement, the frequency of the signals (*f_value*) and the voltage range to analyze (*v_from* and *v_to*). For the frequency scan, the peak voltage value of the signals (*v_value*), and the frequency range to analyze (*f_from* and *f_to*). Finally, for the voltage scan, the frequency value, and the voltage range, same as the resistance measurement. Before running the script, these values can be edited according to the measurement requirements.

³ Developed by John D. Hunter, et al. <https://matplotlib.org>

⁴ Created by Travis Oliphant <https://numpy.org/>

```

options = {
  "device_id": "dev5845",
  "api_level": 6,
  "server_host": "192.168.91.86",
  "server_port": 8004,
  "resistance":{
    "f_value": 100, # Hz
    "v_from": 0, # Vpk
    "v_to": 1, # Vpk
    "num_pts": 10,
    "num_pts_for_avg": 1,
    "t_sleep": 1
  },
  "frequency": {
    "v_value": 3, # Vpk
    "f_from": 2000, # Hz
    "f_to": 20000, # Hz
    "num_pts": 50,
    "num_pts_for_avg": 10,
    "t_sleep": 0.5
  },
  "voltage": {
    "f_value": 1000, # Hz
    "v_from": 0, # Vpk
    "v_to": 5, # Vpk
    "num_pts": 50,
    "num_pts_for_avg": 10,
    "t_sleep": 0.5
  }
}
}

```

Code 3 Editable configurations for the connection and measurements

After establishing the connection with the Lock-in Amplifier a small menu will appear on the screen with the following options.

- 1 3w V vs Frequency
- 2 3w V vs Voltage

- 3 2w V vs Frequency
- 4 2w V vs Voltage

- 5 I vs V

- 9 Close all plots

- 0 Exit Program

Code 4 Available measurements in a numbered menu.

By typing the number of one of the options the measurement will start or, in the case of the option 9, all the plots will be closed or, in the case of the option 0, the script will end.

After selecting a measurement option, a file prompt will show in the screen to give a filename and location to save the data. For each measurement, the in-phase and out-of-phase components of the signals are stored in a list to later process the information. The specified number of measurements for average is considered to make the calculations which lead to the final data point. After each data point is calculated, the information is shown in a plot which updates every time a new data point is measured. The progress of the measurement in percentage can be read in both, the title of the plot and the console as long as the measurement is still running.

Once all the data points were calculated and the plot is complete, the title of the plot will change according to the measurement type. Some files will be generated in the specified location, the data file which contains the measured values, the plot as an image file and the configurations of the measurement as a text file. Finally, the signal outputs of the lock-in amplifier are switched off and the menu is visible to select an option again.

The K device

Lithography is a key technique in the fabrication of electronic and photonic devices. It involves the use of a mask, or a patterned template, to selectively transfer the pattern onto a thin film or substrate, which can then be etched or processed further to create the desired device structure. The photolithography process typically involves the substrate preparation where the sample is cleaned and prepared to ensure the good adhesion and uniformity of the photoresist coating. The photoresist is a light-sensitive material that changes its chemical properties when exposed to light. After this, the mask alignment and exposure take place. The mask, previously designed by a software (KLayout for this work) is aligned over the surface. Then by light exposure, typically using UV light, the pattern is transferred. By using a chemical solution, the exposed areas are removed from the surface to reveal the desired pattern. The lithography process can be made by exposing the pattern or the whole surface except for the pattern by selecting the appropriate photoresist (positive or negative, respectively). Finally, the sample is taken to the desired process which can be a deposition

or an etching which will affect only the area which is not covered by the pattern. By using this technique, the devices describe here were fabricated.

The device for measuring the 3ω voltage requires a heater stripe and a sensor to measure the ΔT generated by Joule Effect. It is also possible to use the same stripe as a heater and as a sensor by identifying the applied voltage and the measured voltage due to their frequencies.

Furthermore, to apply the differential 3ω method two samples must be measured. The difference between the first and the second sample is the thin layer to be measured. This allows us to subtract the ΔT value from both samples to obtain the ΔT only of the desired layer. It is important to isolate the heater from the sample to avoid any current to flow through the semiconductor. To achieve this, a thin 50nm SiO_2 layer is grown in top of the sample before creating the stripe.

The design for the K device consists of two contact pads to apply a 1w current through the stripe and two more contact pads to measure the 1ω voltage and the 3ω voltage. To increase the statistics and reduce the uncertainty, the length and width of the heating stripe can take different values. For this work, 6 different devices were fabricated on the same sample taking 10, 15, and 20 μm for the width ($2b$) and 1000, 1500, and 2000 μm for the length (l) of the stripe.

Available dimensions in microns ($2b \times l$):

1. 10 x 1000
2. 10 x 1500
3. 20 x 1000
4. 20 x 1500
5. 15 x 1000
6. 15 x 1500

Au is a good conductor for the design but it cannot stick properly to the SiO_2 so a thin Cr layer must be deposited before. In summary, the design involves two primary steps which are the SiO_2 thin layer deposition and the Au/Cr deposition. The former does not need a lithography process because the 3ω method requires the semiconductor to be fully isolated from the stripe heater. The latter does require a lithography process to draw the contact

pads and the stripe on the surface of the SiO_2 layer. The mask for the Au/Cr deposition can be found in Complements (Mask for K design). A 3D sketch of the device is shown in Fig. 23.

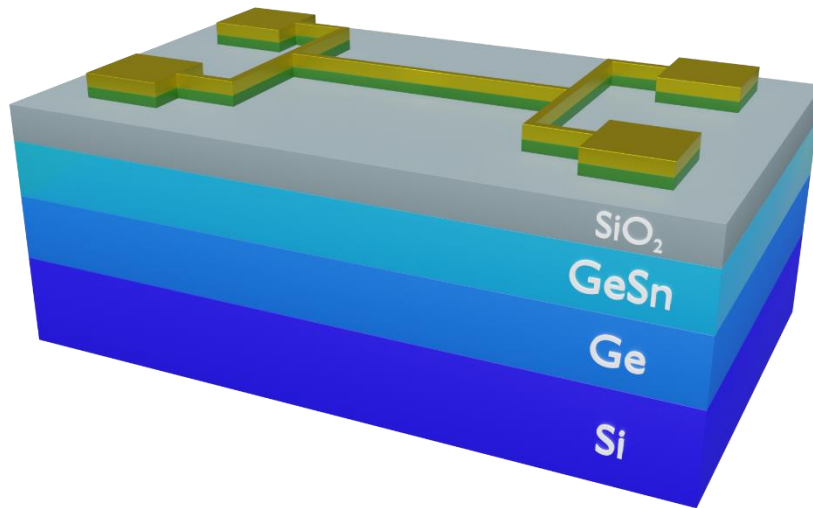


Fig. 23 GeSn sample with a K device on top. The green and golden materials are Cr and Au respectively.

To confirm the fabrication of the devices was successful, before performing any measurements they were analyzed in a microscope to check the pads and wires are not broken. In Fig. 24 a 1000 x 10 K device is shown. The length and width of the stripe heater can be confirmed by this images. It is very important to check the electrical continuity of the device and discard any problems from the beginning.

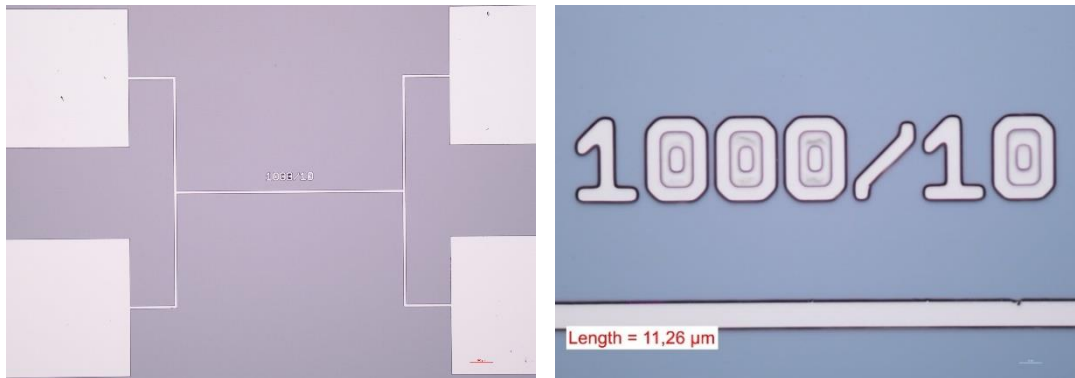


Fig. 24 Microscope images from the K device in a full view (left) and the heater stripe (right) for the 1000x10 device

Results for the TCR

Since the TCR is a property of the metal connections and not of the grown semiconductor, some samples were randomly chosen for these measurements.

Sample	d_{GePDA} (nm)	d_{GeSn} (nm)	Sn %
TCR_1	505	200	11.7
GePDA_2	265	--	--
Sn_3	295	288	11.8

Table 3 Set of samples to measure the TCR

The resistance of the heater stripes of 3 samples and 2 different devices each one, were measured at different temperatures from 50K to 350K in steps of 50K. In Fig. 25 the results for all the measurements are shown. During the experiments, one of the devices was broken. For that reason, only 5 curves were fitted. It is expected, considering the analyzed material is *Au/Cr* to see an increase in resistance as temperature increases as well. Fig. 25 shows an increasing linear behavior for all the measured samples. The fitting parameters can be found in Table 4.

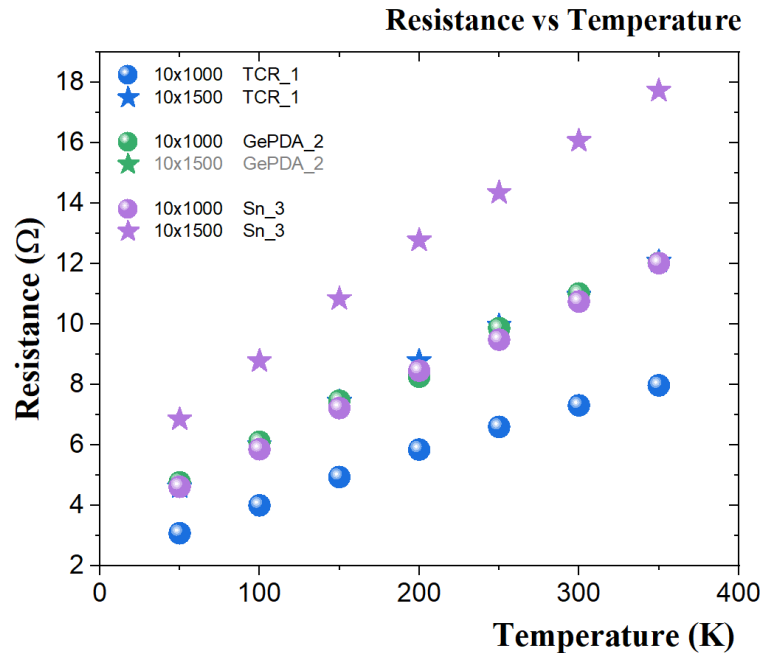


Fig. 25 Resistance vs. Temperature for 5 different devices

With the extracted parameters, the α values were calculated according to Eq. (56). The α shows a decreasing behavior as the temperature increases, as shown in Fig. 26. The variation is small enough to confirm the first order approximation was valid to apply.

Sample	Device	m	n
TCR_1	10x1000	0.0164	2.40731
TCR_1	10x1500	0.02487	3.57963
GePDA_2	10x1000	---	---
GePDA_2	10x1500	0.03577	5.30348
Sn_3	10x1000	0.02416	3.49833
Sn_3	10x1500	0.03577	5.30348

Table 4 Linear fit parameters for the Resistance vs. Temperature curve

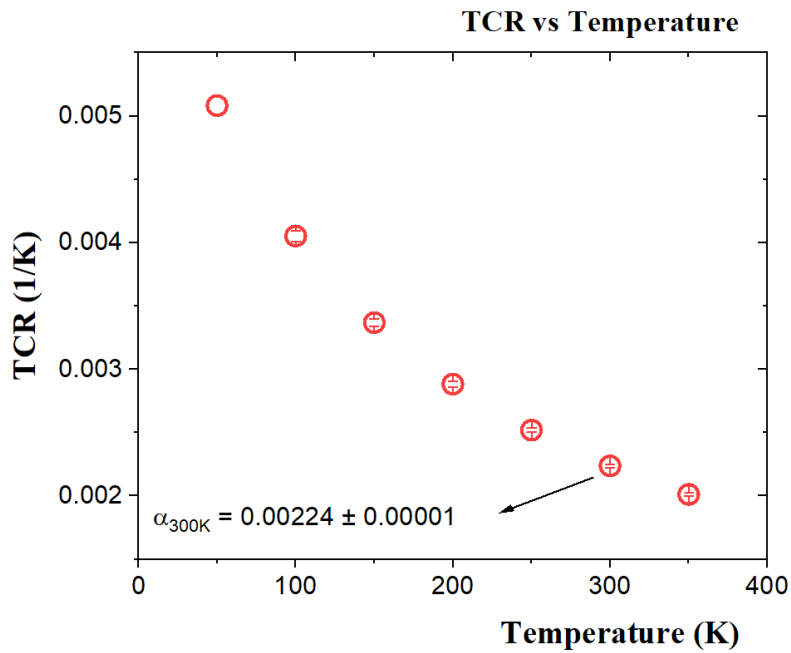


Fig. 26 TCR vs. Temperature plot of Au/Cr

The calculation of the α values at different temperatures make possible to apply the 3ω method in a wide range of temperatures as well. The most important value for our concerns is at room temperature (300K) which has a small error of $\sim 1\%$.

T (K)	α (mK ⁻¹)
50	5.08 ± 0.066
100	4.05 ± 0.042
150	3.37 ± 0.029
200	2.88 ± 0.021
250	2.52 ± 0.016
300	2.24 ± 0.012
350	2.01 ± 0.010

Table 5 Experimental values of the TCR for each measured temperature

Validation of the 3ω method

The validation of the 3ω voltage is carried out in four steps which are defined by the relation between the $V_{1\omega}$ and the $V_{3\omega}$. These steps to validate the method are:

1. To verify the linear tendency and the slope between the $Re\{V_{3\omega}\}$ and the $\ln(f)$

As the substrate is the same (Si) in every fabricated device, the slope of the curve should remain constant for all the measured samples. The slope involves the thermal conductivity and thermal diffusivity of the substrate and not of the thin layers so its value should not be different regardless of the measured sample.

In Fig. 27, the $V_{3\omega}$ of different samples from the Sn concentration set are plotted against the Frequency. The logarithmic scale in the frequency axis makes visible the linear dependency as expected from the theory.

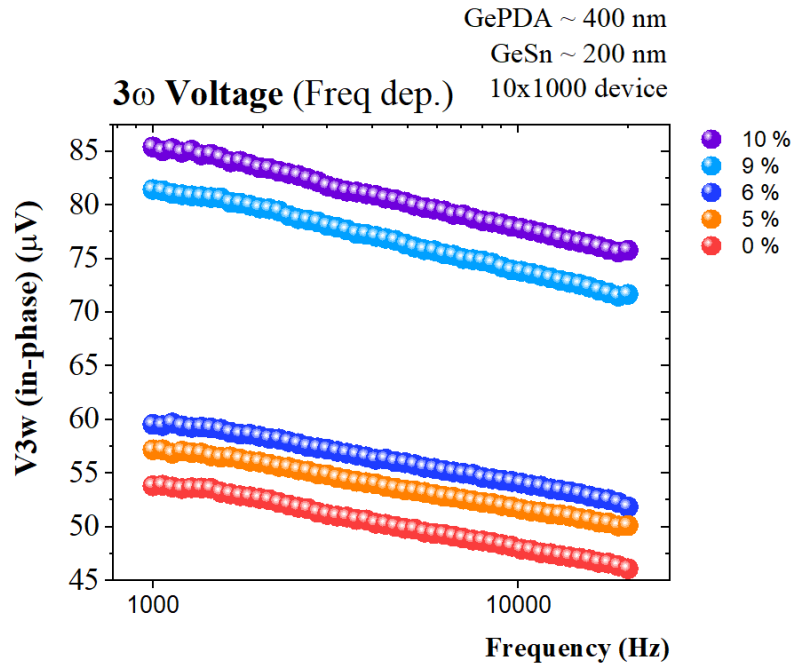


Fig. 27 $Re\{V_{3\omega}\}$ vs. Frequency for the Sn-concentration set of samples

2. The $Im\{V_{3\omega}\}$ is constant in the analyzed frequency range.

The derived theoretical expressions show that there is no dependency between the out of phase part of the $V_{3\omega}$ with the frequency. The expected curve for each sample is a constant value. In Fig. 28 the out-of-phase component of each sample has a very small variation which could be assumed as constant.

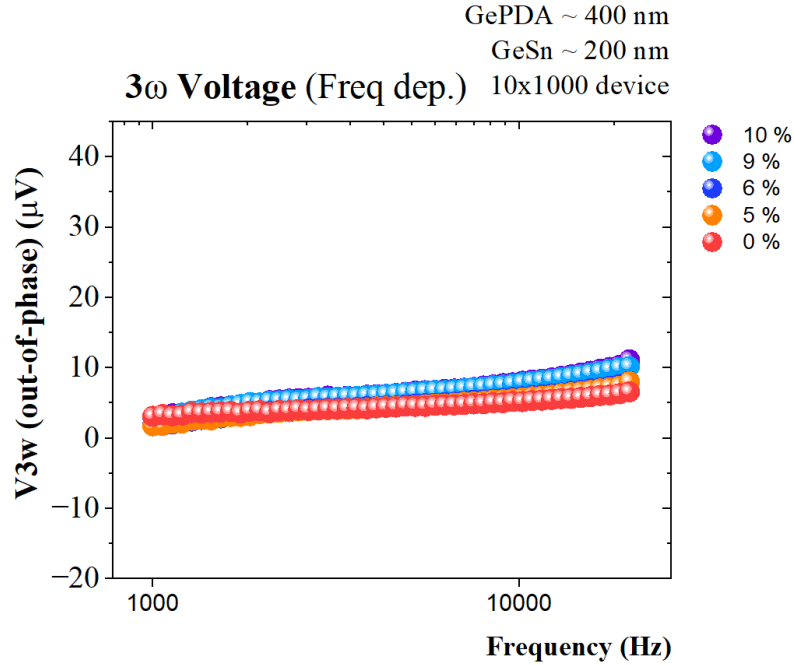


Fig. 28 $Im\{V_{3\omega}\}$ vs. Frequency for the Sn-concentration set of samples

3. The $V_{3\omega}$ has a cubic dependency with the $V_{1\omega}$

To prove the cubic dependency the natural logarithm of both values was plotted. From this plot, the slope of a linear fit curve could tell the grade of dependency between the two values.

$$V_{3\omega} = a V_{1\omega}^3 \quad (59)$$

where a represent all the additional terms multiplied by the $V_{1\omega}^3$ term. By taking the natural logarithm of the whole equation it is possible to extract the power of $V_{1\omega}$ as:

$$\ln(V_{3\omega}) = \ln(a V_{1\omega}^3) \quad (60)$$

$$\ln(V_{3\omega}) = \ln(V_{1\omega}^3) + \ln(a) \quad (61)$$

$$\ln(V_{3\omega}) = 3 \ln(V_{1\omega}) + \ln(a) \quad (62)$$

Now, to ensure the cubic dependency a linear fit of such curve should have a slope value near 3.

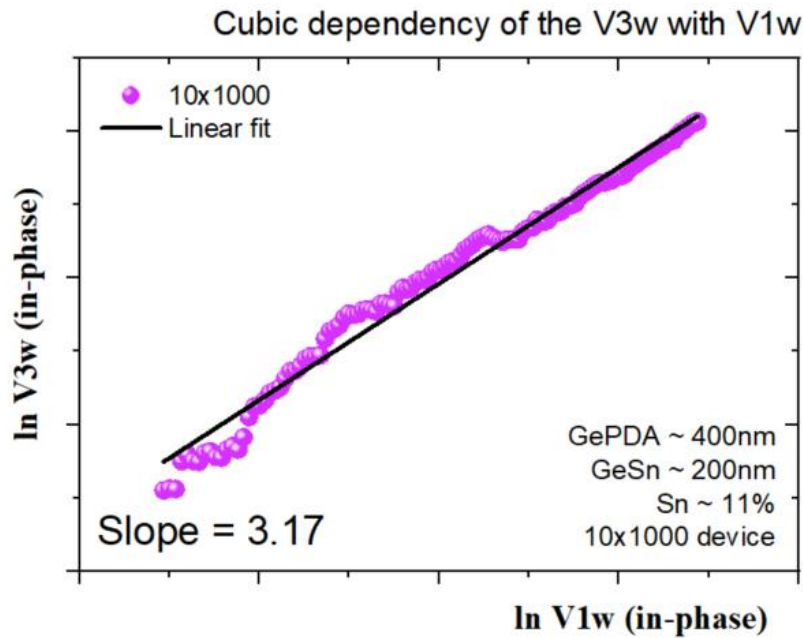


Fig. 29 Linear fit of the $\ln(V_{3\omega})$ vs. $\ln(V_{1\omega})$ for the in-phase component

In Fig. 29 the linear fit shows a slope value of 3.17 which ensure the cubic dependency. The out-of-phase component, according to theoretical expressions, should show the same behavior. The same logarithmic analysis can be made on this component to further confirm the validity of the method.

SiO₂ thickness study

To choose a SiO₂ thickness value for the insulation layers deposition, two samples were chosen (a GePDA and a GeSn sample) to apply the differential 3 ω method and compare the extracted thermal conductivity.

Sample	d_{GePDA} (nm)	d_{GeSn} (nm)	Sn %
SiO ₂ _1	315	310	12
GePDA_2	265	--	--

Table 6 Set of samples to compare the SiO₂ thickness effect on the thermal conductivity

Different SiO₂ thicknesses (50nm, 100nm, 200nm, and 300nm) were measured to analyze the impact it produces on the extracted κ value.

The SiO_2 deposition thickness was confirmed using Transmission Electron Microscopy (TEM). The following images show the results, the left ones for the GeSn layer ($\sim 300\text{nm}$) and the right ones for the SiO_2 layer.

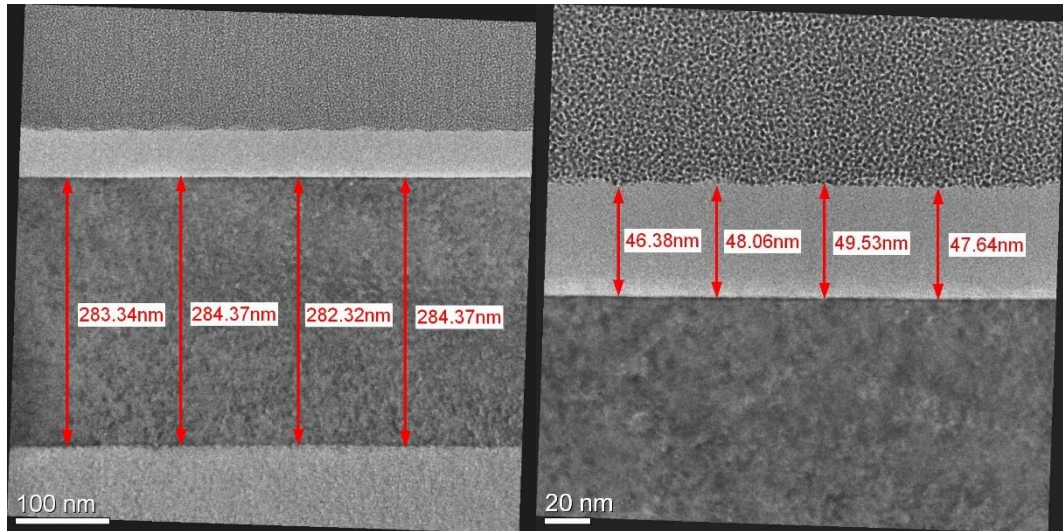


Fig. 30 Image from TEM for the 300nm GeSn layer (left) and the 50nm SiO_2 layer (right)

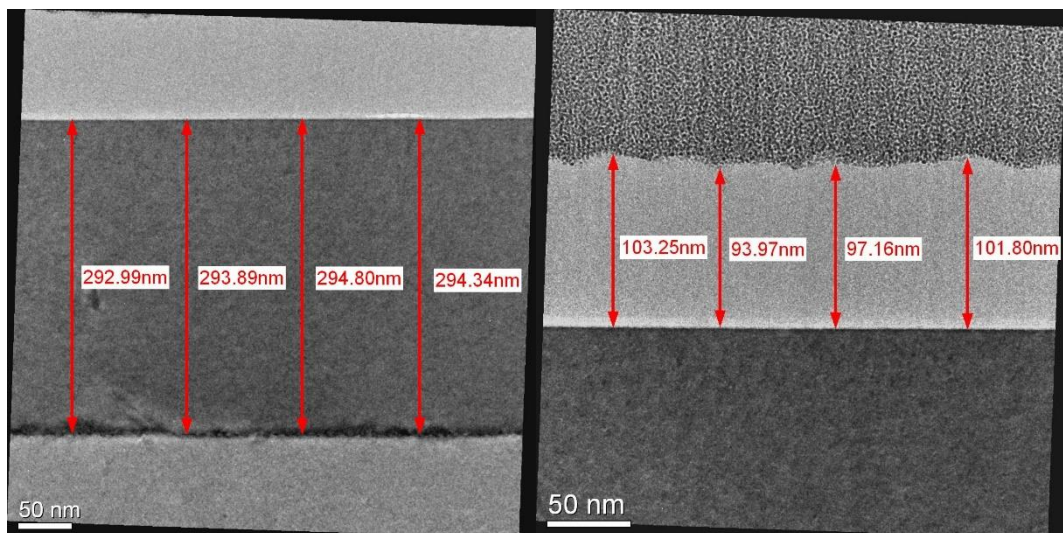


Fig. 31 Image from TEM for the 300nm GeSn layer (left) and the 100nm SiO_2 layer (right)

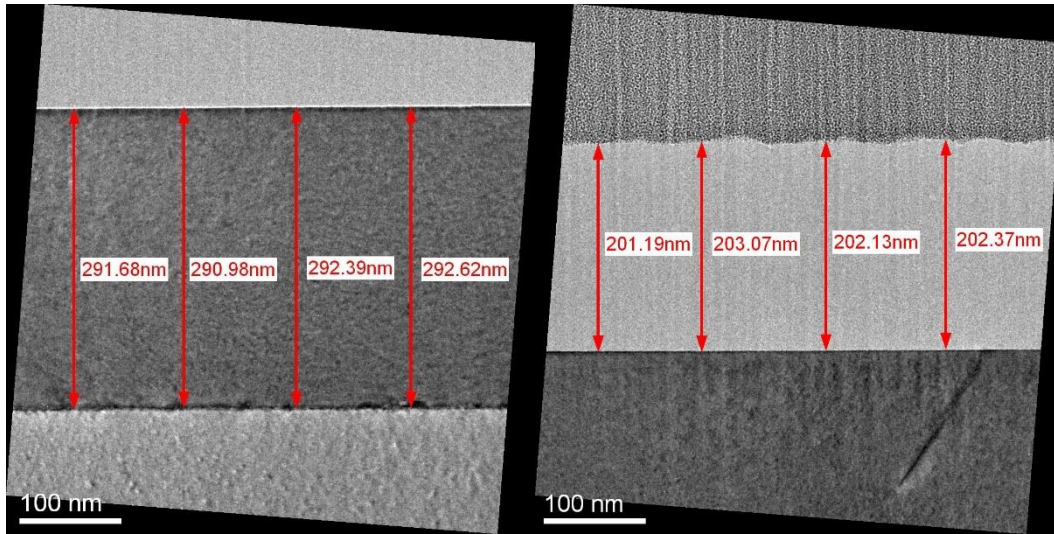


Fig. 32 Image from TEM for the 300nm GeSn layer (left) and the 200nm SiO₂ layer (right)

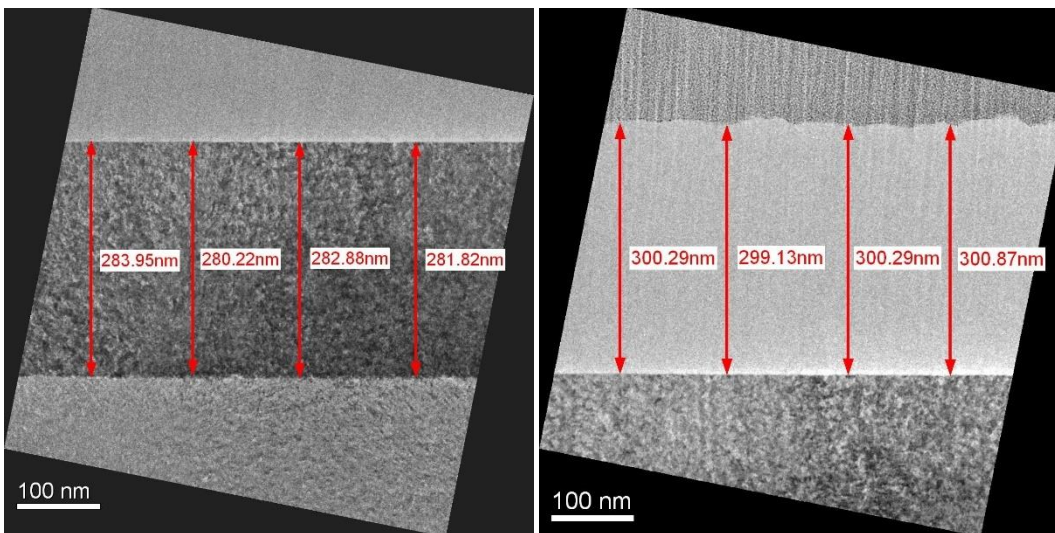


Fig. 33 Image from TEM for the 300nm GeSn layer (left) and the 300nm SiO₂ layer (right)

There is a small variation on the GeSn thickness $\sim 10\text{nm}$ which is acceptable considering the variations in the Sn concentration set of samples. The SiO₂ layer thicknesses are very close to the desired values.

The k of the GeSn of each sample was calculated by the 3ω method, the six K devices on each sample were measured to get a more accurate result.

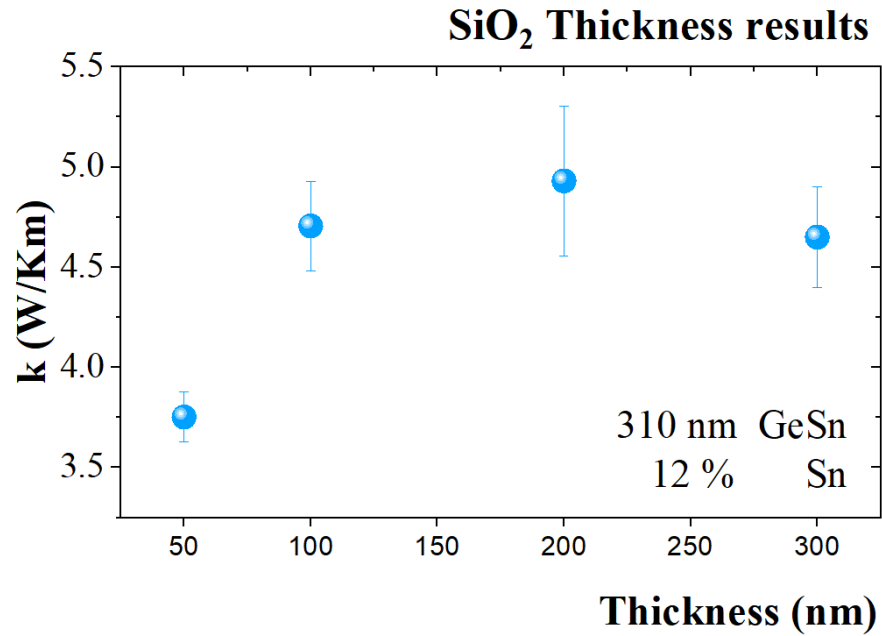


Fig. 34 Thermal conductivity on a 310nm GeSn at 12% Sn concentration for different SiO₂ thicknesses

Sample	d_{SiO_2} (nm)	k_{avg} ($\frac{W}{K m}$)
SiO2_1_50	50	3.75 ± 0.12
SiO2_1_100	100	4.70 ± 0.22
SiO2_1_200	200	4.93 ± 0.37
SiO2_1_300	300	4.65 ± 0.25

Fig. 35 Thermal conductivity for different SiO₂ thicknesses on the same GeSn wafer

After the data processing, the plot in Fig. 34 showed an asymptotic behavior as the SiO₂ thickness increases. The low κ value for the 50nm sample is attributed to the high phonon scattering produced at the interface between the GeSn and the SiO₂ layer. This was previously demonstrated in [27] where different results for SiO₂ layers are compared from several authors at different film thickness values as shown in Fig. 36. For that reason, all further fabricated samples have a 200nm SiO₂ layer.

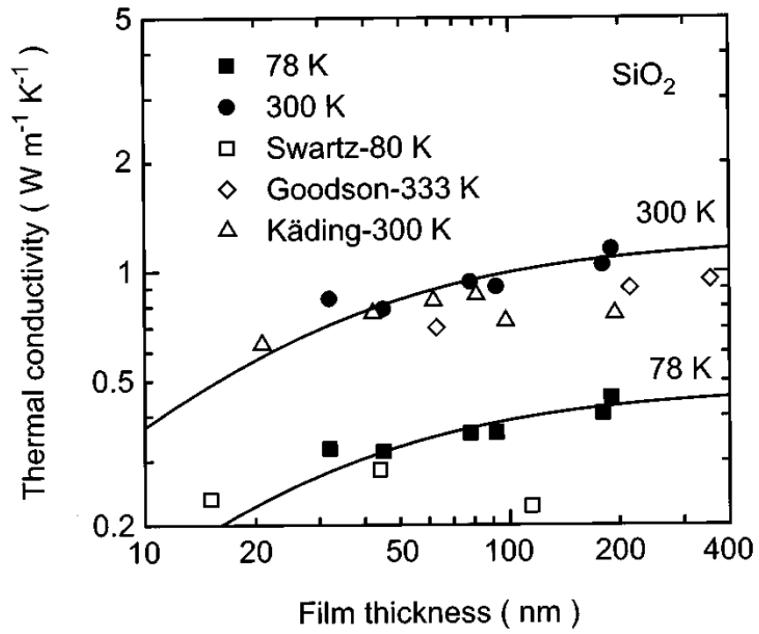


Fig. 36 Thermal conductivity of SiO₂ films at 78K and 300K for different thicknesses as shown in [27]

Lattice thermal conductivity measurements

GeSn thicknesses

The *GeSn* thickness set of samples was measured in two different occasions. The first generation results come from O. Krause [26] as presented in his master thesis, and the second generation results were taken from the same samples to confirm the previous results. In Fig. 37 the thermal conductivity of the thinner layer is much lower than the other ones. Recalling the *SiO₂* results, this behavior is attributed to the interface between materials. As the thickness of the layer increases an asymptotic behavior is visible. To confirm the tendency, a very thick (705nm) *GeSn* layer from the first-generation measurements, grown over a *GeVS* buffer, shows a similar value. The theory for the thermal conductivity of *GeSn* layers establish a value $\sim 5.8 \frac{W}{K m}$ for a 12% *Sn* concentration. Recent results [19] obtained by Raman Thermometry shows an experimental value between 4.2 – 5.4 $\frac{W}{K m}$ for the same *Sn* concentration. Both, the Raman thermometry results, and the theoretical results are shown in the plot as a blue region and a red dashed line, respectively. It is important to notice that the *GePDA* layer to apply the differential 3ω method has a thickness of 265nm which is not exactly the same as the one of every measured sample. This is not the case for the *GeVS* sample which helps to reinforce the reliability of the data and also discard any idea that the Ge buffer thickness has a considerable impact in the extracted thermal conductivity value.

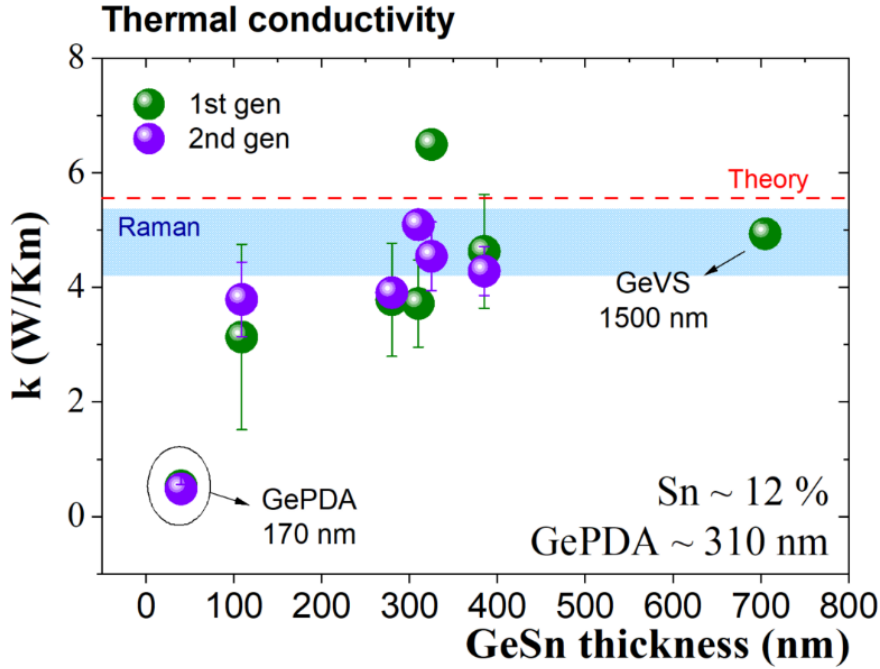


Fig. 37 Thermal conductivity of the GeSn thickness set of samples

Sample	$d_{Ge\,diff}$ (nm)	d_{Ge} (nm)	d_{GeSn} (nm)	$k_{1^{st}\,gen}$ ($\frac{W}{K\,m}$)	$k_{2^{st}\,gen}$ ($\frac{W}{K\,m}$)
GeSn_1	265	170	40	0.53 ± 0.12	0.48 ± 0.07
GeSn_2	265	265	109	3.13 ± 1.61	3.78 ± 0.65
GeSn_3	265	295	280	3.78 ± 0.98	3.90 ± 0.20
GeSn_4	265	315	310	3.71 ± 0.76	5.09 ± 0.26
GeSn_5	265	325	325	6.49 ± 0.24	4.53 ± 0.60
GeSn_6	265	310	385	4.62 ± 0.99	4.28 ± 0.42
GeSn_7	1500 (Ge VS)	1500 (Ge VS)	705	4.93 ± 0.19	---

Table 7 Results for the thermal conductivity of the GeSn thickness set of samples

Sn concentration

The Sn concentration set was analyzed using a 410 nm GePDA buffer layer for the differential 3ω method. Even though the theory establishes there should be a soft decrease going from $\sim 60 \frac{W}{K\,m}$ for pure Ge to $\sim 4 \frac{W}{K\,m}$ for a 12% Sn concentration, the plot in Fig. 38 shows, in blue, very low values for all the samples above 5% of Sn concentration. This is not the expected behavior, but it is a good indicator that the incorporated Sn on the lattice is

negatively affecting the heat conduction which positively affects the thermoelectric properties of the material.

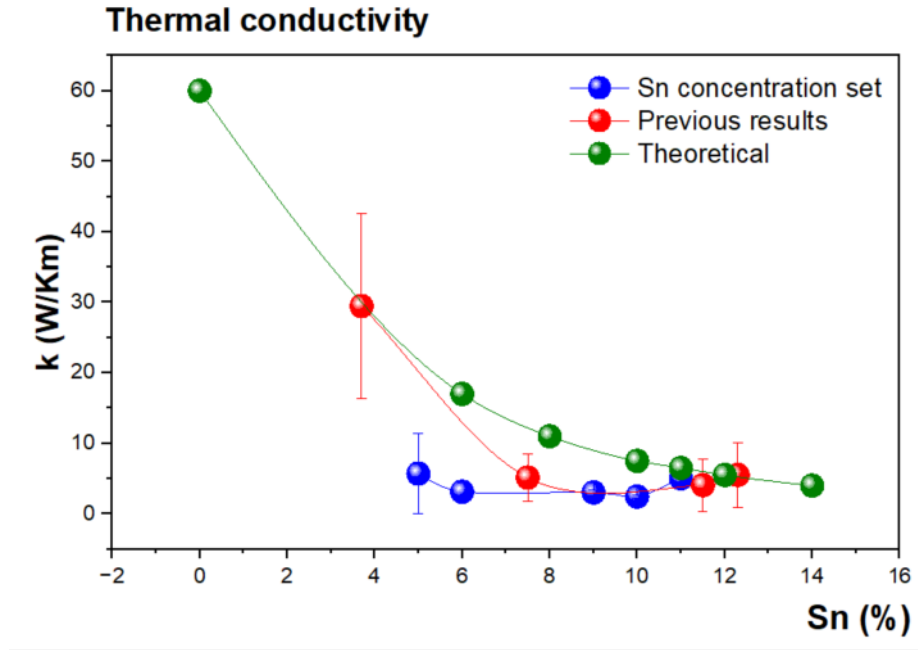


Fig. 38 Thermal conductivity for the Sn concentration set of samples compared to the theoretical results and previous experimental results

Sample	$d_{Ge\,diff}$ (nm)	d_{Ge} (nm)	d_{GeSn} (nm)	Sn %	$k \left(\frac{W}{K\,m} \right)$
Sn_1	410	435	165	5	5.69 ± 3.46
Sn_2	410	388	145	6	3.14 ± 1.30
Sn_3	410	380	180	9	3.03 ± 0.32
Sn_4	410	380	200	10	2.45 ± 0.18
Sn_5	410	390	235	11	5.01 ± 1.31

Table 8 Results of the thermal conductivity for the Sn concentration set of samples

Previous results are also shown, in red, for concentrations above 3.7% which match the theory except for the ~7.5% of Sn sample. In the case of high Sn concentrations, both sets match the theory.

A study of the ΔT values for the different dimensions of the K device is shown in Fig. 39. For the thinner stripe the ΔT value is high compared to the other dimensions. Recalling the mathematical model for the 3ω method, the width of the stripe was assumed to be much

lower than the thermal penetration, so it is reasonable that a thinner stripe gives better results than a thicker one.

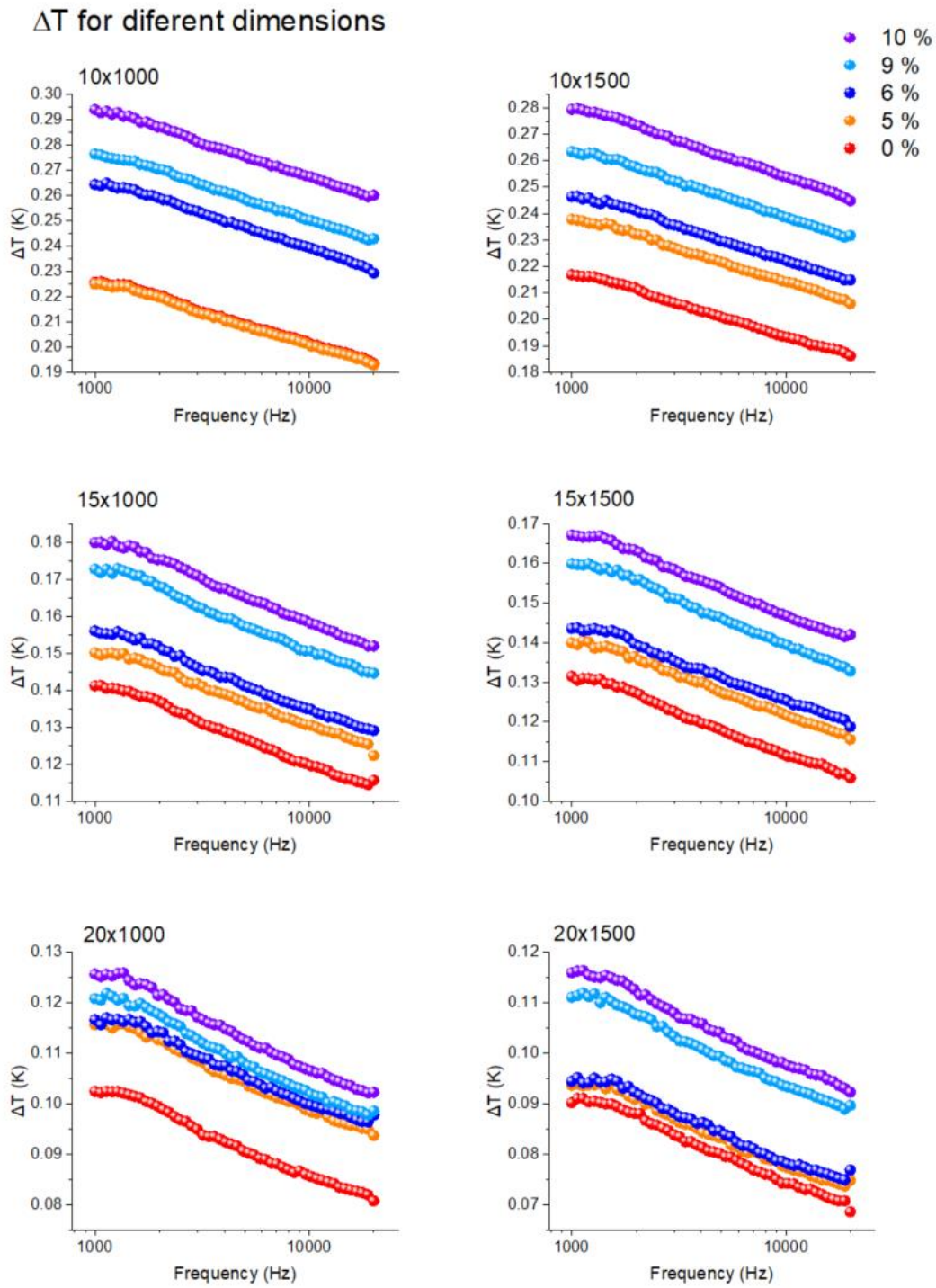


Fig. 39 Change in temperature for each dimension in the K-device for different Sn concentrations

Improved devices

The K-S device

The device to simultaneously measure the thermal conductivity and the Seebeck coefficient is more complex than the K-device. It involves various steps to be fabricated which include depositions and etchings using different lithography masks. Following the design provided by [24] the first step is to etch the layer of interest from everywhere except for a small mesa. After that, an insulation layer is deposited (SiO_2) over the whole sample. Two small windows are etched, one on the mesa and one on the substrate to deposit the Seebeck contact pads. Two more windows are etched for ground (GND) reference contact pads. After the metal deposition the mesa and the substrate are covered again by an insulation layer and finally the heater is deposited over both, the mesa, and the substrate.

In Fig. 40 a K-S device for the mesa is shown. The inner metal deposition is in direct contact with the layer of interest to measure the generated voltage due to the Seebeck effect and the contact pad at the most left part of the device works as GND. The heater on top has a more complex geometry to apply a uniform distribution of heat over the mesa. This device has a single pair of contact pads to apply and measure the voltage.

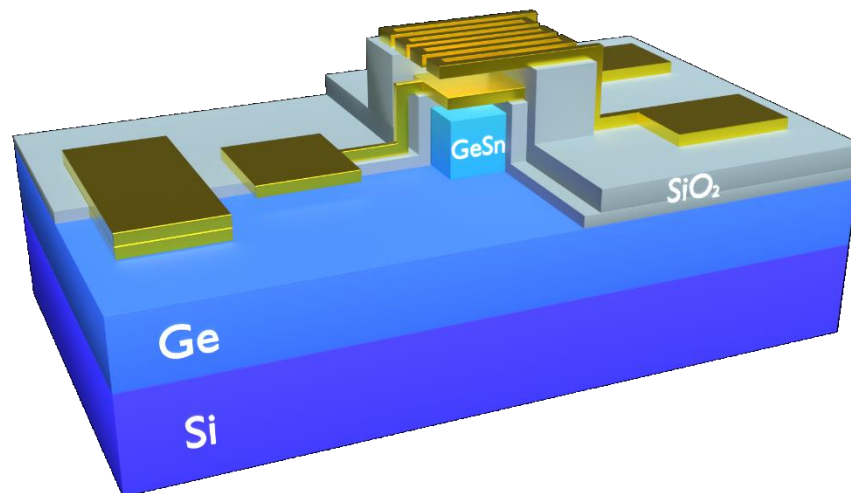


Fig. 40 GeSn sample with a K-S device. A cut was made to show the inner contact pads

For testing purposes, different dimensions of the mesa and the heater wire width were chosen. The goal for testing wire widths is to compare the quality of the deposition and

select the best dimensions to fabricate more devices. For the mesa dimensions, by measuring devices with different areas for the layer of interest the uncertainty can be decreased. Same case of the K device with different dimensions. The values for the heater wire width (w) are $2\mu m$, $3\mu m$, $4\mu m$, and $5\mu m$. The values for the area of the mesa are $100\mu m$, $150\mu m$, and $200\mu m$. A combination of those parameters was taken to create a mask to fabricate different devices for testing purposes. The space between contact pads and devices was also considered for the mask which can be found in the Complements (Mask for K-S design) as well as the run sheet with the detailed fabrication steps (Run sheet for K-S and K-S- σ design)

The K-S device was fabricated following the steps detailed in the Complements (Run sheet for K-S and K-S- σ design). The SiO_2 deposition was not possible to perform after an Au/Cr layer due to contamination of the equipment. For that reason, the first metal deposition was Al/Ti which does not affect the previous TCR calculations because the first metal pads are for measuring the generated Seebeck voltage and not for applying heat to the sample.

For every deposition step the quality of the wires and pads was inspected using a microscope. In Fig. 41 the device was inspected to ensure the Al/Ti deposition was successful, and the wires and pads are not broken. In the image, the right most contact has a small square in the center which is the window etched in the first steps for the metal to make direct contact with the material.

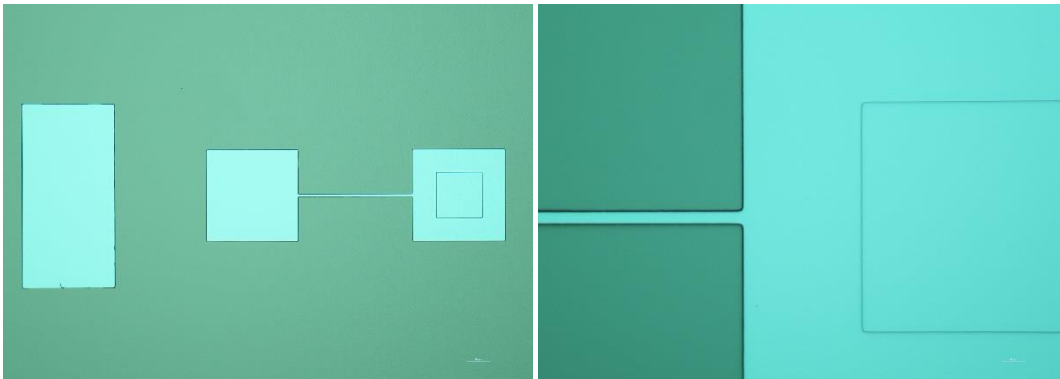


Fig. 41 Microscope images of the Al/Ti deposition for the Seebeck contact pads

After the first metal deposition, a second SiO_2 layer is required to insulate one of the Seebeck contacts for the deposition of the heater. In Fig. 42, the blue rectangle is the SiO_2 layer. The next and final step is the Au/Cr deposition of the heater.

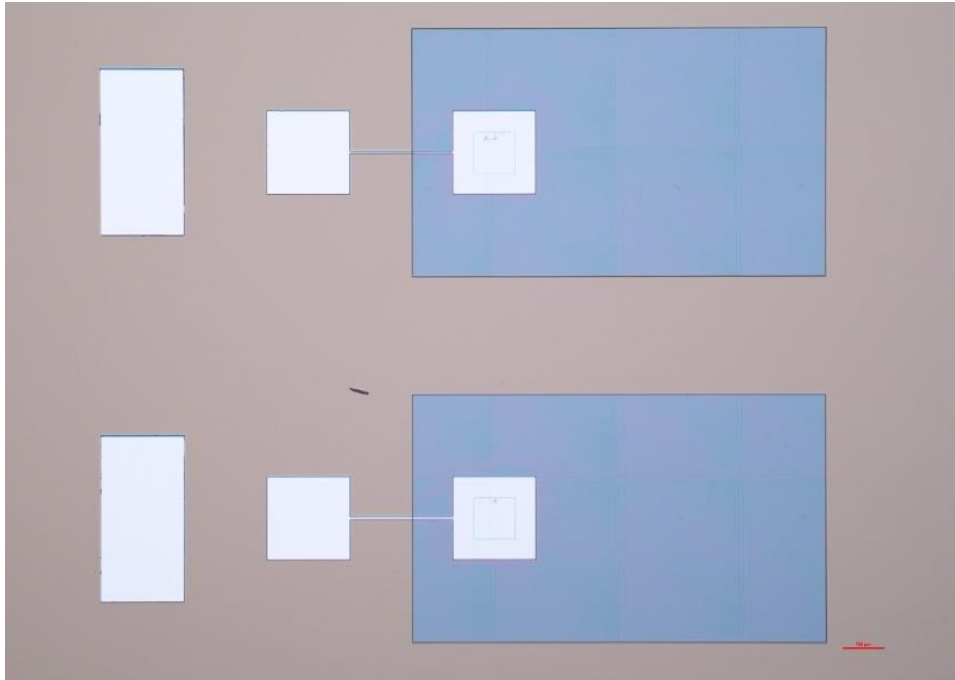


Fig. 42 Microscope images of the second SiO_2 deposition to insulate one of the Seebeck contacts

In Fig. 43 the resist after the lithography exposition is shown. The serpentine is well defined over the insulation layer which is a good indicator that the deposition will be successful.

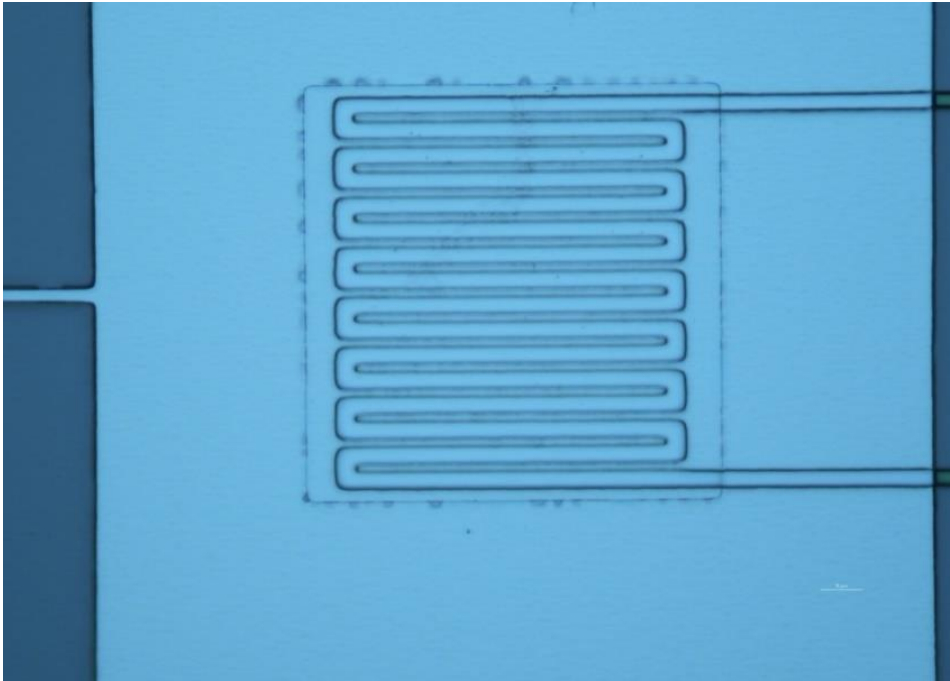


Fig. 43 Microscope image of the resist after exposition for the deposition of the heater

Finally, in Fig. 44 the final device for $5\ \mu\text{m}$ wire and $100\ \mu\text{m}$ mesa are shown. The device on the left has the mesa which can be seen as a square surrounding the heater. On the right side, the device does not have a mesa to apply the differential 3ω method by measuring the Ge buffer.

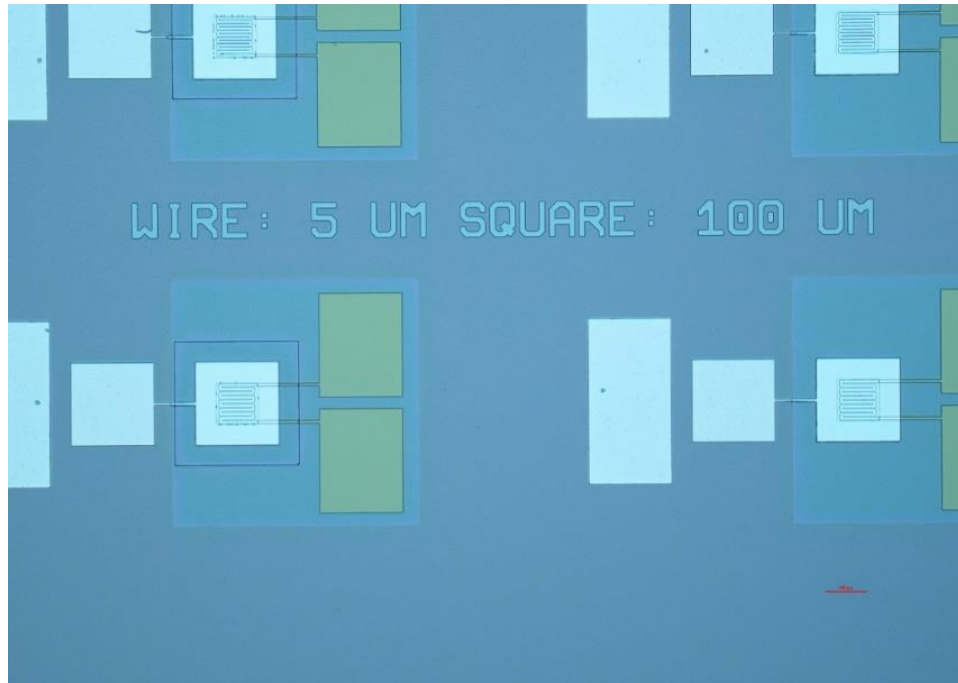


Fig. 44 Microscope image of the finished device after the Au/Cr deposition

The devices for 2 and 3 μm wire were almost all useless because of discontinuities of the serpentine. For the 4 μm wire devices, only some of them had a good heater. All the 5 μm devices were successfully fabricated.

During the process, the photoresist material before the exposure takes places is spread over the surface by a rotating mechanism. Since the samples are square-shaped, depending on the time and rotation speed parameters selected, the photoresist will be thicker on the corners. This was analyzed using a different microscope to prevent the contact pads to be deposited over a non-uniform surface.

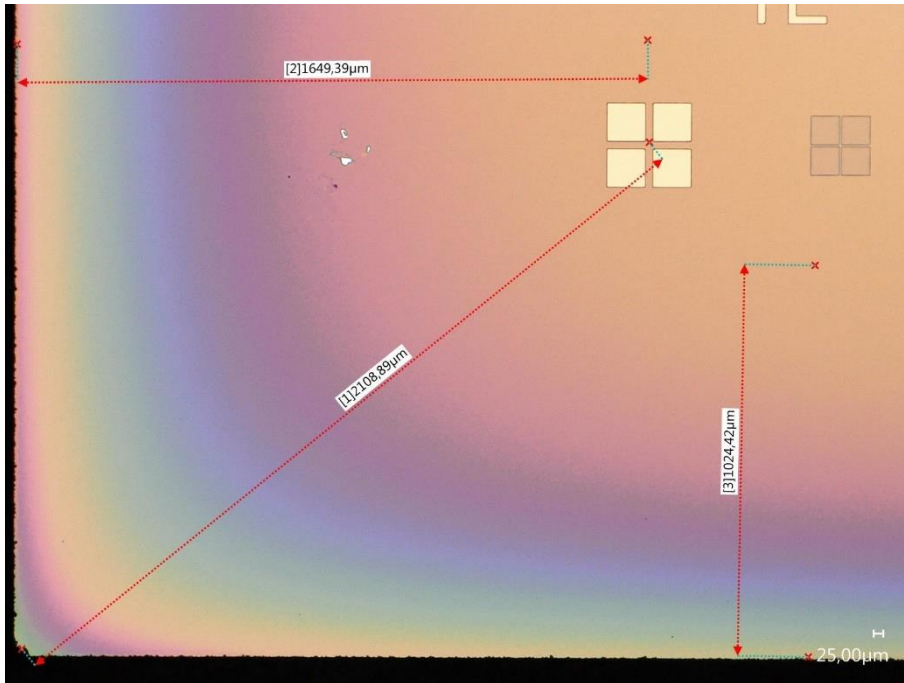


Fig. 45 Bottom left corner of a sample with K-S devices (Highest non-uniformity)

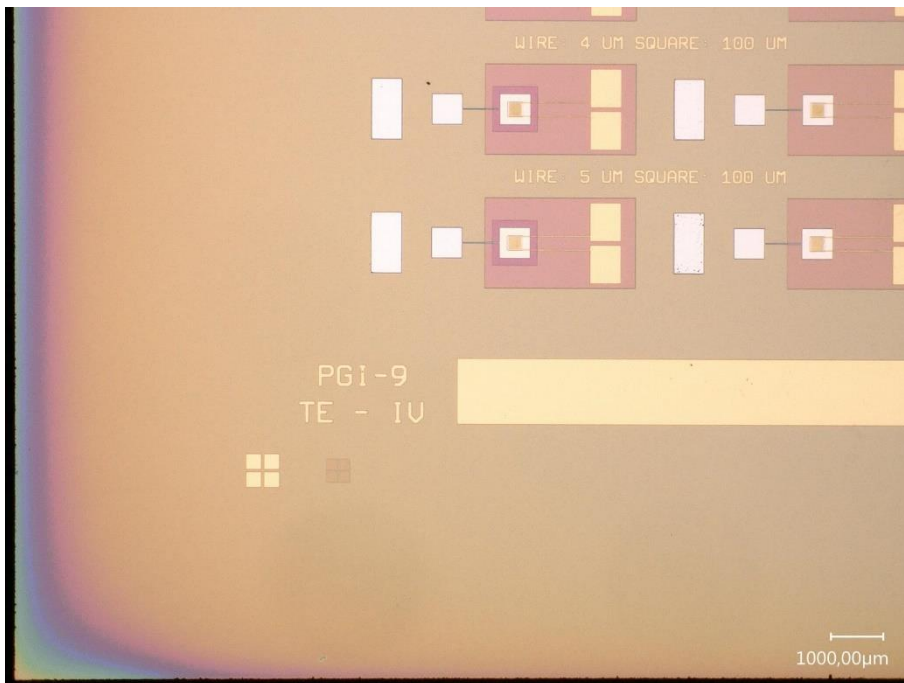


Fig. 46 Bottom left corner of a sample with K-S devices (Low non-uniformity)

In Fig. 45, the corner of the sample shows a color gradient which indicates the thickness of the photoresist was not uniform. This was the worst non-uniformity found through all the samples. Yet, the devices are not affected due to their separation to the edges. In Fig. 46, the non-uniformity of the photoresist does not even reach the marker. This was the typical behavior found in most of the samples.

Further tests can be made on the devices by changing the exposure parameters during the lithography process to obtain better results. The main goal of this is to match the values obtained with the K device for the same samples.

The following figures show the difference between a $5\mu\text{m}$ and a $2\mu\text{m}$ wire for the heaters. In the thinner wire heater, the contacts are broken and there is no clear separation of the wires so a uniform heating of the area may be impossible by using that device.

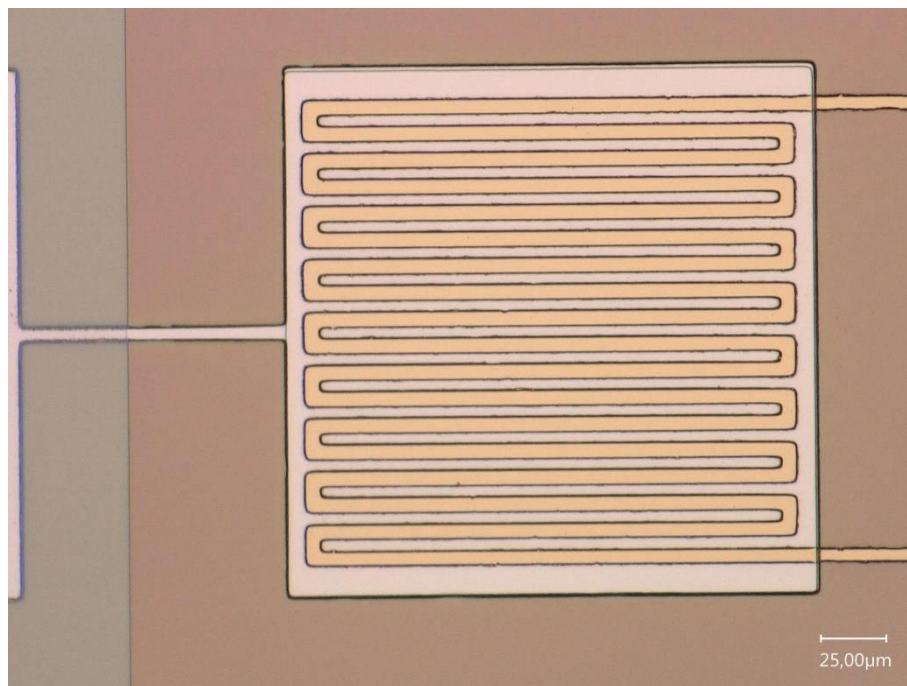


Fig. 47 $5\mu\text{m}$ wire heater for a K-S device

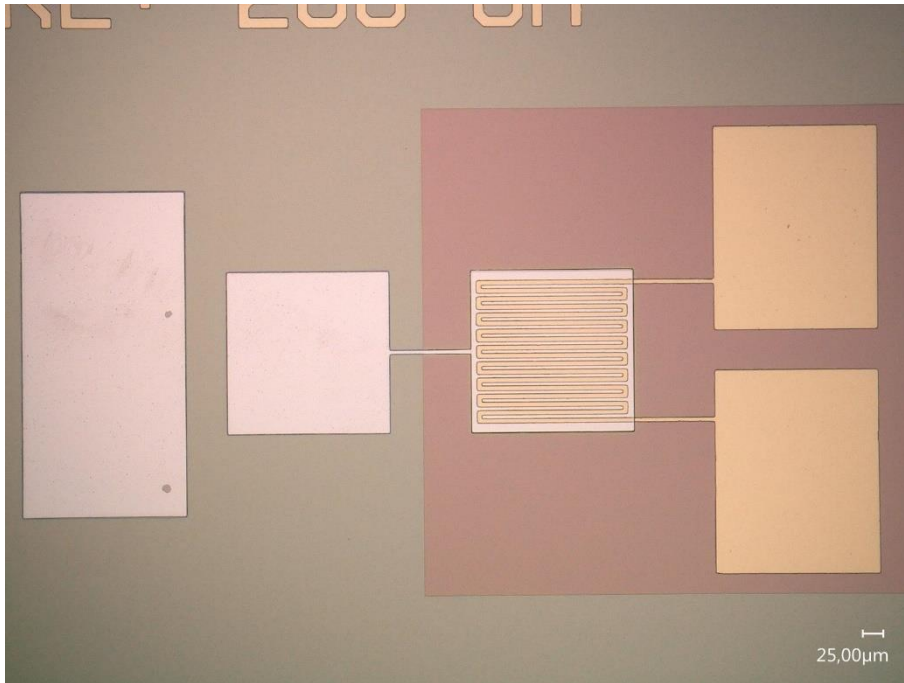


Fig. 48 5 μm wire complete K-S device

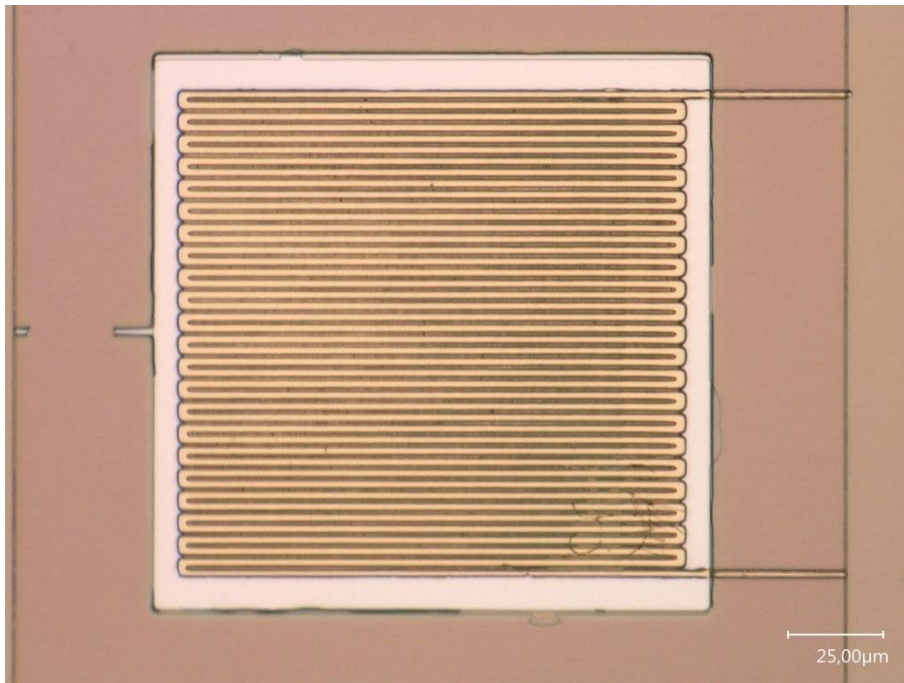


Fig. 49 2 μm wire heater for a K-S device

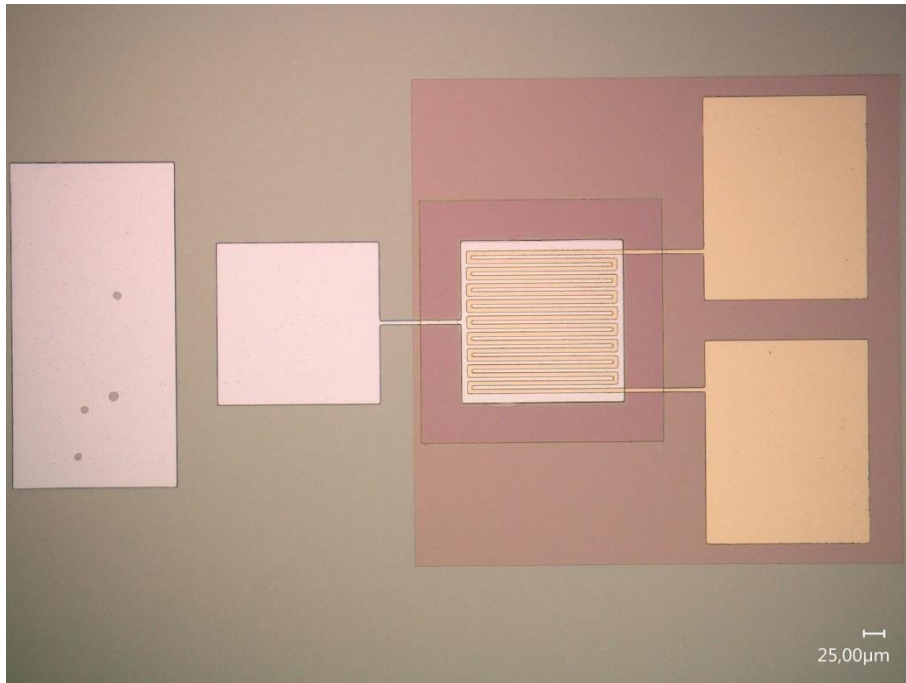


Fig. 50 2 μm wire complete K-S device

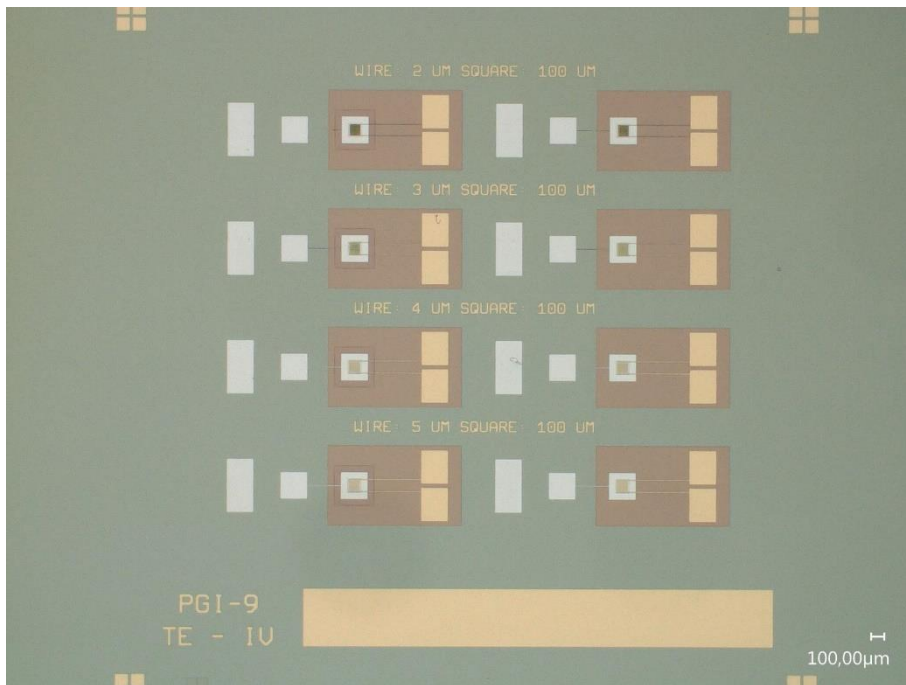


Fig. 51 Chip containing 4 K-S devices with different dimensions

The σ device

The σ device, shown in Fig. 52, can be fabricated in the same process of the K-S device taking advantage of the first steps: the etching of a small mesa, the deposition and etching of a SiO_2 insulation layer and the metal contact deposition. For this reason, a new mask which contains many K-S devices and many σ devices were designed. For this device, the area of the mesa can be varied to reduce the uncertainty of the extracted electrical conductivity value. The following values were selected for the area of the mesa (A), $100\mu m$, $150\mu m$, $200\mu m$, and $250\mu m$. The mask for this device can be found in the Complements (Mask for the K-S- σ design).

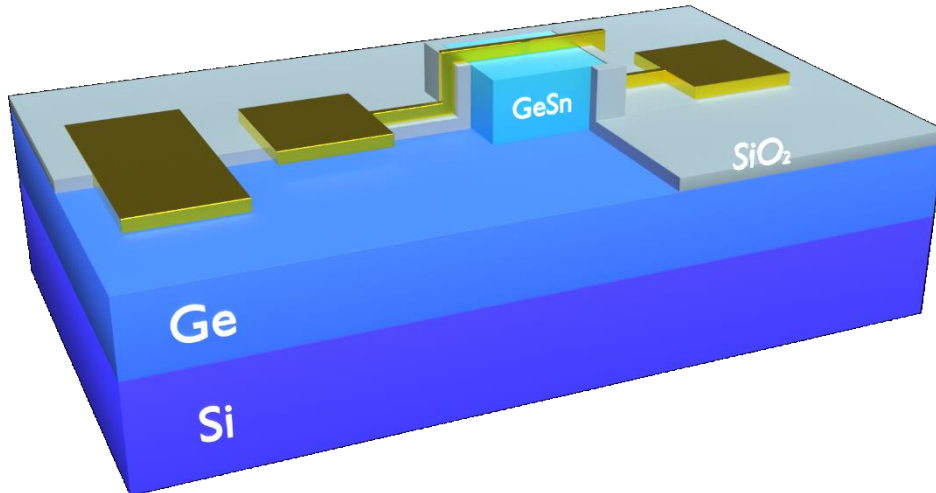


Fig. 52 GeSn sample with a σ device on top. A cut was made to show the GeSn mesa

Chapter 4. Discussion and Conclusions

The *GeSn* varying thickness and the *Sn* varying concentration sets of samples for determine the thermal conductivity of *GeSn* binary alloys showed important results to analyze in detail.

For the *GeSn* varying thickness set, the RBS spectrum for the thinner samples showed a strange behavior in the substrate peak which is attributed to the long path the He^+ ions travel to reach the substrate. In the case of samples with similar thicknesses, the substrate signal looks the same due to a similar energy loss through the sample. Furthermore, the RBS results confirm the presence of *Si* for the substrate. Nevertheless, for the same thinner samples, the XRD signal for the *GeSn* is left-shifted compared to the other samples which could be associated to a different lattice strain compared to the other samples. This would require a more detailed study of the crystalline structure of the sample which is beyond the scope of this work. An indicator of the lattice strain in these two samples is the single peak signal different from the double-peak signal of the other samples indicating its critical thickness after which the lattice is relaxed was not reached. *GeSn* alloys grow as a strained structure and after this critical thickness, they relax and slightly change its *Sn* concentration resulting in this double-peak signal. Despite this, the thermal conductivity results for this set of samples behaves as expected. For very thin layers the high phonon scattering produced near the interface between the *GePDA* and the *GeSn* layers avoid the heat to efficiently propagate through the lattice causing the thermal conductivity value to be lower than that of the material itself. As the thickness increases, the thermal conductivity increases until its real value. After 280 nm the expected value from theory and Raman results is reached and stays almost stable for thicker layers. The 705 nm *GeSn* layer grown on a *GeVS* buffer confirms all the previous data points. To get more reliable results and discard any issue with the thinner layers, a new set of samples all grown in *GeVS* wafers is proposed to be measured.

The *Sn* varying concentration set results clearly show the effect of adding *Sn* to the *Ge* lattice but the expected soft decrease is absent. All the samples, except for the 11% one, are significantly below the theoretical values. As the difference between the *GePDA*

thickness of both samples for the differential 3ω method is not significantly high, the mismatch of the experimental results may be attributed to the growth of the $GeSn$ itself. The RBS spectrum for each sample in this set show reasonable results. The width of all the Ge and the $Ge + Sn$ signals is very similar on each sample, as expected, and the height of the Sn signal decreases as the Sn concentration also decreases. Moreover, the XRD results show a left shift of the signals as the concentration gets higher (assuming similar strain of the lattices), which is also the expected behavior. This could be considered as an indicator that, with the 3ω method, something more than just the $GeSn$ thermal conductivity is being extracted. To discard the sample structure as the cause of this issue, it is proposed as future work to grow a new set of samples over a $GeVS$ buffer and increase the thickness of the $GeSn$ layers.

It was demonstrated that the K-S device fabrication was successful. This new device provides the capability of simultaneously measure the Seebeck coefficient and the thermal conductivity. To continue with the investigation, some tests must be carried out concerning the validation of the 3ω method to ensure the new heater geometry is useful and confirm that the generated Seebeck voltage can be extracted from the 2ω component as the frequency increases. A right indicator that the device is properly working, at least for the thermal conductivity measurements, would be to replicate the $GeSn$ thickness set results using the same samples.

The σ device was only designed and has not been fabricated yet. The advantage of its design is that both, the K-S and the σ devices, can share their fabrication process using the same steps. To have a sample with such devices would make easier to fully characterize the thermoelectric properties of the material.

As further work, once the Sn concentration effect on the thermal conductivity was demonstrated, the electrical conductivity value can be increased by doping the material with B or P for an p-type or n-type doping, respectively. Something important to notice is that the doping also increase the phonon scattering and decreases the thermal conductivity which positively affects the thermoelectric properties of the material. To further reach an even lower thermal conductivity value, additional to the doping the material could be changed from a binary alloy to a ternary $SiGeSn$ alloy. These suggestions along with the

proposed devices can take us closer to demonstrate the *GeSn* and *SiGeSn* alloys are suitable for thermoelectric applications at room temperature.

The confirmation of the theory about the low thermal conductivity for *Sn* concentrations ~11% is the first step through the final goal of fabricating portable energy harvesting devices. Increasing the electrical conductivity, as it was previously discussed, will only negatively affect the conduction of heat which improves the *ZT* figure of merit. Doped *GeSn* and *SiGeSn* layers are the next step in this investigation. Finally, the Seebeck coefficient would be the last parameter to prove these materials to be suitable for thermoelectric applications.

For further investigation on *GeSn* alloys, it is important to create thicker layers on *GeVS* buffers to reduce as much as possible all issues concerning the growth process and to get closer to the theoretical results.

In conclusion, *GeSn* alloys are demonstrated to be promising candidates for thermoelectric devices operating at room temperature.

References

1. Vedernikov, M.V. and E.K. Iordanishvili. *A.F. Ioffe and origin of modern semiconductor thermoelectric energy conversion*. in *Seventeenth International Conference on Thermoelectrics. Proceedings ICT98 (Cat. No.98TH8365)*. 1998.
2. Goldsmid, H.J., *Introduction to Thermoelectricity*. 1 ed. Springer Series in Materials Science. 2012, Berlin: Springer Berlin, Heidelberg. XVI, 242.
3. Kanatzidis, M.G., *Nanostructured Thermoelectrics: The New Paradigm?* Chemistry of Materials, 2010. **22**(3): p. 648-659.
4. LaLonde, A.D., et al., *Lead telluride alloy thermoelectrics*. Materials Today, 2011. **14**(11): p. 526-532.
5. Khshanovska, O., T. Parashchuk, and I. Horichok, *Estimating the upper limit of the thermoelectric figure of merit in n- and p-type PbTe*. Materials Science in Semiconductor Processing, 2023. **160**: p. 107428.
6. Liu, W.-S., et al., *Thermoelectric Property Studies on Cu-Doped n-type $Cu_xBi_2Te_{2.7}Se_{0.3}$ Nanocomposites*. Advanced Energy Materials, 2011. **1**(4): p. 577-587.
7. Poudel, B., et al., *High-Thermoelectric Performance of Nanostructured Bismuth Antimony Telluride Bulk Alloys*. Science, 2008. **320**(5876): p. 634-638.
8. Chen, S. and Z. Ren, *Recent progress of half-Heusler for moderate temperature thermoelectric applications*. Materials Today, 2013. **16**(10): p. 387-395.
9. Han, Z., et al., *Room-temperature thermoelectric materials: Challenges and a new paradigm*. Journal of Materiomics, 2022. **8**(2): p. 427-436.
10. Settaluri, K.T., H. Lo, and R.J. Ram, *Thin Thermoelectric Generator System for Body Energy Harvesting*. Journal of Electronic Materials, 2012. **41**(6): p. 984-988.
11. da Rosa, A.V. and J.C. Ordóñez, *Chapter 5 - Thermoelectricity*, in *Fundamentals of Renewable Energy Processes (Fourth Edition)*, A.V. da Rosa and J.C. Ordóñez, Editors. 2022, Academic Press: Oxford. p. 187-247.
12. Beekman, M., et al., *Charge Transfer in Thermoelectric Nanocomposites: Power Factor Enhancements and Model Systems*, in *Advanced Thermoelectric Materials*. 2019. p. 1-34.
13. Shanks, H.R., et al., *Thermal Conductivity of Silicon from 300 to 1400 K*. Physical Review, 1963. **130**(5): p. 1743-1748.

14. Wirths, S., D. Buca, and S. Mantl, *Si–Ge–Sn alloys: From growth to applications*. Progress in Crystal Growth and Characterization of Materials, 2016. **62**(1): p. 1-39.
15. Wirths, S., et al., *Lasing in direct-bandgap GeSn alloy grown on Si*. Nature Photonics, 2015. **9**(2): p. 88-92.
16. Khatami, S.N. and Z. Aksamija, *Lattice Thermal Conductivity of the Binary and Ternary Group-IV Alloys Si-Sn, Ge-Sn, and Si-Ge-Sn*. Physical Review Applied, 2016. **6**(1): p. 014015.
17. Wirths, S., et al., *Reduced pressure CVD growth of Ge and Ge_{1-x}Sn_x alloys*. Journal of Solid State Science and Technology, 2013. **2**: p. N99-N102.
18. Rubin, S., T.O. Passell, and L.E. Bailey, *Chemical Analysis of Surfaces by Nuclear Methods*. Analytical Chemistry, 1957. **29**(5): p. 736-743.
19. Spirito, D., et al., *Thermoelectric Efficiency of Epitaxial GeSn Alloys for Integrated Si-Based Applications: Assessing the Lattice Thermal Conductivity by Raman Thermometry*. ACS Applied Energy Materials, 2021. **4**(7): p. 7385-7392.
20. Cahill, D.G. and R.O. Pohl, *Thermal conductivity of amorphous solids above the plateau*. Physical Review B, 1987. **35**(8): p. 4067-4073.
21. Chimienti, A.A., *3-omega method for thermal conductivity measurements of GeSn thin films in multilayer structures*, in *Physics department*. 2021, Università di Pisa: Pisa. p. 78.
22. Duquesne, J.Y., D. Fournier, and C. Frétygny, *Analytical solutions of the heat diffusion equation for 3 ω method geometry*. Journal of Applied Physics, 2010. **108**(8): p. 086104.
23. Cahill, D.G., M. Katiyar, and J.R. Abelson, *Thermal conductivity of a-Si:H thin films*. Physical Review B, 1994. **50**(9): p. 6077-6081.
24. Je-Hyeong Bahk, T.F., Ali Shakouri, *Thin Film Thermoelectric Characterization Techniques*, in *Annual Review of Heat Transfer*. 2013, Begell House Inc.: New York. p. 51-99.
25. Concepción, O., et al., *Isothermal Heteroepitaxy of Ge_{1-x}Sn_x Structures for Electronic and Photonic Applications*. ACS Applied Electronic Materials, 2023. **5**(4): p. 2268-2275.
26. Krause, O., *Investigation of Si-based GeSn/SiGeSn Semiconductors for Thermoelectric Applications*, in *Faculty of Mathematics, Computer Science and Natural Sciences*. 2022, RWTH Aachen University: Aachen, Germany. p. 65.
27. Lee, S.M. and D.G. Cahill, *Heat transport in thin dielectric films*. Journal of Applied Physics, 1997. **81**(6): p. 2590-2595.

List of tables

Table 1 Set of samples to compare the thermal conductivity for different GeSn thicknesses	54
Table 2 Set of samples to compare the effect of Sn concentration in the thermal conductivity	54
Table 3 Set of samples to measure the TCR	67
Table 4 Linear fit parameters for the Resistance vs. Temperature curve	68
Table 5 Experimental values of the TCR for each measured temperature.....	69
Table 6 Set of samples to compare the <i>SiO2</i> thickness effect on the thermal conductivity	72
Table 7 Results for the thermal conductivity of the GeSn thickness set of samples	78
Table 8 Results of the thermal conductivity for the Sn concentration set of samples	79

List of figures

Fig. 1 State of the art thermoelectric materials as for 2010 [3]	27
Fig. 2 State of art of common thermoelectric materials as for 2011 [4]	27
Fig. 3 Half-Heusler thermoelectric materials compared to nanostructured compounds [8]	28
Fig. 4 Thermal conductivity of SiGe, GeSn, and SiSn alloys at different concentrations [16].	32
Fig. 5 Schematic of the reaction chamber of the CVD machine as shown in [17]	34
Fig. 6 GeSn thin film grown over a Ge buffer on a Si substrate	34
Fig. 7 Schematic drawing of RBS apparatus taken from [18].....	36
Fig. 8 Schematic of RBS technique.....	37
Fig. 9 RBS experimental over simulation curve for the reference sample	39
Fig. 10 Schematic drawing of the XRD technique	41
Fig. 11 XRD ω - 2θ rocking curves for GeSn/Ge/Si samples as shown in [19].....	41
Fig. 12 Schematic drawing of the device for the 3ω method as presented by Cahill and Pohl in [20] .	42
Fig. 13 Device for Seebeck coefficient and Thermal conductivity differential measurements, as shown in [24]......	49
Fig. 14 Schematic of the cross-section view of a thin film electrical conductivity measuring device as shown in [24]	52
Fig. 15 (left) Grow rate as a function of Sn content for different reactor pressure (P) and total gas flow (QT) values. (right) Sn content as a function of the total gas flow (QT) at different temperatures as shown in [25].	53
Fig. 16 RBS spectrum from GeSn-thickness set samples	55
Fig. 17 RBS spectrum from Sn-concentration set samples	56
Fig. 18 XRD curves from GeSn-thickness set samples	57
Fig. 19 XRD curves from Sn-concentration set samples	58
Fig. 20 Bonding map for the K device within the chip carrier.....	59
Fig. 21 K device sample glued and bonded to the chip carrier.....	59
Fig. 22 Connections diagram between the chip carrier, the PCB and the Lock-in amplifier for the Frequency scan measurement and the Resistance measurement for the K device.....	61
Fig. 23 GeSn sample with a K device on top. The green and golden materials are Cr and Au respectively.....	66
Fig. 24 Microscope images from the K device in a full view (left) and the heater stripe (right) for the 1000x10 device.....	66

Fig. 25 Resistance vs. Temperature for 5 different devices	67
Fig. 26 TCR vs. Temperature plot of Au/Cr.....	68
Fig. 27 $Re\{V3\omega\}$ vs. Frequency for the Sn-concentration set of samples	70
Fig. 28 $Im\{V3\omega\}$ vs. Frequency for the Sn-concentration set of samples.....	71
Fig. 29 Linear fit of the $\ln V3\omega$ vs. $\ln V1\omega$ for the in-phase component.....	72
Fig. 30 Image from TEM for the 300nm <i>GeSn</i> layer (left) and the 50nm <i>SiO2</i> layer (right)	73
Fig. 31 Image from TEM for the 300nm <i>GeSn</i> layer (left) and the 100nm <i>SiO2</i> layer (right)	73
Fig. 32 Image from TEM for the 300nm <i>GeSn</i> layer (left) and the 200nm <i>SiO2</i> layer (right)	74
Fig. 33 Image from TEM for the 300nm <i>GeSn</i> layer (left) and the 300nm <i>SiO2</i> layer (right)	74
Fig. 34 Thermal conductivity on a 310nm <i>GeSn</i> at 12% Sn concentration for different <i>SiO2</i> thicknesses.....	75
Fig. 35 Thermal conductivity for different <i>SiO2</i> thicknesses on the same <i>GeSn</i> wafer	75
Fig. 36 Thermal conductivity of <i>SiO2</i> films at 78K and 300K for different thicknesses as shown in [27]	76
Fig. 37 Thermal conductivity of the GeSn thickness set of samples	78
Fig. 38 Thermal conductivity for the Sn concentration set of samples compared to the theoretical results and previous experimental results.....	79
Fig. 39 Change in temperature for each dimension in the K-device for different Sn concentrations ...	80
Fig. 40 GeSn sample with a K-S device. A cut was made to show the inner contact pads.....	81
Fig. 41 Microscope images of the Al/Ti deposition for the Seebeck contact pads	82
Fig. 42 Microscope images of the second SiO ₂ deposition to insulate one of the Seebeck contacts .	83
Fig. 43 Microscope image of the resist after exposition for the deposition of the heater	84
Fig. 44 Microscope image of the finished device after the Au/Cr deposition.....	85
Fig. 45 Bottom left corner of a sample with K-S devices (Highest non-uniformity).....	86
Fig. 46 Bottom left corner of a sample with K-S devices (Low non-uniformity)	86
Fig. 47 5 μm wire heater for a K-S device	87
Fig. 48 5 μm wire complete K-S device	88
Fig. 49 2 μm wire heater for a K-S device	88
Fig. 50 2 μm wire complete K-S device	89
Fig. 51 Chip containing 4 K-S devices with different dimensions.....	89
Fig. 52 GeSn sample with a σ device on top. A cut was made to show the GeSn mesa	90

Complements

Python scripts

utils.py

```
def base_message(msg,sym=' ',fg_color='',bg_color='',style=''):
    print(fg_color,bg_color,style,f"\n{sym}{sym} {msg}\n",'\x1b[0m')

def welcome_message():
    base_message("""
*** 3-OMEGA MEASUREMENTS ***
Zurich lockin MFLI

Before running this script you should have already run "LabOne User Interface"!
If not press Ctrl+c to abort the execution.
""",',',colors.fg.lightblue)

def general_message(msg,marker = '>', fg_color = '\x1b[1;33m', bg_color = '',style
= ''):
    base_message(msg,marker,fg_color,bg_color,style)

def error_message(msg):
    base_message(msg,"!",colors.fg.lightred)

def info_message(msg):
    base_message(msg,"*",colors.fg.lightblue)

def success_message(msg):
    base_message(msg,"+",colors.fg.lightgreen)

def plain_message(msg):
    base_message(msg)

class colors:

    # '''Colors class:reset all colors with colors.reset; two
    # sub classes fg for foreground
    # and bg for background; use as colors.subclass.colorname.
    # i.e. colors.fg.red or colors.bg.greenalso, the generic bold, disable,
    # underline, reverse, strike through,
    # and invisible work with the main class i.e. colors.bold'''

    reset = '\x1b[0m'
    bold = '\x1b[01m'
    disable = '\x1b[02m'
    underline = '\x1b[04m'
    reverse = '\x1b[07m'
    strikethrough = '\x1b[09m'
```

```

invisible = '\x1b[08m'

class fg:
    black = '\x1b[30m'
    red = '\x1b[31m'
    green = '\x1b[32m'
    orange = '\x1b[33m'
    blue = '\x1b[34m'
    purple = '\x1b[35m'
    cyan = '\x1b[36m'
    lightgrey = '\x1b[1;37m'
    darkgrey = '\x1b[1;30m'
    lightred = '\x1b[1;31m'
    lightgreen = '\x1b[1;32m'
    yellow = '\x1b[1;33m'
    lightblue = '\x1b[1;34m'
    pink = '\x1b[1;35m'
    lightcyan = '\x1b[1;36m'

class bg:
    black = '\x1b[40m'
    red = '\x1b[41m'
    green = '\x1b[42m'
    orange = '\x1b[43m'
    blue = '\x1b[44m'
    purple = '\x1b[45m'
    cyan = '\x1b[46m'
    lightgrey = '\x1b[47m'

```

TE_measurement.py

```

# Import libraries
import signal,sys
import time
import os
from datetime import datetime
import numpy as np
import matplotlib.pyplot as plt
from scipy.optimize import curve_fit
import tkinter as tk
from tkinter import filedialog as fd
from tkinter import messagebox as mb
from src import utils as te_u
from src.utils import colors as te_c

# Load options
def load_options():

    options = {

        "device_id": "dev5845",

        "api_level": 6,

        "server_host": "192.168.91.86",

```

```

"server_port": 8004,
"resistance":{
    "f_value": 100, # Hz
    "v_from": 0, # Vpk
    "v_to": 1, # Vpk
    "num_pts": 10,
    "num_pts_for_avg": 1,
    "t_sleep": 1
},
"frequency": {
    "v_value": 3, # Vpk
    "f_from": 2000, # Hz
    "f_to": 20000, # Hz
    "num_pts": 50,
    "num_pts_for_avg": 10,
    "t_sleep": 0.5
},
"voltage": {
    "f_value": 1000, # Hz
    "v_from": 0, # Vpk
    "v_to": 5, # Vpk
    "num_pts": 50,
    "num_pts_for_avg": 10,
    "t_sleep": 0.5
}
}

return options

# Check zhinst installation
try:
    import zhinst.utils
except ModuleNotFoundError:

```

```

    te_u.error_message("module 'zhinst' is not installed. Try running: pip install
zhinst")
    sys.exit()

# On abort event handler
def signal_handling(signum, frame):
    print("Program aborted! (>_<)")
    # Turn the voltage off
    sys.exit()

signal.signal(signal.SIGINT, signal_handling)

# Configure GUI
root = tk.Tk()
root.wm_attributes('-topmost', 1)
root.withdraw()
filename = ""
filedir = ""
filename_no_ext = ""

# Load options
opt = load_options()

# Welcome message
te_u.welcome_message()

# Stablish connection.
# Call a zhinst utility function that returns:
# - an API session `daq` in order to communicate with devices via the data
server.
# - the device ID string that specifies the device branch in the server's node
hierarchy.
# - the device's discovery properties.
te_u.general_message(
f"""Stablishing connection with the Lock-in Amplifier
Device id: \t{opt['device_id']}
Server host:\t{opt['server_host']}
Server port:\t{opt['server_port']}
Api level: \t{opt['api_level']}
...wait a moment please...""")

try:
    (daq, device, props) = zhinst.utils.create_api_session(
        opt["device_id"],
        opt["api_level"],
        opt["server_host"],
        opt["server_port"]
    )
    zhinst.utils.api_server_version_check(daq)
except:
    te_u.error_message(
    """Connection failed.
- Check the device is on and connected properly.
- Check the LabOne User Interface is running.
- Check the connection options at src/options.py are correct""")
    sys.exit()

# Enable the API's log.
# uncomment the following line to enable the API's log.
# daq.setDebugLevel(3)

```



```

# Create a base configuration: Disable all available outputs, awgs, demods,
scopes,...
# uncomment the following line only if it's safe to disable everything
# zhinst.utils.disable_everything(daq, device)

te_u.success_message("Connection stablished :)")

measurement = 1

while measurement != 0 :

    te_u.general_message(
    """Choose an option to measure:

        - 1 3w V vs Frequency
        - 2 3w V vs Voltage

        - 3 2w V vs Frequency
        - 4 2w V vs Voltage

        - 5 I vs V

        - 9 Close all plots

    - 0 Exit Program
    """)
    )

    measurement_str = input("Write the number of the desired option: ")
    try:
        measurement = float(measurement_str)
    except:
        te_u.info_message("Invalid option, try again.")
        continue

    if measurement == 0:
        plt.close('all')
        print("Bye bye :)")
    elif measurement == 1: # Frequency scan code

        te_u.general_message("Initializing measurement...")

        ## Configure the device.
        # Start scopeModule
        scopeModule = daq.scopeModule()

        # Signal output
        # OUTPUT 1 (index 0)
        daq.setInt("/%s/sigouts/0/imp50" % device, 0) #set load impedance OFF (the
impedence of the output is always 50Ohm)
        ampl = opt["frequency"]["v_value"]
        daq.setInt("/%s/sigouts/0/enables/0" % device, 1) #enable output channel 1
        daq.setDouble("/%s/sigouts/0/amplitudes/0" % device, ampl) #set amplitude
Vpk [V]
        daq.setInt("/%s/sigouts/0/autorange" % device, 1) #autorange
        daq.setInt("/%s/sigouts/0/offset" % device, 0) #set offset = 0
        daq.setInt("/%s/sigouts/0/diff" % device, 1) #set differential output ON
        daq.setInt("/%s/sigouts/0/on" % device, 1) #switch on signal output

        # Demodulators (the first demodulator is indexed by 0)

```

```

daq.setInt("/%/demods/0/harmonic" % device,1) #set harmonic
daq.setInt("/%/demods/2/harmonic" % device,1)
daq.setDouble("/%/demods/0/phaseshift" % device,0) #set phaseshift=0°
daq.setDouble("/%/demods/2/phaseshift" % device,0)
daq.setInt("/%/demods/0/order" % device,4)
daq.setInt("/%/demods/1/order" % device,4) #set low pass filter order
daq.setInt("/%/demods/2/order" % device,4)
daq.setDouble("/%/demods/0/timeconstant" % device,0.1)
daq.setDouble("/%/demods/1/timeconstant" % device,0.1) #set time constant

[s]
daq.setDouble("/%/demods/2/timeconstant" % device,0.1)
# adjusting the phase according to the 1 Omega signal
daq.setInt("/%/demods/0/phaseadjust" % device,1)
daq.setInt("/%/demods/2/phaseadjust" % device,1) #autophase

# 3 Omega measurements
daq.setInt("/%/demods/2/harmonic" % device,3) # for measuring 3 Omega

signal
# daq.setInt("/%/demods/0/sinc" % device,1) #Enable sinc filter

## V3omega vs frequency measurement
Npt = opt["frequency"]["num_pts"]
f1 = opt["frequency"]["f_from"]
f2 = opt["frequency"]["f_to"]

fv = np.logspace(np.log10(f1),np.log10(f2),Npt)
daq.setDouble("/%/oscs/0/freq" % device, fv[0])
time.sleep(5)

# Perform a global synchronisation between the device and the data server:
# Ensure that the signal input and output configuration has taken effect
# before calculating the signal input autorange.
daq.sync()

X1v = []
Y1v = []
X3v = []
Y3v = []

## Plot parameters
# Further options:
https://matplotlib.org/3.5.1/api/_as_gen/matplotlib.pyplot.plot.html
markerfacecolors = ['none','none']
markeredgecolors = ['red','blue']
markers = ['o','o']
markersizes = [5,5]
labels = [r'$V_{3x}$',r'$V_{3y}$']

x_label = r'Frequency [Hz]'
y_label = r'Voltage [V]'

fig, axis = plt.subplots(1,1)
axis.set_xlabel(x_label)
axis.set_ylabel(y_label)
#axis.set_xscale('log')
# Uncomment to set axis limits (see line axis.relim() below)
# axis.set_ylim([0, 100])
# axis.set_xlim([0, 100])

# Open file to save data

```

```

        data = [('Data file (*.dat)', '*.dat'),('Text file (*.txt)', '*.txt'),('All
files', '*.*')]
        f = fd.asksaveasfile(mode = 'w', defaultextension = data, confirmoverwrite
= True, filetypes = data, title = 'Save calculation results to a file', parent =
root, initialfile = filename, initialdir = filedir)
        if f == None:
            filename_no_ext = "freq_scan"+datetime.now().strftime("%y-%m-
%d_%H_%M_%S")
            filename = filename_no_ext+".dat"
            filedir = "measurements"

            if not os.path.isdir(filedir):
                os.makedirs(filedir)

            f = open(filedir+"/"+filename, 'w+')
            te_u.info_message("Your data file was saved at "+filedir+"/"+filename)
        else:
            filedir = os.path.dirname(f.name)
            filename = os.path.basename(f.name)
            filename_no_ext = os.path.splitext(filename)[0]

plt.ion()

te_u.general_message("Measuring...")

for ii in range(len(fv)):
    ff = fv[ii]
    daq.setDouble("/%s/oscs/0/freq" % device, ff)
    time.sleep(opt["frequency"]["t_sleep"])

    NN = opt["frequency"]["num_pts_for_avg"] # Averaging over NN
measurement values, this number can be changed to adjust the measurement speed and
accuracy
    V1XX = 0
    V1YY = 0
    V3XX = 0
    V3YY = 0

    for jj in range(NN):
        sample1 = daq.getSample("/%s/demods/0/sample" % device) #Get
measurement result
        sample3 = daq.getSample("/%s/demods/2/sample" % device) #Get
measurement result
        V1XX = V1XX + sample1['x']
        V1YY = V1YY + sample1['y']
        V3XX = V3XX + sample3['x']
        V3YY = V3YY + sample3['y']

    # Append new data to arrays
    X1v.append(V1XX/NN)
    Y1v.append(V1YY/NN)
    X3v.append(V3XX/NN)
    Y3v.append(V3YY/NN)

    axis.set_title(f"Progress of data acquisition:
{float(ii+1)/Npt*100:.2f}%.")

    te_u.general_message(f"\tProgress: {float(ii+1)/Npt*100:.2f}%")

    # Plot new data (point by point)

```

```

axis.plot(
    ff,
    V3XX/NN,
    color='none',
    markerfacecolor = markerfacecolors[0],
    markeredgecolor = markeredgecolors[0],
    marker=markers[0],
    markersize=markersizes[0],
    label=labels[0]
)

axis.plot(
    ff,
    V3YY/NN,
    color='none',
    markerfacecolor = markerfacecolors[1],
    markeredgecolor = markeredgecolors[1],
    marker=markers[1],
    markersize=markersizes[1],
    label=labels[1]
)

axis.set_xscale('log')

# Auto axis limits
axis.relim()

plt.pause(0.01)
if(ii == 0):
    axis.legend()

## Write data to file
# Set data and headers to be written to file
data_to_write =[fv[ii],X1v[ii],Y1v[ii],X3v[ii],Y3v[ii]]
headers = ["freq", "V1X", "V1Y", "V3X", "V3Y"]

if(ii==0):
    for k,h in enumerate(headers):
        f.write(h)
        if k != len(headers)-1:
            f.write("\t")
        f.write("\n")

    for j,e1 in enumerate(data_to_write):
        # Adjust precision of data ex. {var:.2f} for 2 decimal places
        f.write(f"{float(e1):.8f}")
        if j != len(data_to_write)-1:
            f.write("\t")
        f.write("\n")

f.close()

daq.setInt("/%s/sigouts/0/on" % device, 0) #switch off signal output

axis.set_title("Frequency Scan Measurement")

plt.pause(0.01)

plt.savefig(filedir + "/" + filename_no_ext + ".jpg", dpi=300)
plt.ioff()

```

```

f_config = open(filedir + "/" + filename_no_ext + "_config.txt", "w+")
for k,v in opt["frequency"].items():
    f_config.write(k+"\t"+str(v)+"\n")
f_config.close()

# Comment the following line to close the plot after acquisition
plt.show()

elif measurement == 2: # Voltage scan code

    te_u.general_message("Initializing measurement...")

    ## Configure the device.
    # Start scopeModule
    scopeModule = daq.scopeModule()

    # Set frequency
    freq = opt["voltage"]["f_value"]
    daq.setDouble("/%s/oscs/0/freq" % device, freq)

    # Signal output
    # OUTPUT 1 (index 0)
    daq.setInt("/%s/sigouts/0/imp50" % device, 0) #set load impedance OFF (the
impedance of the output is always 50ohm)
    ampl = 4
    daq.setDouble("/%s/sigouts/0/amplitudes/0" % device, ampl) #set amplitude
Vpk [V]
    daq.setInt("/%s/sigouts/0/autorange" % device, 1) #autorange
    daq.setInt("/%s/sigouts/0/enables/0" % device, 1) #enable output channel 1
    daq.setInt("/%s/sigouts/0/offset" % device, 0) #set offset = 0 V
    daq.setInt("/%s/sigouts/0/diff" % device, 1) #set differential output ON
    daq.setInt("/%s/sigouts/0/on" % device, 1) #switch on signal output

    # Demodulators (the first demodulator is indexed by 0)
    daq.setInt("/%s/demods/0/harmonic" % device,1) #set harmonic
    daq.setInt("/%s/demods/2/harmonic" % device,1)
    daq.setDouble("/%s/demods/0/phaseshift" % device,0) #set phaseshift=0°
    daq.setDouble("/%s/demods/2/phaseshift" % device,0)
    daq.setInt("/%s/demods/0/order" % device,4)
    daq.setInt("/%s/demods/1/order" % device,4) #set low pass filter order
    daq.setInt("/%s/demods/2/order" % device,4)
    daq.setDouble("/%s/demods/0/timeconstant" % device,0.1)
    daq.setDouble("/%s/demods/1/timeconstant" % device,0.1) #set time constant
[s]
    daq.setDouble("/%s/demods/2/timeconstant" % device,0.1)
    daq.setInt("/%s/demods/0/phaseadjust" % device,1)
    daq.setInt("/%s/demods/2/phaseadjust" % device,1) #autophase
    daq.setInt("/%s/demods/2/harmonic" % device,3)
    # daq.setInt("/%s/demods/0/sinc" % device,1) #Enable sinc filter

    # Signal input
    # VOLTAGE INPUT 1
    daq.setDouble("/%s/sigins/0/scaling" % device,1) #set scaling = 1 V/V
    daq.setInt("/%s/sigins/0/ac" % device,0) #AC coupling OFF
    daq.setInt("/%s/sigins/0/imp50" % device,0) #OFF=10MOhm
    daq.setInt("/%s/sigins/0/float" % device,0) #GROUND connection (floating
connection OFF)
    daq.setInt("/%s/sigins/0/diff" % device,1) #set differential measurements
    # daq.setInt("/%s/sigins/0/autorange" % device,1) #autorange
    daq.setDouble("/%s/sigins/0/range" % device,1) #Set range [V]

```

```

## V3omega vs Vinput measurement
Npt = opt["voltage"]["num_pts"]
V1 = opt["voltage"]["v_from"] #Vpk values!
V2 = opt["voltage"]["v_to"]

Vv = np.linspace(V1,V2,Npt)
daq.setDouble("/%s/sigouts/0/amplitudes/0" % device, V1)
time.sleep(5)

# Perform a global synchronisation between the device and the data server:
# Ensure that the signal input and output configuration has taken effect
# before calculating the signal input autorange.
daq.sync()

X1v = []
Y1v = []
X3v = []
Y3v = []

## Plot parameters
# Further options:
https://matplotlib.org/3.5.1/api/\_as\_gen/matplotlib.pyplot.plot.html
markerfacecolors = ['none', 'none']
markeredgecolors = ['red', 'blue']
markers = ['o', 'o']
markersizes = [5,5]
labels = [r'$V_{3x}$', r'$V_{3y}$']

x_label = r'$1\omega$ Voltage$ [V]'
y_label = r'$3\omega$ Voltage$ [V]'

fig, axis = plt.subplots(1,1)
axis.set_xlabel(x_label)
axis.set_ylabel(y_label)
# Uncomment to set axis limits (see line axis.relim() below)
# axis.set_ylim([0, 100])
# axis.set_xlim([0, 100])

# Open file to save data
data = [('Data file (*.dat)', '*.dat'), ('Text file (*.txt)', '*.txt'), ('All
files', '*.*')]
f = fd.asksaveasfile(mode = 'w', defaultextension = data, confirmoverwrite
= True, filetypes = data, title = 'Save calculation results to a file', parent =
root, initialfile = filename, initialdir = filedir)
if f == None:
    filename_no_ext = "voltage_scan"+datetime.now().strftime("%y-%m-
%d_%H_%M_%S")
    filename = filename_no_ext+".dat"
    filedir = "measurements"

    if not os.path.isdir(filedir):
        os.makedirs(filedir)

    f = open(filedir+"/"+filename, 'w+')
    te_u.info_message("Your data file was saved at "+filedir+"/"+filename)
else:

```

```

        filedir = os.path.dirname(f.name)
        filename = os.path.basename(f.name)
        filename_no_ext = os.path.splitext(filename)[0]

plt.ion()

te_u.general_message("Measuring...")

for ii in range(len(Vv)):
    Vv = Vv[ii]
    daq.setDouble("/%s/sigouts/0/amplitudes/0" % device, Vv)
    time.sleep(opt["voltage"]["t_sleep"])

    NN = opt["voltage"]["num_pts_for_avg"]
    V1XX = 0
    V1YY = 0
    V3XX = 0
    V3YY = 0

    for jj in range(NN):
        sample1 = daq.getSample("/%s/demods/0/sample" % device) #Get
measurement result
        sample3 = daq.getSample("/%s/demods/2/sample" % device) #Get
measurement result
        V1XX = V1XX + sample1['x']
        V1YY = V1YY + sample1['y']
        V3XX = V3XX + sample3['x']
        V3YY = V3YY + sample3['y']

    # Append new data to arrays
    X1v.append(V1XX/NN)
    Y1v.append(V1YY/NN)
    X3v.append(V3XX/NN)
    Y3v.append(V3YY/NN)

    axis.set_title(f"Progress of data acquisition:
{float(ii+1)/Npt*100:.2f}%.")

    te_u.general_message(f"\tProgress: {float(ii+1)/Npt*100:.2f}%")

# Plot new data (point by point)
axis.plot(
    Vv,
    V3XX/NN,
    color='none',
    markerfacecolor = markerfacecolors[0],
    markeredgecolor = markeredgecolors[0],
    marker=markers[0],
    markersize=markersizes[0],
    label=labels[0]
)

axis.plot(
    Vv,
    V3YY/NN,
    color='none',
    markerfacecolor = markerfacecolors[1],
    markeredgecolor = markeredgecolors[1],
    marker=markers[1],

```

```

        markersize=markersizes[1],
        label=labels[1]
    )

    # Auto axis limits
    axis.relim()

    plt.pause(0.01)
    if(ii == 0):
        axis.legend()

    ## Write data to file
    # Set data and headers to be written to file
    data_to_write = [Vv[ii],X3v[ii],Y3v[ii]]
    headers = ["V1", "V3X", "V3Y"]

    if(ii==0):
        for k,h in enumerate(headers):
            f.write(h)
            if k != len(headers)-1:
                f.write("\t")
            f.write("\n")

        for j,e1 in enumerate(data_to_write):
            # Adjust precision of data ex. {var:.2f} for 2 decimal places
            f.write(f"{float(e1):.8f}")
            if j != len(data_to_write)-1:
                f.write("\t")
            f.write("\n")

    f.close()

    daq.setInt("/%s/sigouts/0/on" % device, 0) #switch off signal output

    axis.set_title("Voltage Scan Measurement")

    plt.pause(0.01)

    plt.savefig(filedir + "/" + filename_no_ext + ".jpg", dpi=300)
    plt.ioff()

    f_config = open(filedir + "/" + filename_no_ext + "_config.txt", "w+")
    for k,v in opt["voltage"].items():
        f_config.write(k+"\t"+str(v)+"\n")
    f_config.close()

    # Comment the following line to close the plot after acquisition
    plt.show()

elif measurement == 3: # Seebeck Frequency

    te_u.general_message("Initializing measurement...")

    ## Configure the device.
    # Start scopeModule
    scopeModule = daq.scopeModule()

    # Signal output
    # OUTPUT 1 (index 0)
    daq.setInt("/%s/sigouts/0/imp50" % device, 0) #set load impedance OFF (the
impedence of the output is always 500hm)

```



```

    ampl = opt["frequency"]["v_value"]
    daq.setInt("/%s/sigouts/0/enables/0" % device, 1) #enable output channel 1
    daq.setDouble("/%s/sigouts/0/amplitudes/0" % device, ampl) #set amplitude
Vpk [V]
    daq.setInt("/%s/sigouts/0/autorange" % device, 1) #autorange
    daq.setInt("/%s/sigouts/0/offset" % device, 0) #set offset = 0
    daq.setInt("/%s/sigouts/0/diff" % device, 1) #set differential output ON
    daq.setInt("/%s/sigouts/0/on" % device, 1) #switch on signal output

# Demodulators (the first demodulator is indexed by 0)
    daq.setInt("/%s/demods/0/harmonic" % device,1) #set harmonic
    daq.setInt("/%s/demods/2/harmonic" % device,1)
    daq.setDouble("/%s/demods/0/phaseshift" % device,0) #set phaseshift=0°
    daq.setDouble("/%s/demods/2/phaseshift" % device,0)
    daq.setInt("/%s/demods/0/order" % device,4)
    daq.setInt("/%s/demods/1/order" % device,4) #set low pass filter order
    daq.setInt("/%s/demods/2/order" % device,4)
    daq.setDouble("/%s/demods/0/timeconstant" % device,0.1)
    daq.setDouble("/%s/demods/1/timeconstant" % device,0.1) #set time constant
[s]
    daq.setDouble("/%s/demods/2/timeconstant" % device,0.1)
    # adjusting the phase according to the 1 Omega signal
    daq.setInt("/%s/demods/0/phaseadjust" % device,1)
    daq.setInt("/%s/demods/2/phaseadjust" % device,1) #autophase

# 3 Omega measurements
    daq.setInt("/%s/demods/2/harmonic" % device,2) # for measuring 3 Omega
signal
    # daq.setInt("/%s/demods/0/sinc" % device,1) #Enable sinc filter

## V3omega vs frequency measurement
    Npt = opt["frequency"]["num_pts"]
    f1 = opt["frequency"]["f_from"]
    f2 = opt["frequency"]["f_to"]

    fv = np.logspace(np.log10(f1),np.log10(f2),Npt)
    daq.setDouble("/%s/oscs/0/freq" % device, fv[0])
    time.sleep(5)

# Perform a global synchronisation between the device and the data server:
# Ensure that the signal input and output configuration has taken effect
# before calculating the signal input autorange.
    daq.sync()

    X1v = []
    Y1v = []
    X2v = []
    Y2v = []

## Plot parameters
    # Further options:
https://matplotlib.org/3.5.1/api/\_as\_gen/matplotlib.pyplot.plot.html
    markerfacecolors = ['none', 'none']
    markeredgecolors = ['red', 'blue']
    markers = ['o', 'o']
    markersizes = [5,5]
    labels = [r'$V_{2x}$', r'$V_{2y}$']

    x_label = r'Frequency [Hz]'
    y_label = r'Voltage [V]'

```

```

fig, axis = plt.subplots(1,1)
axis.set_xlabel(x_label)
axis.set_ylabel(y_label)
#axis.set_xscale('log')
# Uncomment to set axis limits (see line axis.relim() below)
# axis.set_ylim([0, 100])
# axis.set_xlim([0, 100])

# Open file to save data
data = [('Data file (*.dat)', '*.dat'),('Text file (*.txt)', '*.txt'),('All
files', '*.*')]
f = fd.asksaveasfile(mode = 'w', defaultextension = data, confirmoverwrite
= True, filetypes = data, title = 'Save calculation results to a file', parent =
root, initialfile = filename, initialdir = filedir)
if f == None:
    filename_no_ext = "seebeck_freq_scan"+datetime.now().strftime("%y-%m-
%d_%H_%M_%S")
    filename = filename_no_ext+".dat"
    filedir = "measurements"

    if not os.path.isdir(filedir):
        os.makedirs(filedir)

    f = open(filedir+"/"+filename,'w+')
    te_u.info_message("Your data file was saved at "+filedir+"/"+filename)
else:
    filedir = os.path.dirname(f.name)
    filename = os.path.basename(f.name)
    filename_no_ext = os.path.splitext(filename)[0]

plt.ion()

te_u.general_message("Measuring...")

for ii in range(len(fv)):
    ff = fv[ii]
    daq.setDouble("/%s/oscs/0/freq" % device, ff)
    time.sleep(opt["frequency"]["t_sleep"])

    NN = opt["frequency"]["num_pts_for_avg"] # Averaging over NN
measurement values, this number can be changed to adjust the measurement speed and
accuracy
    V1XX = 0
    V1YY = 0
    V2XX = 0
    V2YY = 0

    for jj in range(NN):
        sample1 = daq.getSample("/%s/demods/0/sample" % device) #Get
measurement result
        sample2 = daq.getSample("/%s/demods/2/sample" % device) #Get
measurement result
        V1XX = V1XX + sample1['x']
        V1YY = V1YY + sample1['y']
        V2XX = V2XX + sample2['x']
        V2YY = V2YY + sample2['y']

# Append new data to arrays

```

```

X1v.append(V1XX/NN)
Y1v.append(V1YY/NN)
X2v.append(V2XX/NN)
Y2v.append(V2YY/NN)

axis.set_title(f"Progress of data acquisition:
{float(ii+1)/Npt*100:.2f}%.")

te_u.general_message(f"\tProgress: {float(ii+1)/Npt*100:.2f}%")

# Plot new data (point by point)
axis.plot(
    ff,
    V2XX/NN,
    color='none',
    markerfacecolor = markerfacecolors[0],
    markeredgecolor = markeredgecolors[0],
    marker=markers[0],
    markersize=markersizes[0],
    label=labels[0]
)

axis.plot(
    ff,
    V2YY/NN,
    color='none',
    markerfacecolor = markerfacecolors[1],
    markeredgecolor = markeredgecolors[1],
    marker=markers[1],
    markersize=markersizes[1],
    label=labels[1]
)

axis.set_xscale('log')

# Auto axis limits
axis.relim()

plt.pause(0.01)
if(ii == 0):
    axis.legend()

## Write data to file
# Set data and headers to be written to file
data_to_write =[fv[ii],X1v[ii],Y1v[ii],X2v[ii],Y2v[ii]]
headers = ["freq", "V1X", "V1Y", "V2X", "V2Y"]

if(ii==0):
    for k,h in enumerate(headers):
        f.write(h)
        if k != len(headers)-1:
            f.write("\t")
        f.write("\n")

for j,el in enumerate(data_to_write):
    # Adjust presicion of data ex. {var:.2f} for 2 decimal places
    f.write(f"{float(el):.8f}")
    if j != len(data_to_write)-1:
        f.write("\t")
f.write("\n")

```

```

f.close()

daq.setInt("/s/sigouts/0/on" % device, 0) #switch off signal output

axis.set_title("Seebeck Frequency Scan Measurement")

plt.pause(0.01)

plt.savefig(filedir + "/" + filename_no_ext + ".jpg", dpi=300)
plt.ioff()

f_config = open(filedir + "/" + filename_no_ext + "_config.txt", "w+")
for k,v in opt["frequency"].items():
    f_config.write(k+"\t"+str(v)+"\n")
f_config.close()

# Comment the following line to close the plot after acquisition
plt.show()

elif measurement == 4: # Seebeck Voltage

    te_u.general_message("Initializing measurement...")

    ## Configure the device.
    # Start scopeModule
    scopeModule = daq.scopeModule()

    # Set frequency
    freq = opt["voltage"]["f_value"]
    daq.setDouble("/s/oscs/0/freq" % device, freq)

    # Signal output
    # OUTPUT 1 (index 0)
    daq.setInt("/s/sigouts/0/imp50" % device, 0) #set load impedance OFF (the
impedence of the output is always 50ohm)
    ampl = 4
    daq.setDouble("/s/sigouts/0/amplitudes/0" % device, ampl) #set amplitude
Vpk [V]
    daq.setInt("/s/sigouts/0/autorange" % device, 1) #autorange
    daq.setInt("/s/sigouts/0/enables/0" % device, 1) #enable output channel 1
    daq.setInt("/s/sigouts/0/offset" % device, 0) #set offset = 0 V
    daq.setInt("/s/sigouts/0/diff" % device, 1) #set differential output ON
    daq.setInt("/s/sigouts/0/on" % device, 1) #switch on signal output

    # Demodulators (the first demodulator is indexed by 0)
    daq.setInt("/s/demods/0/harmonic" % device,1) #set harmonic
    daq.setInt("/s/demods/2/harmonic" % device,1)
    daq.setDouble("/s/demods/0/phaseshift" % device,0) #set phaseshift=0°
    daq.setDouble("/s/demods/2/phaseshift" % device,0)
    daq.setInt("/s/demods/0/order" % device,4)
    daq.setInt("/s/demods/1/order" % device,4) #set low pass filter order
    daq.setInt("/s/demods/2/order" % device,4)
    daq.setDouble("/s/demods/0/timeconstant" % device,0.1)
    daq.setDouble("/s/demods/1/timeconstant" % device,0.1) #set time constant
[s]
    daq.setDouble("/s/demods/2/timeconstant" % device,0.1)
    daq.setInt("/s/demods/0/phaseadjust" % device,1)
    daq.setInt("/s/demods/2/phaseadjust" % device,1) #autophase
    daq.setInt("/s/demods/2/harmonic" % device,2)
    # daq.setInt("/s/demods/0/sinc" % device,1) #Enable sinc filter

```

```

# Signal input
# VOLTAGE INPUT 1
daq.setDouble("/%s/sigins/0/scaling" % device,1) #set scaling = 1 V/V
daq.setInt("/%s/sigins/0/ac" % device,0) #AC coupling OFF
daq.setInt("/%s/sigins/0/imp50" % device,0) #OFF=10MOhm
daq.setInt("/%s/sigins/0/float" % device,0) #GROUND connection (floating
connection OFF)
daq.setInt("/%s/sigins/0/diff" % device,1) #set differential measurements
# daq.setInt("/%s/sigins/0/autorange" % device,1) #autorange
daq.setDouble("/%s/sigins/0/range" % device,1) #Set range [V]

## V3omega vs Vinput measurement
Npt = opt["voltage"]["num_pts"]
V1 = opt["voltage"]["v_from"] #Vpk values!
V2 = opt["voltage"]["v_to"]

Vv = np.linspace(V1,V2,Npt)
daq.setDouble("/%s/sigouts/0/amplitudes/0" % device, V1)
time.sleep(5)

# Perform a global synchronisation between the device and the data server:
# Ensure that the signal input and output configuration has taken effect
# before calculating the signal input autorange.
daq.sync()

X1v = []
Y1v = []
X2v = []
Y2v = []

## Plot parameters
# Further options:
https://matplotlib.org/3.5.1/api/\_as\_gen/matplotlib.pyplot.plot.html
markerfacecolors = ['none', 'none']
markeredgecolors = ['red', 'blue']
markers = ['o', 'o']
markersizes = [5,5]
labels = [r'$V_{2x}$', r'$V_{2y}$']

x_label = r'$1\omega$ Voltage$ [V]'
y_label = r'$2\omega$ Voltage$ [V]'

fig, axis = plt.subplots(1,1)
axis.set_xlabel(x_label)
axis.set_ylabel(y_label)
# Uncomment to set axis limits (see line axis.relim() below)
# axis.set_ylim([0, 100])
# axis.set_xlim([0, 100])

# Open file to save data
data = [('Data file (*.dat)', '*.dat'),('Text file (*.txt)', '*.txt'),('All
files', '*.*')]
f = fd.asksaveasfile(mode = 'w', defaultextension = data, confirmoverwrite
= True, filetypes = data, title = 'Save calculation results to a file', parent =
root, initialfile = filename, initialdir = filedir)
if f == None:

```

```

filename_no_ext = "seebeck_voltage_scan"+datetime.now().strftime("%y-
%m-%d_%H_%M_%S")
filename = filename_no_ext+".dat"
filedir = "measurements"

if not os.path.isdir(filedir):
    os.makedirs(filedir)

f = open(filedir+"/"+filename,'w+')
te_u.info_message("Your data file was saved at "+filedir+"/"+filename)
else:
    filedir = os.path.dirname(f.name)
    filename = os.path.basename(f.name)
    filename_no_ext = os.path.splitext(filename)[0]

plt.ion()

te_u.general_message("Measuring...")

for ii in range(len(Vv)):
    Vv = Vv[ii]
    daq.setDouble("/%s/sigouts/0/amplitudes/0" % device, Vv)
    time.sleep(opt["voltage"]["t_sleep"])

    NN = opt["voltage"]["num_pts_for_avg"]
    V1XX = 0
    V1YY = 0
    V2XX = 0
    V2YY = 0

    for jj in range(NN):
        sample1 = daq.getSample("/%s/demods/0/sample" % device) #Get
measurement result
        sample2 = daq.getSample("/%s/demods/2/sample" % device) #Get
measurement result
        V1XX = V1XX + sample1['x']
        V1YY = V1YY + sample1['y']
        V2XX = V2XX + sample2['x']
        V2YY = V2YY + sample2['y']

    # Append new data to arrays
    X1v.append(V1XX/NN)
    Y1v.append(V1YY/NN)
    X2v.append(V2XX/NN)
    Y2v.append(V2YY/NN)

    axis.set_title(f"Progress of data acquisition:
{float(ii+1)/Npt*100:.2f}%.")

    te_u.general_message(f"\tProgress: {float(ii+1)/Npt*100:.2f}%")

    # Plot new data (point by point)
    axis.plot(
        Vv,
        V2XX/NN,
        color='none',
        markerfacecolor = markerfacecolors[0],
        markeredgecolor = markeredgecolors[0],
        marker=markers[0],

```

```

        markersize=markersizes[0],
        label=labels[0]
    )

    axis.plot(
        Vv,
        V2Yy/NN,
        color='none',
        markerfacecolor = markerfacecolors[1],
        markeredgecolor = markeredgecolors[1],
        marker=markers[1],
        markersize=markersizes[1],
        label=labels[1]
    )

    # Auto axis limits
    axis.relim()

    plt.pause(0.01)
    if(ii == 0):
        axis.legend()

    ## Write data to file
    # Set data and headers to be written to file
    data_to_write = [Vv[ii],X2v[ii],Y2v[ii]]
    headers = ["V1", "V2X", "V2Y"]

    if(ii==0):
        for k,h in enumerate(headers):
            f.write(h)
            if k != len(headers)-1:
                f.write("\t")
            f.write("\n")

        for j,e1 in enumerate(data_to_write):
            # Adjust precision of data ex. {var:.2f} for 2 decimal places
            f.write(f"{float(e1):.8f}")
            if j != len(data_to_write)-1:
                f.write("\t")
            f.write("\n")

    f.close()

    daq.setInt("/%s/sigouts/0/on" % device, 0) #switch off signal output

    axis.set_title("Seebeck Voltage Scan Measurement")

    plt.pause(0.01)

    plt.savefig(filedir + "/" + filename_no_ext + ".jpg", dpi=300)
    plt.ioff()

    f_config = open(filedir + "/" + filename_no_ext + "_config.txt", "w+")
    for k,v in opt["voltage"].items():
        f_config.write(k+"\t"+str(v)+"\n")
    f_config.close()

    # Comment the following line to close the plot after acquisition
    plt.show()

elif measurement == 5: # Resistance code

```

```

te_u.general_message("Initializing measurement...")

## Configure the device.
# Start scopeModule
scopeModule = daq.scopeModule()

# Set frequency
freq = opt["resistance"]["f_value"]
daq.setDouble("/%s/oscs/0/freq" % device, freq)

# Signal output
# OUTPUT 1 (index 0)
daq.setInt("/%s/sigouts/0/imp50" % device, 0) #set load impedance OFF (the
impedence of the output is always 50Ohm)
daq.setInt("/%s/sigouts/0/enables/0" % device, 1) #enable output channel 1
ampl = 1
daq.setDouble("/%s/sigouts/0/amplitudes/0" % device, ampl) #set amplitude
Vpk [V]
daq.setInt("/%s/sigouts/0/autorange" % device, 1) #autorange
daq.setInt("/%s/sigouts/0/offset" % device, 0) #set offset = 0 V
daq.setInt("/%s/sigouts/0/diff" % device, 0) #set differential output ON
daq.setInt("/%s/sigouts/0/on" % device, 1) #switch on signal output

# Demodulators (the first demodulator is indexed by 0)
daq.setInt("/%s/demods/0/harmonic" % device,1) #set harmonic
daq.setInt("/%s/demods/1/harmonic" % device,1)
daq.setInt("/%s/demods/2/harmonic" % device,1)
daq.setDouble("/%s/demods/0/phaseshift" % device,0) #set phaseshift=0°
daq.setDouble("/%s/demods/1/phaseshift" % device,0)
daq.setDouble("/%s/demods/2/phaseshift" % device,0)
daq.setInt("/%s/demods/0/order" % device,4)
daq.setInt("/%s/demods/1/order" % device,4) #set low pass filter order
daq.setInt("/%s/demods/2/order" % device,4)
daq.setDouble("/%s/demods/0/timeconstant" % device,0.1)
daq.setDouble("/%s/demods/1/timeconstant" % device,0.1) #set time constant
[s]
daq.setDouble("/%s/demods/2/timeconstant" % device,0.1)
daq.setInt("/%s/demods/0/phaseadjust" % device,1)
daq.setInt("/%s/demods/1/phaseadjust" % device,1)
daq.setInt("/%s/demods/2/phaseadjust" % device,1) #autophase
daq.setInt("/%s/demods/2/harmonic" % device,3)
# daq.setInt("/%s/demods/0/sinc" % device,1) #Enable sinc filter

# Signal input
# VOLTAGE INPUT 1
daq.setDouble("/%s/sigins/0/scaling" % device,1) #set scaling = 1 V/V
daq.setInt("/%s/sigins/0/ac" % device,0) #AC coupling OFF
daq.setInt("/%s/sigins/0/imp50" % device,0) #OFF=10MOhm
daq.setInt("/%s/sigins/0/float" % device,0) #GROUND connection (floating
connection OFF)
daq.setInt("/%s/sigins/0/diff" % device,1) #set differential measurements
# daq.setInt("/%s/sigins/0/autorange" % device,1) #autorange
daq.setDouble("/%s/sigins/0/range" % device,1) #Set range [V]

## V3omega vs Vinput measurement
Npt = opt["resistance"]["num_pts"]
V1 = opt["resistance"]["v_from"] #Vpk values!
V2 = opt["resistance"]["v_to"]

```



```

Vv = np.linspace(V1,V2,Npt)
daq.setDouble("/%/sigouts/0/amplitudes/0" % device, V1)
time.sleep(5)

# Perform a global synchronisation between the device and the data server:
# Ensure that the signal input and output configuration has taken effect
# before calculating the signal input autorange.
daq.sync()

X1v = np.array([])
Y1v = np.array([])
X1i = np.array([])
Y1i = np.array([])
X3v = np.array([])
Y3v = np.array([])

## Plot parameters
# Further options:
https://matplotlib.org/3.5.1/api/\_as\_gen/matplotlib.pyplot.plot.html
markerfacecolors = ['none','none']
markeredgecolors = ['red','blue']
markers = ['o','o']
markersizes = [5,5]
labels = ['r','r']

x_label = r'$I$ [A]'
y_label = r'$V$ [V]'

fig, axis = plt.subplots(1,1)
axis.set_xlabel(x_label)
axis.set_ylabel(y_label)
# Uncomment to set axis limits (see line axis.relim() below)
# axis.set_ylim([0, 100])
# axis.set_xlim([0, 100])

# Open file to save data
data = [('Data file (*.dat)', '*.dat'),('Text file (*.txt)', '*.txt'),('All
files','*.*')]
f = fd.asksaveasfile(mode = 'w', defaultextension = data, confirmoverwrite
= True, filetypes = data, title = 'Save calculation results to a file', parent =
root, initialfile = filename, initialdir = filedir)
if f == None:
    filename_no_ext = "resistance"+datetime.now().strftime("%y-%m-
%d_%H_%M_%S")
    filename = filename_no_ext+".dat"
    filedir = "measurements"

    if not os.path.isdir(filedir):
        os.makedirs(filedir)

    f = open(filedir+"/"+filename,'w+')
    te_u.info_message("Your data file was saved at "+filedir+"/"+filename)
else:
    filedir = os.path.dirname(f.name)
    filename = os.path.basename(f.name)
    filename_no_ext = os.path.splitext(filename)[0]

```

```

plt.ion()

te_u.general_message("Measuring...")
for ii in range(len(Vv)):
    Vv = Vv[ii]
    daq.setDouble("/s/sigouts/0/amplitudes/0" % device, Vv)
    time.sleep(opt["resistance"]["t_sleep"])

    NN = opt["resistance"]["num_pts_for_avg"]
    V1XX = 0
    V1YY = 0
    I1XX = 0
    I1YY = 0
    V3XX = 0
    V3YY = 0

    for jj in range(NN):
        sample1 = daq.getSample("/s/demods/0/sample" % device) #Get
measurement result
        sample2 = daq.getSample("/s/demods/1/sample" % device) #Get
measurement result
        sample3 = daq.getSample("/s/demods/2/sample" % device) #Get
measurement result
        V1XX = V1XX + sample1['x']
        I1XX = I1XX + sample2['x']
        V3XX = V3XX + sample3['x']

    # Append new data to arrays
    X1v = np.append(X1v, V1XX/NN)
    X1i = np.append(X1i, I1XX/NN)
    X3v = np.append(X3v, V3XX/NN)

    axis.set_title(f"Progress of data acquisition:
{float(ii+1)/Npt*100:.2f}%.")

    te_u.general_message(f"\tProgress: {float(ii+1)/Npt*100:.2f}%")

    # Plot new data (point by point)
    axis.plot(
        I1XX/NN,
        V1XX/NN,
        color='none',
        markerfacecolor = markerfacecolors[0],
        markeredgecolor = markeredgecolors[0],
        marker=markers[0],
        markersize=markersizes[0],
        label='I vs V'
    )

    # Auto axis limits
    axis.relim()

    plt.pause(0.01)
    if(ii == 0):
        axis.legend()

    ## Write data to file
    # Set data and headers to be written to file
    headers = ["V1", "V1X", "V3X", "I1x"]
    data_to_write = [Vv[ii], X1v[ii], X3v[ii], X1i[ii]]

```

```

        if(ii==0):
            for k,h in enumerate(headers):
                f.write(h)
                if k != len(headers)-1:
                    f.write("\t")
            f.write("\n")

            for j,e1 in enumerate(data_to_write):
                # Adjust precision of data ex. {var:.2f} for 2 decimal places
                f.write(f"{float(e1):.7f}")
                if j != len(data_to_write)-1:
                    f.write("\t")
            f.write("\n")

    f.close()

    daq.setInt("/%s/sigouts/0/on" % device, 0) #switch off signal output

    def linear_curve(x,m,b):
        return m*x+b

    x = X1i
    y = X1v
    params,_ = curve_fit(linear_curve,x,y)
    m,b = params[0],params[1]
    yfit = m*x+b

    axis.plot(x,yfit,'b-',label='linear fit')

    axis.relim()

    axis.set_title(f"Resistance Measurement R={float(np.abs(m)):.4f}")

    plt.pause(0.01)

    plt.savefig(filedir + "/" + filename_no_ext + ".jpg", dpi=300)

    plt.ioff()

    te_u.general_message(f"\tSlope: {m}")

    f_config = open(filedir + "/" + filename_no_ext+"_config.txt","w+")
    for k,v in opt["resistance"].items():
        f_config.write(k+"\t"+str(v)+"\n")
    f_config.close()

    # Comment the following line to close the plot after acquisition
    plt.show()

    elif measurement == 9: # Close all plots
        plt.close('all')
    else:
        te_u.error_message("Invalid option, try again.")

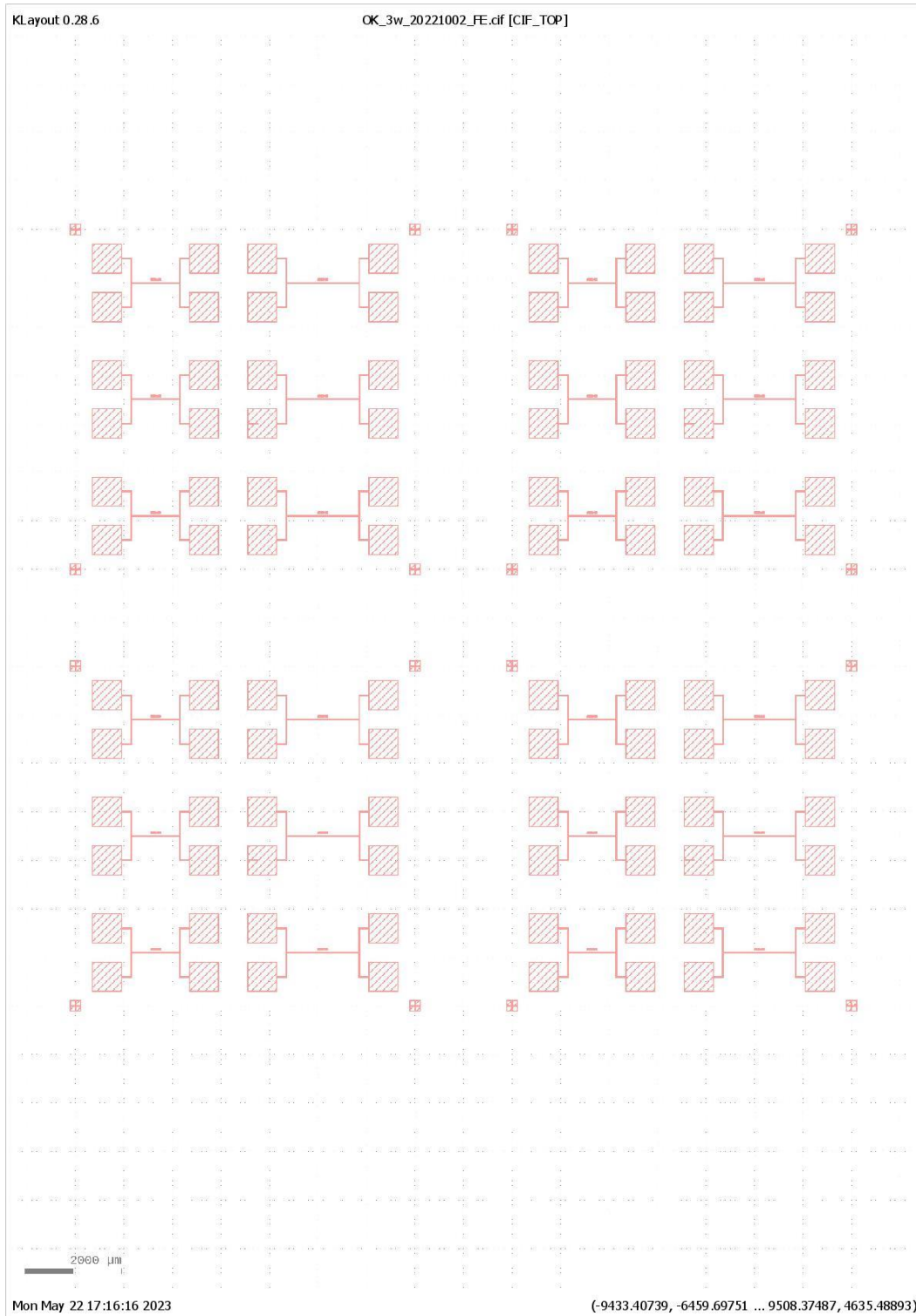
    if measurement in [1,2]:
        mb.showinfo("TE measurement completed","The measurement was successfully
completed")

root.destroy()

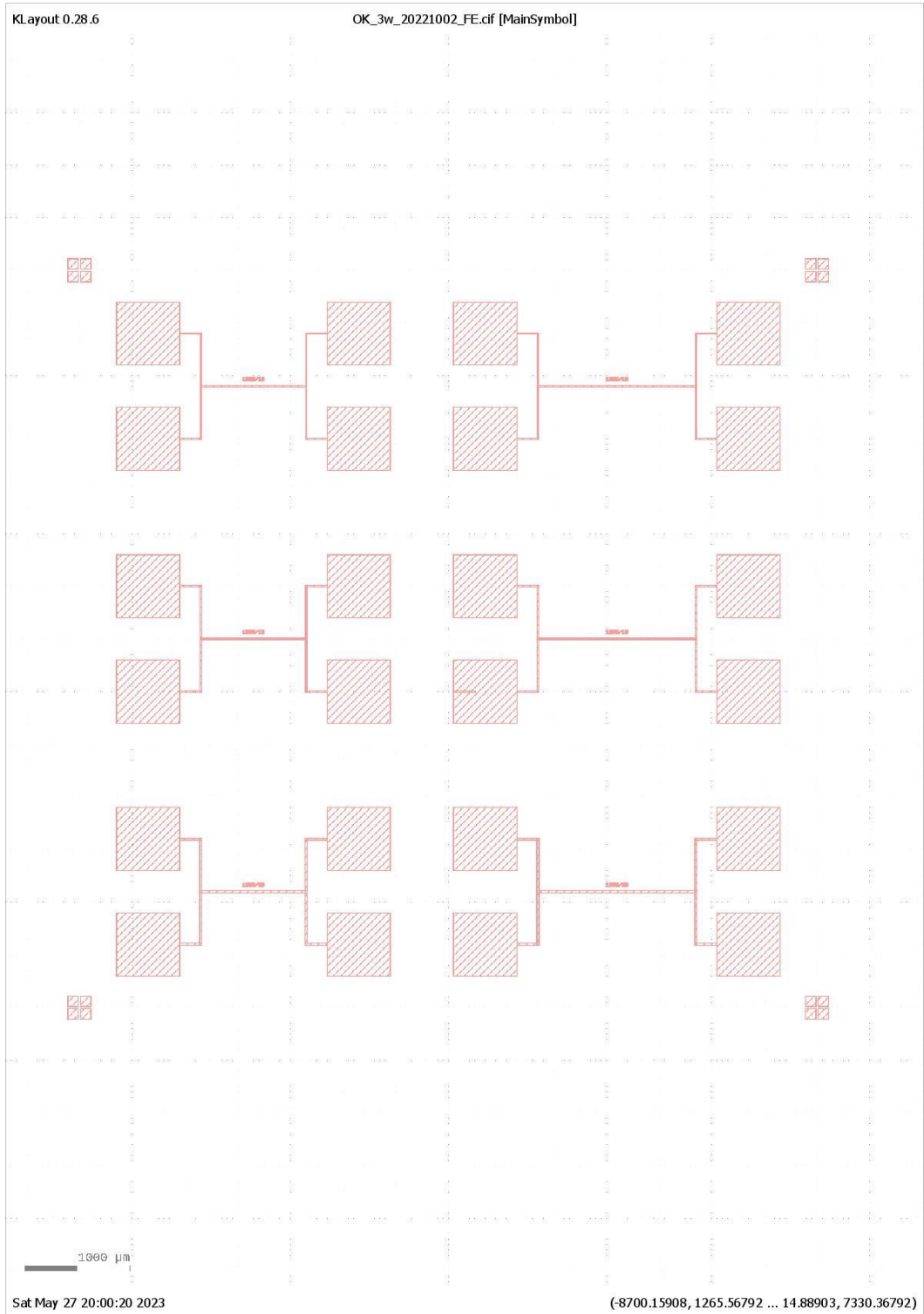
```

Mask for K design

Complete

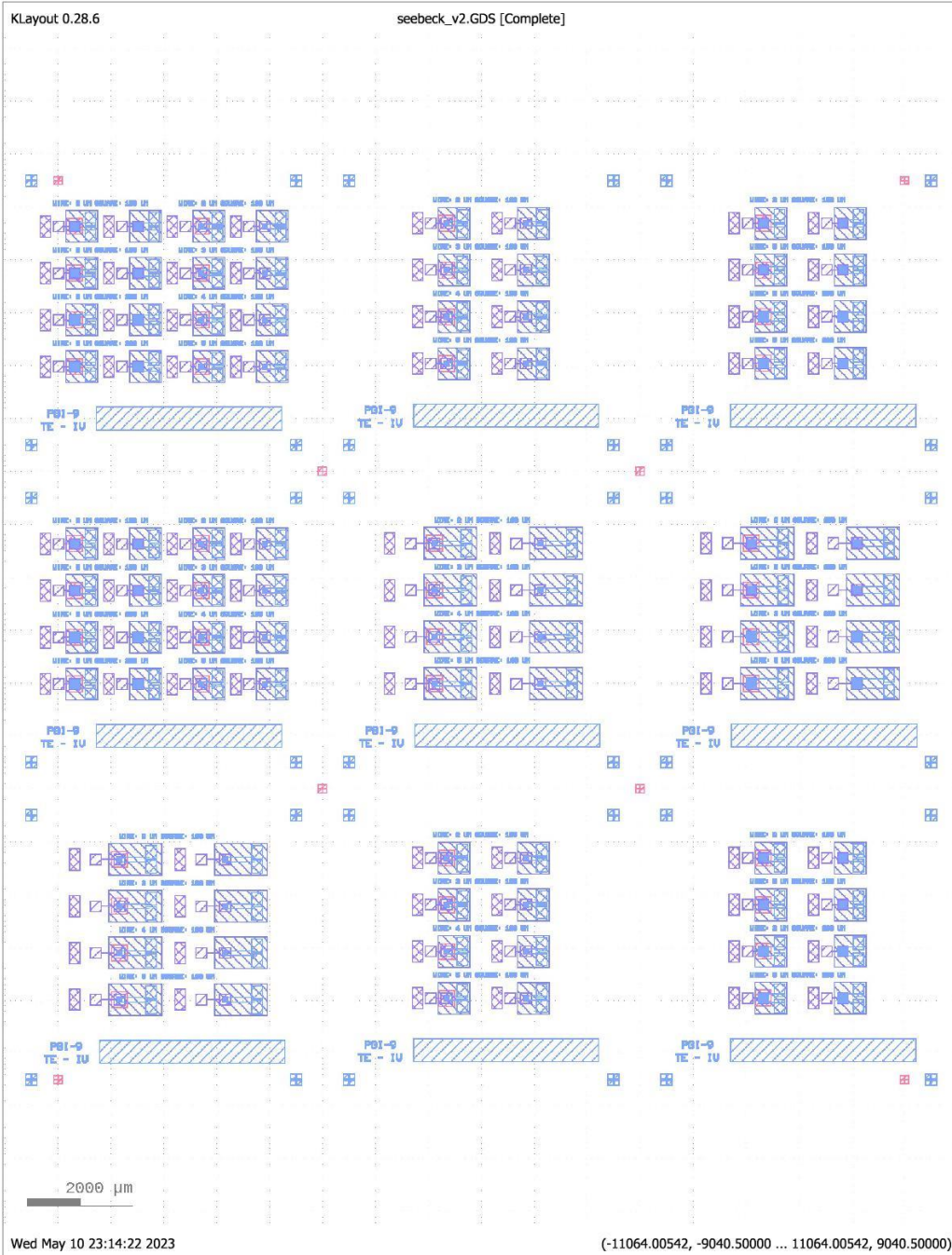


Detail

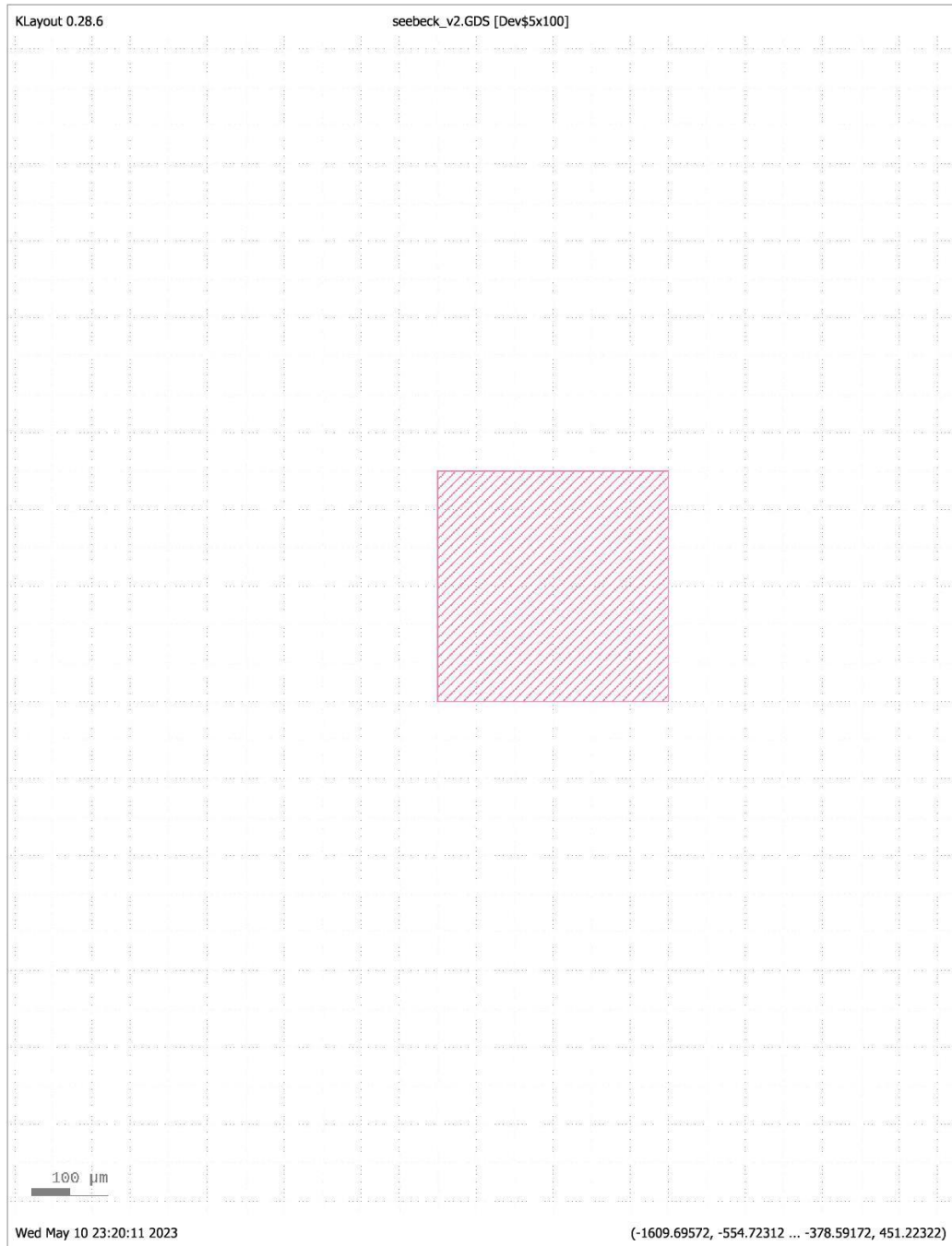


Mask for K-S design

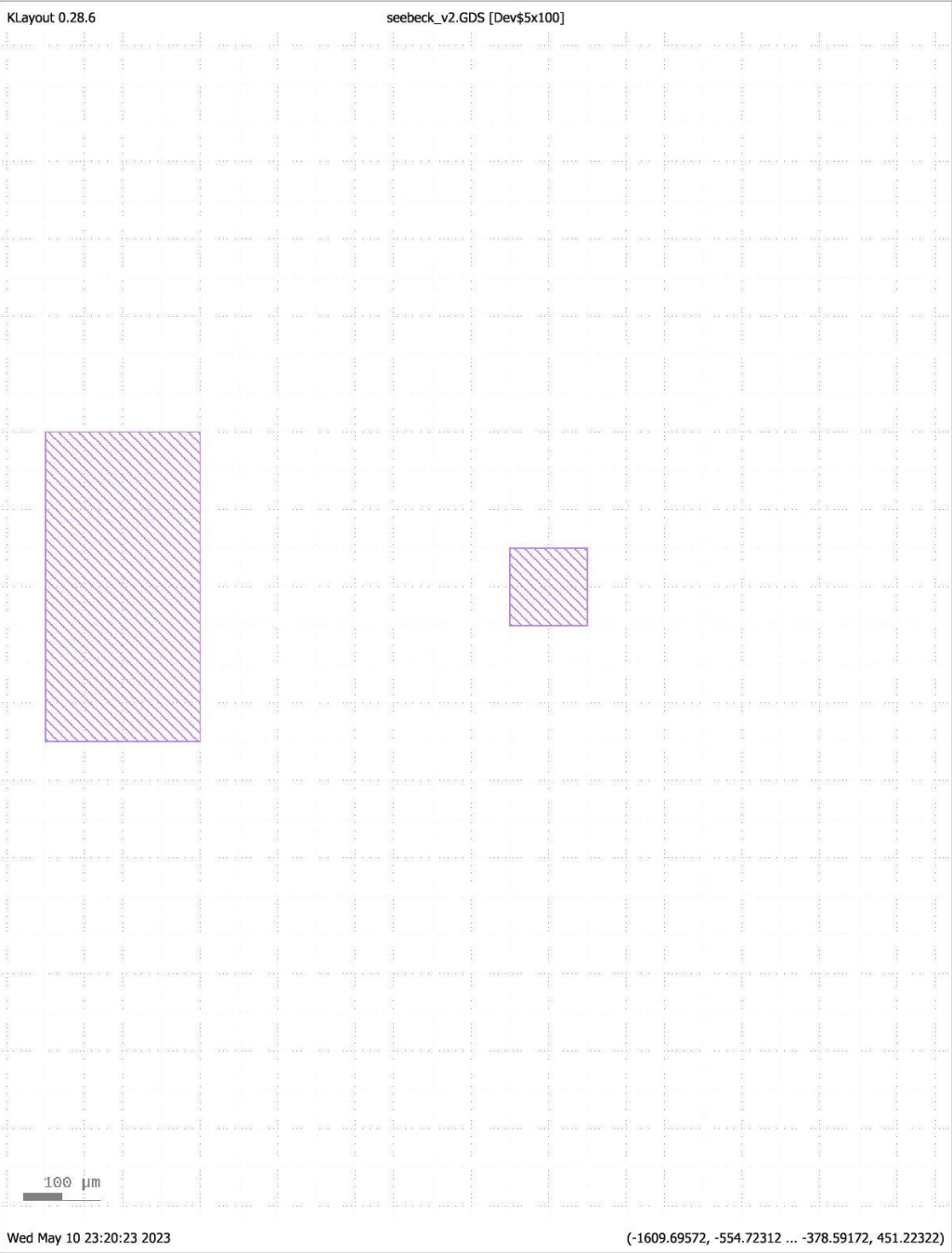
All layers



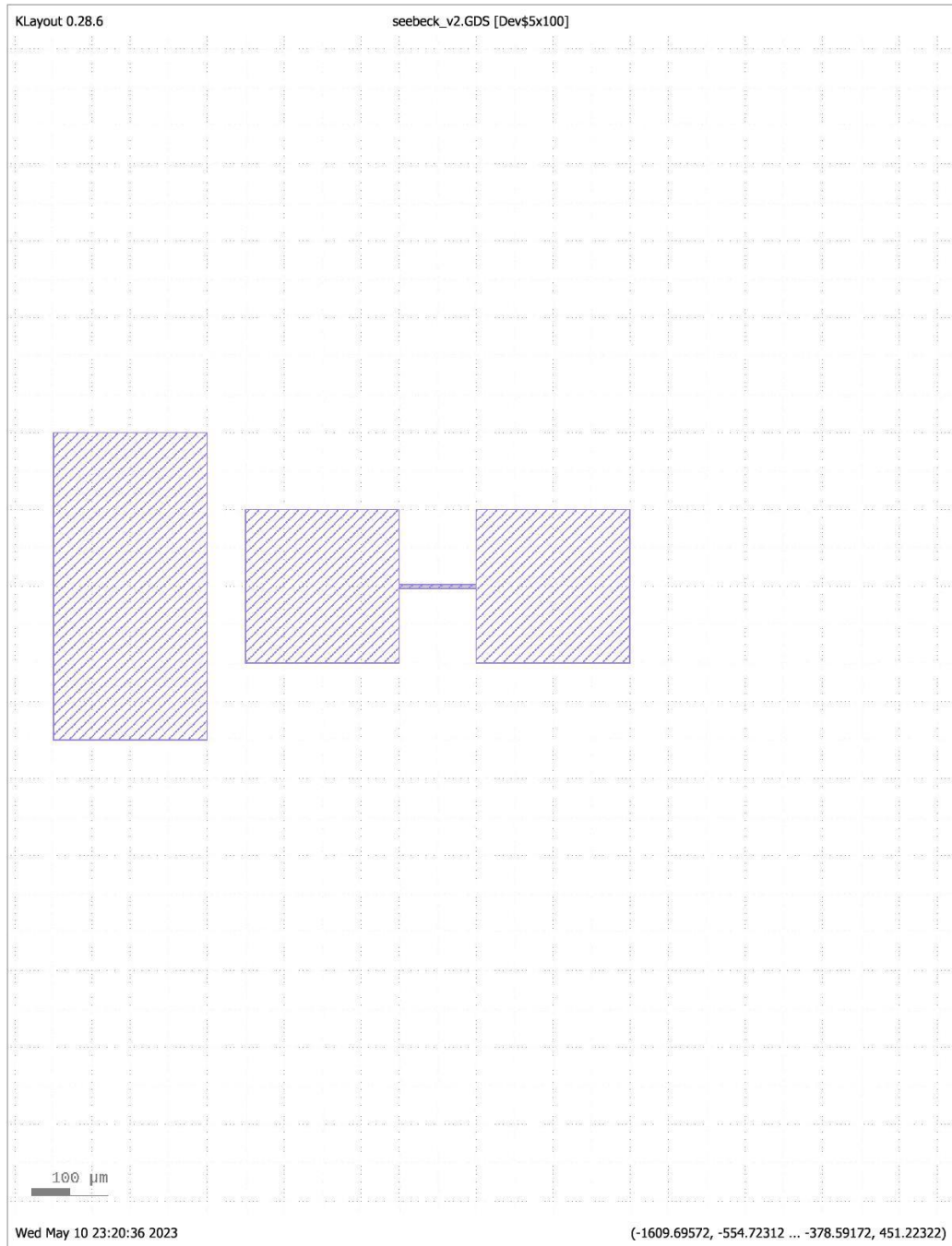
First layer



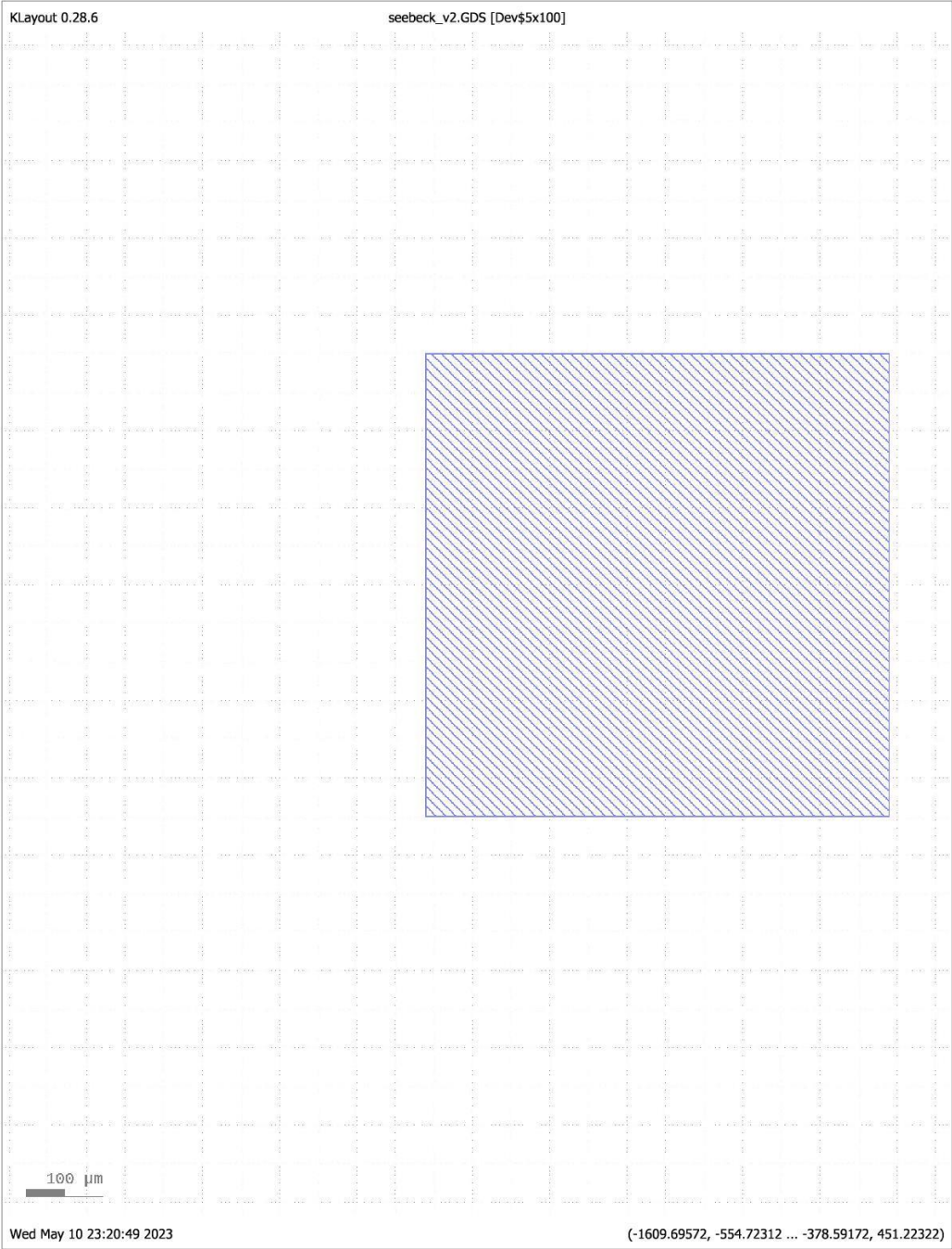
Second layer



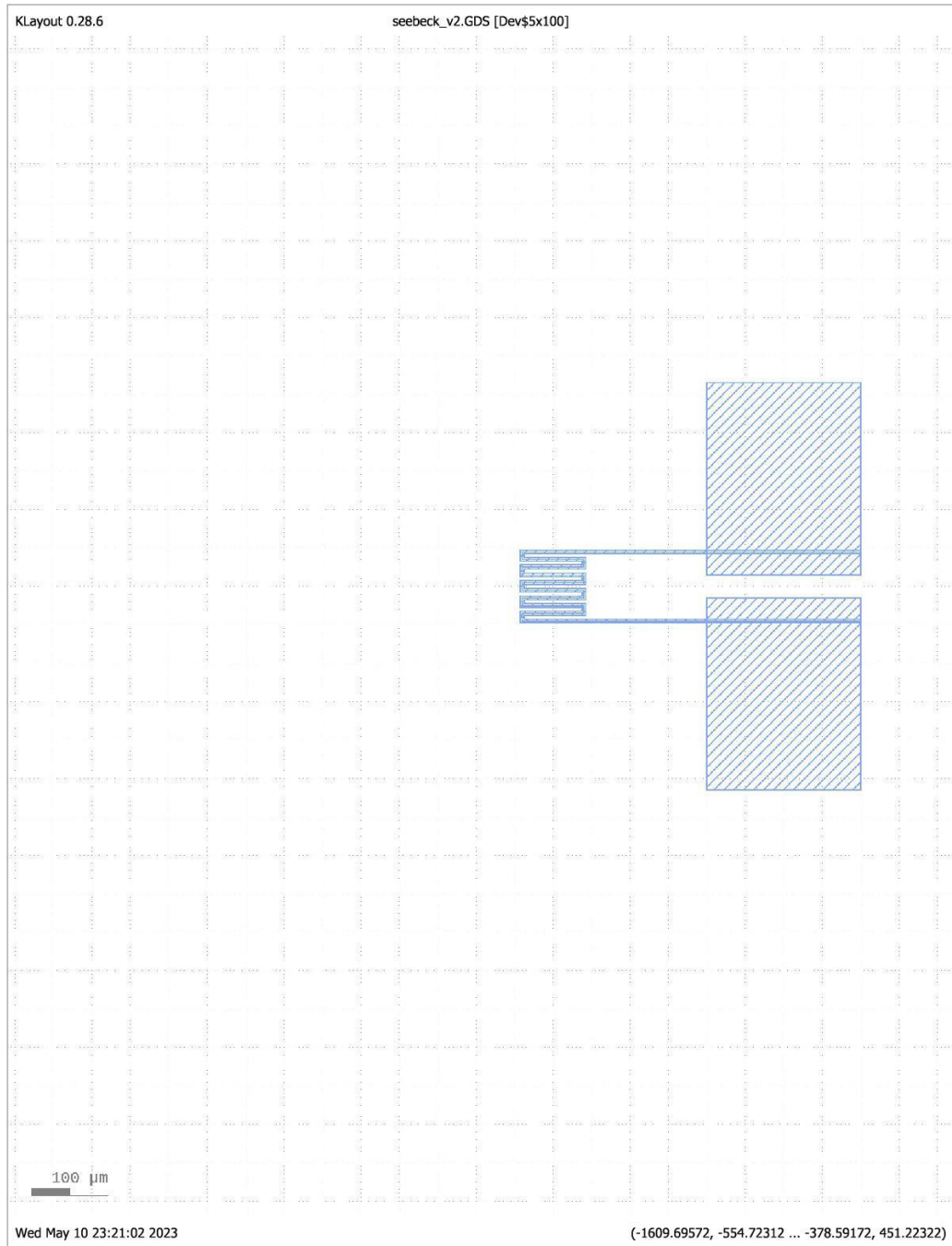
Third layer



Fourth layer

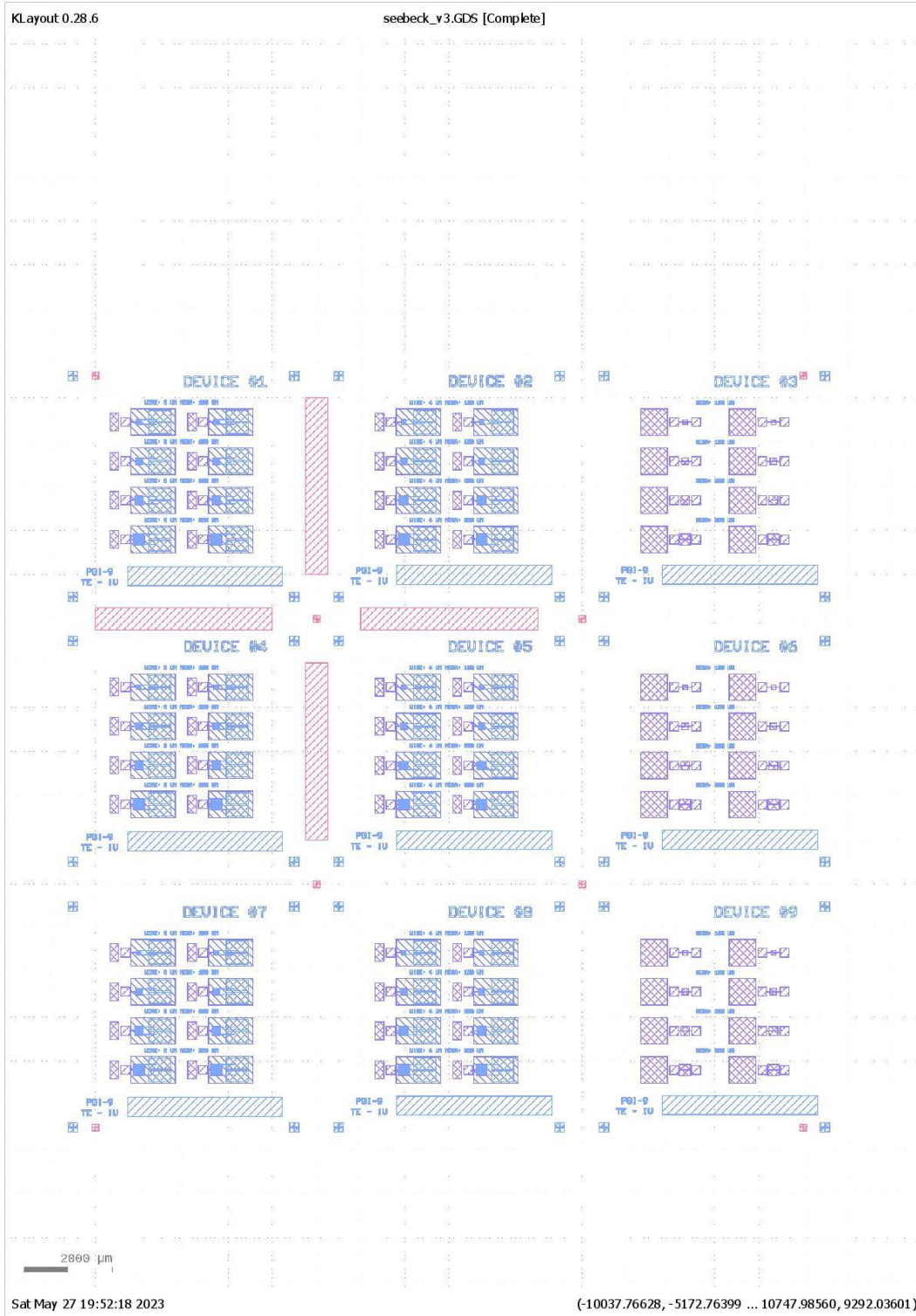


Fifth layer

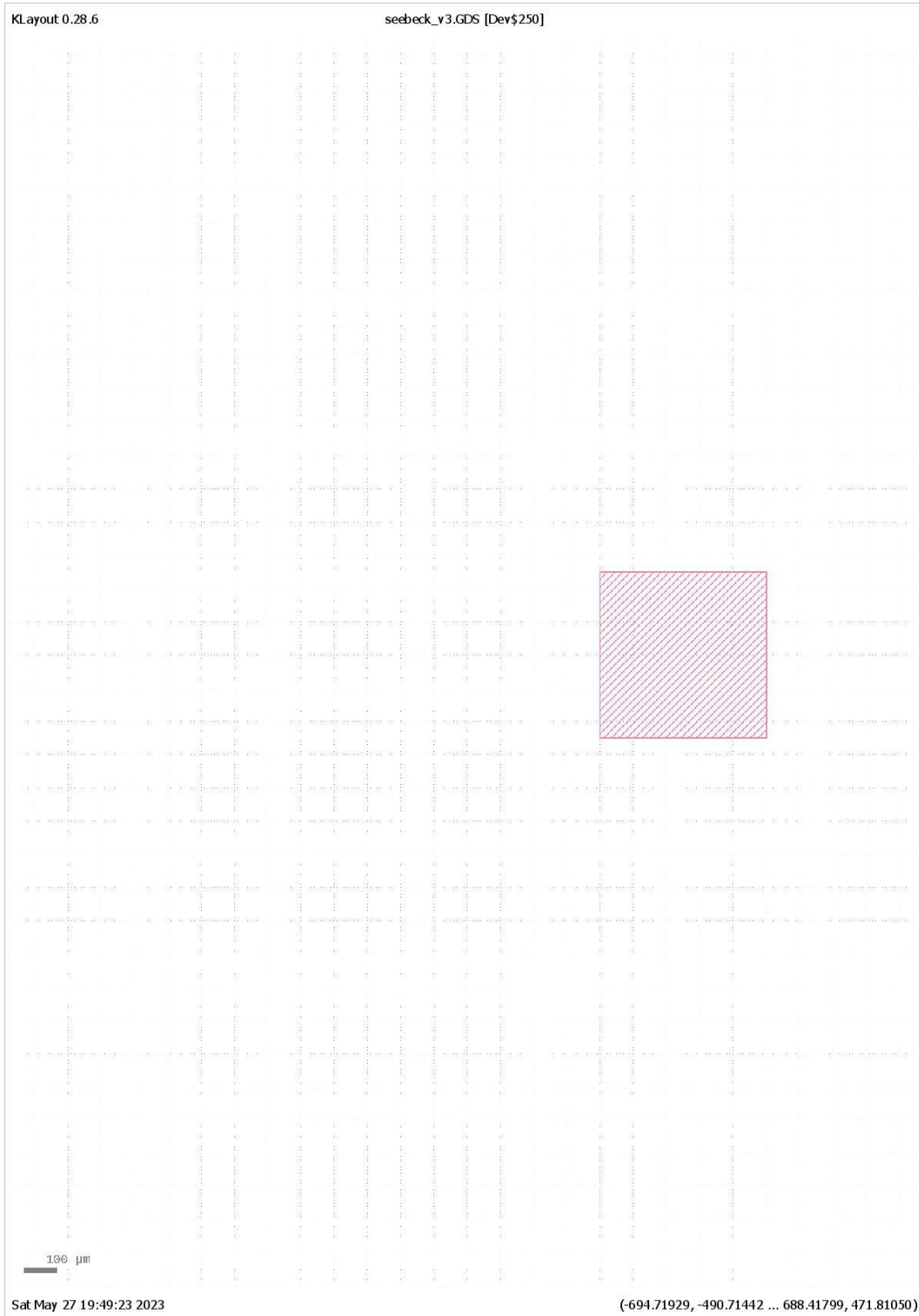


Mask for the K-S- σ design

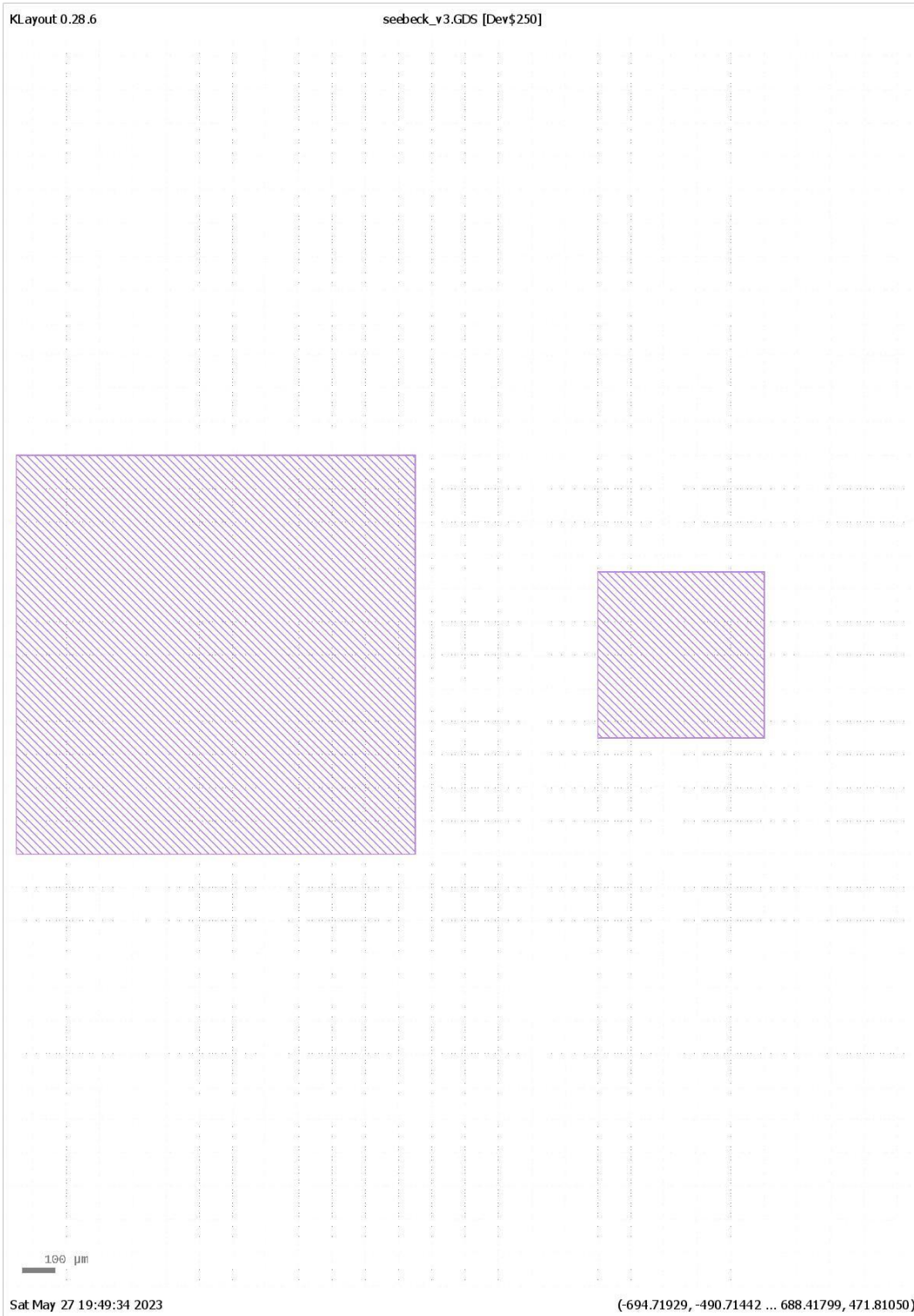
All layers



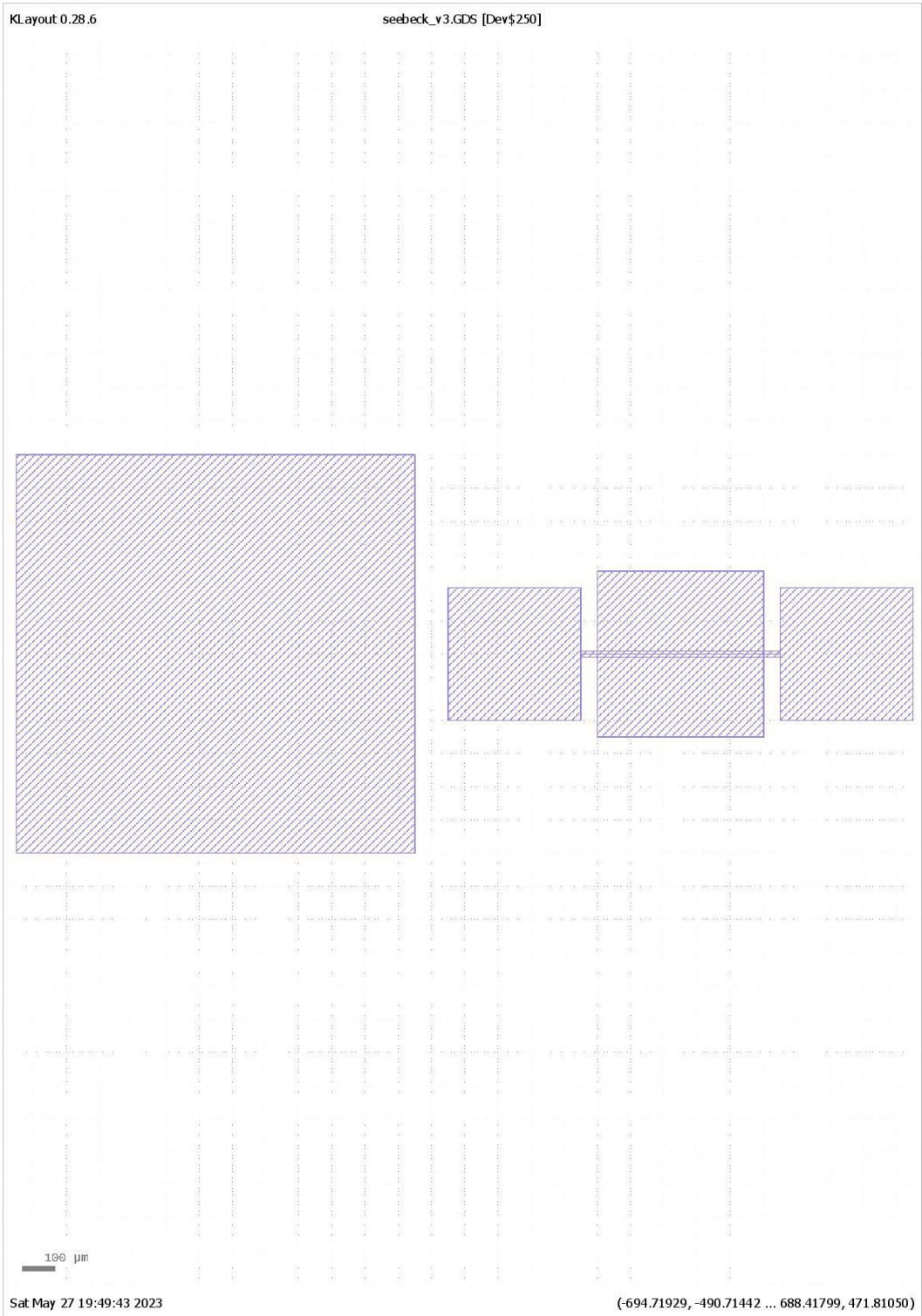
First layer (only σ device)



Second layer (only σ device)



Third layer (only σ device)



Run sheet for K-S and K-S- σ design

Helmholtz Nano Facility
22.02.2022, Juelich
Omar Concepción Díaz

Title: Seebeck Coefficient and Thermal Conductivity measuring device.

Abstract: Fabrication of a device for measuring Seebeck and thermal coefficient on a of GeSn/SiGeSn thin film and on a Ge layer simultaneously from samples grown by chemical vapor deposition for thermoelectric characterization purposes.

Growth Techniques: Chemical vapor deposition

Substrate: 200 mm Silicon (100) wafers, one-side polished

Deposited materials: Ge, Sn, Si doped with B and/or P

Size of the samples: 20 mm x 20 mm

Process:

Step	Process	Tools & Chemicals	Target Parameters	Commentary	Team
1a	Cleaning (Solvent) 1. Acetone 2. Isopropanol	WB 2.1 Acetone Isopropanol	5min, RT, US-9 5min, RT, US-9		WB
1b	Spin Coating AZnLOF2020 (-) 1. Dehydration 2. Cool down on chuck 3. Spin on 4. Softbake	WB 2.2 HotPlate 1. AZ nLOF2020 2. settle on chuck HP left	110°C x 3min 60s ii. Acc/Speed:2500rpm; t=5s iii. Acc/Speed:5000rpm; t=60s 60s 110°C x 60s	Program: SeebeckN	WB
1c	Optical Lithography 1. Exposure	MLA 100 MLA - Lambda=365nm	Dose: 300mJ/cm ² Defoc: 0	2x2cm Proben Design: OC_Seebeck_FE With Alignment	Litho
1d	Post Exposure Bake 1. PEB	WB 2.2 Hot-Plate	110°C x 60s		WB
1e	Development 1. Development 2. Cleaning	WB 2.3 AZ326 MIF DI-Water	60s i. Pre-rinse 1 min. ii. Quality-rinse 3 min.	Stiring all time	WB
1f	Etching	RIE 4 Cl ₂ Ar	YJ-GeSn-Cl ₂ /Ar-v2	Etch rate: 200nm in 45s	
1g	Photoresist removal	Gigabatch	O2-300w-200sccm-5min		
2	Deposition 1. SiO ₂	PECVD 2 Oxford SiO ₂	200 nm @ 250°C	Rec: Oxide_(OPT)_@_250C Etch rate: 100 nm in 1:32	Depo
3a	Spin Coating ECI 3012 (+) 1. Dehydration 2. Cool down on chuck	WB 2.2 HotPlate	130°C x 3min 60s		WB

	3. Spin on	1. ECI 3012 2. settle on chuck HP left	ii. Acc/Speed:500rpm; t=5s iii. Acc/Speed:3000rpm; t=60s 60s 90°C x 90s	Program SeebeckP	
3b	Optical Lithography 1. Exposure	4. Softbake			
		MLA 100 MLA - Lambda=365nm	Dose: 450mJ/cm ² Defoc: 0	2x2cm Proben Design: OC_Seebeck_AE1 With Alignment	Litho
3c	Post Exposure Bake 1. PEB	WB 2.2 Hot-Plate	110°C x 90s		WB
3d	Development 1. Development 2. Cleaning	WB 2.3 AZ326 MIF DI-Water	70s i. Pre-rinse 1 min. ii. Quality-rinse 3 min.	Stiring all the time	WB
3e	Etching 1. Plasma	RIE 4 CHF3	Ch1-TG-CHF3-Ar	Etch rate: 95 nm in 4:10	
	2. Wet Etching	WB 4	1% HF	20s dip	WB
3f	Photoresist removal 1. Acetone 2. Isopropanol	WB 2.1 Acetone Isopropanol	5min, RT, US-4 5min, RT, US-4		WB
4a	Spin Coating ECI 3012 (+) 1. Dehydration 2. Cool down on chuck 3. Spin on	WB 2.2 HotPlate	130°C x 3min 60s		WB
	4. Softbake	1. ECI 3012 2. settle on chuck HP left	ii. Acc/Speed:500rpm; t=5s iii. Acc/Speed:3000rpm; t=60s 60s 90°C x 90s	Program SeebeckP	
4b	Optical Lithography 1. Exposure	MLA 100 MLA - Lambda=365nm	Dose: 450mJ/cm ² Defoc: 0	2x2cm Proben Design: OC_Seebeck_AE2 With Alignment	Litho
4c	Post Exposure Bake 1. PEB	WB 2.2 Hot-Plate	110°C x 90s		WB
4d	Development 1. Development 2. Cleaning	WB 2.3 AZ326 MIF DI-Water	70s i. Pre-rinse 1 min. ii. Quality-rinse 3 min.	Stiring all the time	WB
4e	Metal-Deposition 1. Ti 2. Al	PLS 500 Ti Al	d = 20nm d = 150nm		Depo
4f	Lift off 1. Acetone 2. Isopropanol	WB 9.1 or 9.2 Acetone Isopropanol	5-10min 10min	Ultrasonic at 4-5, RT	WB
5	Deposition 1. SiO2	PECVD 2 Oxford SiO2	200 nm @ 250°C	Rec: Oxide_(OPT)_@_250C Etch rate: 100 nm in 1:32	Depo
6a	Spin Coating AZnLOF2020 (-) 1. Dehydration 2. Cool down on chuck 3. Spin on	WB 2.2 HotPlate	110°C x 3min 60s		WB
		1. AZ nLOF2020 2. settle on chuck	ii. Acc/Speed:2500rpm; t=5s iii. Acc/Speed:5000rpm; t=60s 60s	Program: SeebeckN	

	4. Softbake	HP left	110°C x 60s		
6b	Optical Lithography 1. Exposure	MLA 100 MLA - Lambda=365nm	Dose: 300mJ/cm ² Defoc: 0	2x2cm Proben Design: OC_Seebeck_AE3 With Alignment	Litho
6c	Post Exposure Bake 1. PEB	WB 2.2 Hot-Plate	110°C x 60s		WB
6d	Development 1. Development 2. Cleaning	WB 2.3 AZ326 MIF DI-Water	60s i. Pre-rinse 1 min. ii. Quality-rinse 3 min.	Stiring all time	WB
6f	Etching 1. Plasma	RIE 4 CHF3	Ch1-TG-CHF3-Ar	Etch rate: 95 nm in 4:10	
	2. Wet Etching	WB 4	1% HF	20s dip	WB
6g	Photoresist removal 1. Acetone 2. Isopropanol	WB 2.1 Acetone Isopropanol	5min, RT, US-4 5min, RT, US-4		WB
7a	Spin Coating ECI 3012 (+) 1. Dehydration 2. Cool down on chuck 3. Spin on	WB 2.2 HotPlate	130°C x 3min 60s	Program SeebeckP	WB
		1. ECI 3012	ii. Acc/Speed:500rpm; t=5s iii. Acc/Speed:3000rpm; t=60s		
		2. settle on chuck	60s		
	4. Softbake	HP left	90°C x 90s		
7b	Optical Lithography 1. Exposure	MLA 100 MLA - Lambda=365nm	Dose: 450mJ/cm ² Defoc: 0	2x2cm Proben Design: OC_Seebeck_AE4 With Alignment	Litho
7c	Post Exposure Bake 1. PEB	WB 2.2 Hot-Plate	110°C x 90s		WB
7d	Development 1. Development 2. Cleaning	WB 2.3 AZ326 MIF DI-Water	70s i. Pre-rinse 1 min. ii. Quality-rinse 3 min.	Stiring all the time	WB
7e	Metal-Deposition 1. Cr - Deposition 2. Au - Deposition	PLS 500 Cr Au	d = 50nm d = 250nm	0.2 nm/s 0.3 nm/s	Depo
7f	Lift off 1. Acetone 2. Isopropanol	WB 9.1 or 9.2 Acetone Isopropanol	5-10min 10min	Ultrasonic at 4-5, RT	WB
8	Dicing 1. Dicing	Disco 1	Dice into 7mm x 7mm		ANA